Title

The Ras-GAP Proteins Ira2 and Neurofibromin Are Negatively Regulated by Ubiquitin-associated Proteins Gpb1 in Yeast and ETEA/UBXD8 in Human Cells

Permalink

https://escholarship.org/uc/item/8st7h9w5

Author

Phan, Vernon T

Publication Date

2008-04-07

Peer reviewed|Thesis/dissertation

The Ras-GAP Proteins Ira2 and Neurofibromin Are Negatively Regulated by Ubiquitin-associated Proteins Gpb1 in Yeast and ETEA/UBXD8 in Human Cells

by

Vernon Truong Phan

DISSERTATION

Submitted in partial satisfaction of the requirements for the degree of

DOCTOR OF PHILOSOPHY

In

Biomedical Sciences

in the

GRADUATE DIVISION

of the

UNIVERSITY OF CALIFORNIA, SAN FRANCISCO

UMI Number: 3297797

UMI®

To my parents, who gave us the gifts of life,

and of freedom.

Acknowledgements

I acknowledge with my deepest gratitude and appreciation the many people I have met during my graduate studies who have helped me with both personal and scientific advice. First, I thank my advisor Frank McCormick for guiding me through my graduate studies, and for sharing with me his deep passion in teaching and dissecting the Ras signaling pathway. It was a privilege to study under Frank's guidance. He taught me how to think critically as a scientist, and gave me the freedom to explore my scientific curiosity. While studied under Frank, I had the opportunity to attend many national and international scientific meetings and conferences that had greatly sharpened my skills and my thinking as a scientist. Dear Frank, thank you for giving me many opportunities during my graduate studies. I am extremely grateful for your teaching and guidance.

I also want to thank my thesis committee faculty members, Allan Balmain and Kevin Shannon for their scientific advice and encouragement. I want to thank my committee chairman, Allan, for the many helpful comments and suggestions that guided me toward completion of my dissertation projects. I want to thank Kevin for teaching and sharing with me his deep scientific knowledge of the NF1 diseases. Kevin, thank you for all the help you gave me to complete this dissertation.

I was fortunate to spend the past four years of my graduate studies with the most wonderful and kind people at the UCSF Cancer Center. My special thanks to David Stokoe and David Toczyski for devoting their precious time, expertise and scientific advice to help me with my dissertation proposals for the Qualifying Examination. I want to thank David Stokoe for being so patient

with me. David Toczyski, thank you for allowing me to do my research rotation in your lab in my first year of graduate school, and letting me used the instruments and reagents from your lab. I have learned a lot from you and your lab members, and most of the techniques I learned from your lab directly applied to the many techniques I used in this dissertation.

I also want to thank Scott Kogan, my first scientific advisor, who gave me the first research job after graduated from UC Santa Cruz that would allowed me to move to San Francisco. The three years I worked with Scott had greatly helped me getting interested in medical research. Scott, I thank you for trusting and believing in me, for encouraging me present at the ASH conference, and for letting me lead many research projects in your lab at the time. You have given me the greatest opportunity, one that created the foundation that allowed me to be where I am today.

This dissertation would not be completed without mastering the many techniques I performed to address my scientific hypothesis and curiosity. I learned these techniques over the years from the many truly wonderful and artistic scientists. With deepest gratitude, I want to thank Pablo Rodriquez-Viciana. Pablo, thank you for the intelligent, generosity, and inspiration that you possess that greatly inspired me. Thank you for teaching me the best cloning technique which allowed me to clone so many genes that I thought could not be possible during a short period of time. Thank you for introducing me the TAP-tagged technology, which allowed me to experience the wonder of protein-protein interactions and greatly enhanced my interests in signaling transduction. My special thanks to Vivianne Ding for teaching me the wonder of yeast genetics, for helping me design the many experiments described in this dissertation, and for reading the many proposals and manuscripts I wrote. I want to thank Sang Lee for teaching me new techniques and sharing with me his reagents. I also want to thank Erika Woodbury for her enthusiasm and excellent suggestions. Erika, thank you. I will miss discussing science with you.

I am very fortunate to have the best lab manager Madhu Macrae to help me as a graduate student in Frank lab. Madhu, thank you for letting me obtain the best reagents in the world to tackle the scientific questions I had. Also, I owed many thanks to Jacqueline Galeas for all her wonderful help with obtaining reagents and lab space which allowed me to work smoothly and efficiently.

My graduate years were filled with great memories, many of which had helped and sharpened my life experiences. I would like to thank the many friends I have met over the years that greatly contribute to my growth as a person and as a scientist. Most of all, I want to thank Sarah Choi and Abby Miller for spending the many nights with me in the lab to run western blots and to discuss science with me. I would like to thank Amy Young, Irma Rangel and Cynthia Mysinger for being the best bench mates in the world, and for allowing me to use the lab benches whenever I needed space. Amy, thank you so much for your all help, for sharing your reagents, for reading my manuscripts, and for spending the many weekends with me in the lab running gel electrophoresis and looking over the western blot results with me. Irma, I want to thank you for your attention, for getting me sandwiches and making sure that I won't be hungry while running my experiments. Cynthia, thank you for correct my grammar and reading my many written proposals and manuscripts. Without your help, I might not have won the Children's Foundation Fellowship. I am greatly appreciated your time and generosity. Also, I want to thank Jessie Castillo for all your help processing the paper work that I created. Dear friends, you all have a special place in my heart. Sincerely, I want to thank you for your presence in my life.

Most importantly, I would like to thank my family, to my parents and sisters, for being the greatest angels of my life. Dear mom and dad, you have sacrificed your lives to better ours. From the bottom of my heart, I want to thank you for bringing my sisters and me to America, and for giving us the gift of freedom.

Finally, I would like to thank my best friend and my life partner, Kent Allen Williams. Kent, thank you for the support and encouragement that you have always given me through the many years we have spent together. I know I have given you so many headaches. I want to thank you for being the greatest person that you are, and for being supportive with all my career decisions.

Declaration

The studies presented in this dissertation were performed under the guidance of Dr. Frank McCormick. Part of chapter 3 of this thesis is based on previously written proposals for my dissertation and fellowship application for the Young Investigator Award from the Children's Tumor Foundation. Part of chapter 1 of this thesis is written for a review article about Neurofibromatosis Type 1 and is contributed as a chapter that will be submitted for publication, entitled "Ras signaling and therapies." The following co-authors contributed to "Ras signaling and therapies" chapter: Jesse Lyons, Abigail Miller, Vernon Phan, Irma Rangel and Amy Young and Frank McCormick (UCSF Helen Diller Family Comprehensive Cancer Center, San Francisco, California). Chapters 4-6 of this dissertation are based on a manuscript that will be submitted for publication, entitled "The Ras-GAP Proteins Ira2 and Neurofibromin Are Negatively Regulated by Ubiquitin-associated Proteins Gpb1 in Yeast and ETEA/UBXD8 in Human Cells". The following co-authors contributed to this work: Vivianne W Ding, Fenglei Li, Robert Chalkley, Al Burlingame and Frank McCormick (University of California, San Francisco).

The RasGAP Proteins Ira2 and Neurofibromin Are Regulated by Ubiquitin-Associated Enzymes Gpb1 in Yeast and ETEA/UBXD8 in Human Cells

By

Vernon T. Phan

Abstract

The Neurofibromatosis type 1 (NF1) gene encodes the GTPase activating protein (GAP) neurofibromin which negatively regulates Ras activity. The yeast *Saccharomyces cerevisiae* has two neurofibromin homologs, Ira1 and Ira2. Similar to mammalian cells, mutations or deletions of the IRA genes result in hyperactive Ras. I utilized an unbiased proteomics approach to investigate Ira2 and neurofibromin binding partners and their involvement in regulating Ras signaling. I demonstrated that the Gpb1 protein negatively regulates Ira2 by promoting Ira2 proteolysis. Loss and gain of function experiments showed the Gpb1 protein is essential for Ira2 function. Whereas deletion of *GPB1* increased Ira2 protein levels, overexpression of Gpb1 destabilized Ira2. In addition, the purified Gpb1complex can ubiquitinate Ira2 *in vitro*. I demonstrated that Gpb1 is required for the Rpn1 proteasome base subunit to trigger Ira2 proteolysis. In addition, I showed that the deubiquitination enzyme Ubp6 interacts with Ira2 and antagonizes Gpb1-mediated degradation of Ira2. Finally, I showed that the serine/threonine kinase CK2 binds and phosphorylates Ira2, preventing Ira2 from protein degradation.

I extended the findings to the mammalian system to show that the ETEA/UBXD8 protein directly interacts and negatively regulates neurofibromin. ETEA contains both UBA and UBX domains. Similar to Gpb1 negative regulation of Ira2 in yeast, ETEA over-expression down-regulates neurofibromin in human cells. Purified ETEA, but not a mutant of ETEA that lacks the UBX domain, ubiquitinates the neurofibromin GAP-related domain *in vitro*. Importantly, ETEA shares approximately 18% homology with Gpb1 N-terminal domain, including amino acid sequence homology in the UBA and UBX domains. Silencing of ETEA increases neurofibromin levels and downregulates Ras activities. These findings provide evidence for conserved ubiquitination pathways regulating the RasGAP proteins Ira2 in yeast and neurofibromin in humans.

x

Table of Contents

List of Figures

List of Tables

Chapter 2

Table 2.1: List of Gateway Entry/Destination and shRNA vectors

Chapter 3

Table 3.1: Micro arrays analysis of gene expression in the *ypt7Δ* yeast strain

Chapter 4

Table 4.1: Mass Spectrometry Results of proteins binding to Ira2 complex

Chapter 5

Table 5.1: Mass Spectrometry Results of proteins binding to Gpb1 complex

Chapter 1: Introduction

1.1 Neurofibromatosis Type 1

Neurofibromatosis is the common term used to describe three completely different genetic disorders: Neurofibromatosis Type 1 (NF1), Neurofibromatosis Type 2 (NF2), and Schwannomatosis. These three disorders all cause the development of benign and malignant tumors in the myelin sheath surrounding the nerves. This dissertation focuses on the molecular pathways that control neurofibromin, the protein that when mutated causes Neurofibromatosis Type 1.

Neurofibromatosis type 1 (NF1) is an autosomal dominant genetic disease that affects 1 in 3500 individuals worldwide each year. Individuals with NF1 develop multiple benign neurofibromas and malignant peripheral nerve sheath tumors (MPNSTs). Approximately half of NF1 patients have learning disabilities. Other features of NF1 include café-au-lait spots, hamartomatous lesions of the iris, bone deformations, and a small percentage of NF1 patients can develop gliomas and pheochromocytomas. Children who have NF1 are predisposed to developing myeloid leukemia (Bader, 1986; Riccardi, 1992; Side et al., 1997).

NF1 is characterized as a familial genetic disease. However, about half of the NF1 patients can acquire sporadic mutations of the *NF1* gene. The *NF1* gene functions as a tumor suppressor because loss of functions of the remaining wild-type *NF1* allele, or loss of heterozygosity (LOH), has been detected in malignant tumors of NF1 patients (Legius et al., 1993; Shannon et al., 1994; Upadhyaya et al., 1998). Fredrich von Recklinghausen first described a patient who had NF1 in 1882. The NF1 gene was cloned in 1990 by the laboratories of Collins and White (Cawthon et al., 1990; Wallace et al., 1990). The *NF1* gene locus is located on chromosome 17, and contains 60 exons spanning approximately 350kB (Li et al., 1995). In addition, depending of the cell

types, *NF1* exists in many different isoforms, which can differentially express depending on the tissue types. Even though *NF1* mRNA can be easily detected in many tissue compartments, it is found to be highly expressed in neuronal cells, including the spinal cord and the peripheral nervous systems (Daston and Ratner, 1992; Daston et al., 1992).

1.2 RasGTPase

Ras is a small GTP-binding protein and an important downstream effector of the growth factor tyrosine kinase signaling pathways. Ras functions as a molecular switch that oscillates between its active GTP-bound state and its inactive GDP-bound state. Ras activation can be achieved by extracellular growth factor signals, which activate receptor tyrosine kinases or G-coupling receptor proteins (Figure 1.1). Once activated, RasGTP binds to and activates Ras effectors, which include the oncogenic BRAF or PI3K family of kinases that control cell division, growth and differentiation (Downward, 2003). Uncontrolled activation of the Ras signaling pathway occurs in approximately 30% of human cancers. Additionally, mutations in Ras or Ras effector pathways, which are signaling pathway downstream of the Ras protein, have been found in many different human genetic diseases and cancers (Schubbert et al., 2007). These include mutations in the BRAF protein in malignant melanoma and colorectal cancers, and activation of the Ras/PI3K/AKT signaling pathway in human astrocytomas and gliomas.

Similar to other GTPase family members, Ras is tightly regulated by GTP-exchange factors (GEFs) that induce the release of GDP from Ras for activation, and GTPase-activating proteins (GAPs) that accelerate the hydrolysis of the gamma phosphate from the GTP bound to Ras to attenuate its activities (Bourne et al., 1991). Receptor tyrosine kinases activations recruit GEFs

to the cell plasma membrane to accelerate the displacement of RasGDP for RasGTP. In addition

to GEFs mobilization to the plasma membrane, receptor tyrosine kinases activation results in the

recruitment of the p120RasGAP protein to downregulate Ras activity. GAPs accelerates the

hydrolysis of RasGTP to RasGDP, thereby completes the RasGDP/RasGTP activation cycle

(Donovan et al., 2002).

Loss of functions of GAP proteins result in hyperactive Ras signaling (Kulkarni et al., 2000;

Tanaka et al., 1990a; van der Geer et al., 1997; Viskochil et al., 1990). One of the RasGAP genes

is the *NF1* tumor suppressor gene. Neurofibromin down-regulates Ras through its GAP domain.

Not surprisingly, mutations in the *NF1* gene lead to the development of tumors in humans.

Therefore, loss of neurofibromin function results in Ras hyper-activation and is believed to be

involved in the many clinical pathogenesis seen in NF1 patients. This signifies the importance of

this RasGAP protein in regulating Ras signaling.

1.3 Neurofibromin

Neurofibromin, the *NF1* gene product, is a tumor suppressor which negatively regulates Ras

activity by facilitating the hydrolysis of active RasGTP to inactive RasGDP through its GTPase

activating protein (GAP) domain (Ballester et al., 1990; Martin et al., 1990; Xu et al., 1990b).

Loss of neurofibromin results in hyperactive Ras signaling and activation of Ras downstream

effectors, including the Raf/MEK/ERK, the PI3Kinase/Akt and the mTOR pathways (Cichowski

and Jacks, 2001; Johannessen et al., 2005; Schubbert et al., 2007; Zhu and Parada, 2001).

Neurofibromin is conserved in flies, yeast, and humans. Early studies in *S. cerevisae* showed

that loss of the neurofibromin-like proteins Ira1 and Ira2 results in hyper-activation of the Ras.

4

In addition to regulating Ras, neurofibromin positively regulates the G-protein coupling receptor protein and its downstream effectors. In yeast cells, the G-coupling protein receptor, Gpr1, signals up-stream of the Ras/adenylyl cyclase/PKA pathway. However, in *Drosophila* and mice, neurofibromin signals downstream of G-coupling receptors to control memory and learning (Costa et al., 2002; Guo et al., 1997; The et al., 1997; Tong et al., 2007). Loss of Ira functions in yeast activates Ras. However, loss of neurofibromin in *Nf1*-deficient *Drosophila* reduced adenylyl cyclase activity, and as a result decreased cAMP production in a Ras-independent mechanism (The et al., 1997). Interestingly, in the neurofibromin mutant mice, the learning deficits are reduced when treated with inhibitors targeting Ras pathway, suggesting that cognitive defects in neurofibromin mutant mice are controlled by Ras activity (Costa et al., 2002). In humans, mutations of the *NF1* gene cause learning disability, although the exact molecular function underlying the disease is less clear. Therefore, in yeast and flies, neurofibromin acts downstream of the adenylyl cyclase/cAMP/PKA pathway, whereas the complexity of neurofibromin in controlling cognitive functions in mice and humans is less well understood and needs further investigation.

The GAP domain represents approximately10% of the neurofibromin protein (Figure 1.2). Mutations flanking the GAP domain have been detected in patients with NF1 (Serra et al., 2001). Studies in humans showed that loss of neurofibromin functions leads to a diverse genetic and tumorigenic diseases. These studies suggest that neurofibromin may have other uncharacterized functions. Identifying these unknown functions of neurofibromin will be critical to better design therapeutic targets for the treatment of NF1.

1.4 The Ira1 and Ira2 proteins are Homologous to Neurofibromin

In the yeast *Saccharomyces cerevisiae*, there are two NF1-like genes, *IRA1* and *IRA2*, which encode Ira1 and Ira2 proteins, respectively (Figure 1.2). Ira proteins are negative regulators of Ras1 and Ras2 proteins in yeast and were first identified as components of the adenylyl cyclase /cAMP/PKA pathway (Figure 3.1) (Toda et al., 1985). In yeast cells, Ras deletion causes cell arrest at the G0 phase due to lack of adenylyl cyclase activity (Nikawa et al., 1987; Toda et al., 1985). Hyperactivation of Ras, either by *IRA* genes deletion or expression of activated RAS alleles, activates adenylyl cyclase/cAMP/PKA pathway (Thevelein and de Winde, 1999). Constitutive Ras activation causes yeast cells to die at high temperature. However, this Ras-induced heat shock phenotype is reversed when the GAP domain of neurofibromin is expressed in *ira*-deleted yeast strains, suggesting conserved functions between Ira and neurofibromin (Ballester et al., 1990; Xu et al., 1990a; Xu et al., 1990b).

Recently, Ras was also identified as an effector for the G coupling receptor Gpr1, a glucose receptor that acts upstream of the adenylyl cyclase/cAMP/PKA pathway. Based on their findings, Harashima and coworkers proposed that Gpr1 binds to a Gα subunit Gpa2 and its Gβ-like subunits Gpb1 and Gpb2 to control adenylyl cyclase activity (Harashima and Heitman, 2002). Both Gpb1 and Gpb2 possess a kelch-repeat domain with similar WD40-like folding motifs at their C-terminal domains and unique N-terminal domains (Gettemans et al., 2003; Harashima and Heitman, 2002).

1.5 Haplo-insufficient Activity of Neurofibromin

Although a complete loss of neurofibromin function (LOH) is present in many of the tumors observed in humans with NF1, haplo-insufficiency is thought to be associated with a variety of NF1-related diseases resulting from the low *NF1* gene levels (Cichowski and Jacks, 2001; Upadhyaya et al., 1998). Current studies suggest that retaining neurofibromin activities in the haplotype stromal cells of the NF1 tumors environment are critical for normal cellular functions. The most clear evidence of neurofibromin haploid-inefficiency has been reported *Nf1*$^{+/-}$ mouse models. For example, while somatic inactivation of Nf1 in mice results in almost complete disease penetrance, approximately 10-15% of the *Nf1*$^{+/-}$ mice developed the myeloproliferative leukemia (Jacks et al., 1994; Le et al., 2004). Consistent with this view, studies of heterozygous *Nf1*$^{+/-}$ mouse models showed an increase in the activity of *Nf1*$^{+/-}$ mast cells toward Nf1-deficient Schwann cells in the Nf1 tumor environment (Yang et al., 2003; Zhu et al., 2002). Furthermore, studies have shown that the *Nf1*$^{+/-}$ mice have defects in c-Kit signaling (Dang et al., 2005; Ingram et al., 2000; Yang et al., 2003). In addition, *Nf1*$^{+/-}$ mast cells have been reported to secrete high levels of growth factors that greatly contribute to tumor formation. In the *NF1* heterozygous cells from the tumors environment, reduced neurofibromin activity dosage greatly contribute to the inflammation and enhancement of tumor development. Furthermore, a study showed that neurofibromin is downregulated in response to growth factors stimulation (Cichowski et al., 2003). Therefore, growth factors that are being secreted from the *NF1* heterozygous cells can further downregulate neurofibromin level and activity, thereby greatly increases Ras activity. These studies suggest that heterozygous *Nf1*$^{+/-}$ stromal cells play an important role in NF1 tumor development and raise the possibility of controlling tumor growth by retaining, or increasing,

neurofibromin activity in the stromal cell environment. Identification of physiological signals regulating neurofibromin could lead to strategies for regulating Ras in NF1 patients.

1.6 Known Cellular Mechanisms that Regulate Neurofibromin

Studies have shown that neurofibromin can be regulated by protein phosphorylation or ubiquitination. Positive regulation of neurofibromin can be achieved by protein phosphorylation. Mangoura et. al. showed that PKC phosphorylation of neurofibromin increased the Ras-GAP activity in response to EGF (Mangoura et al., 2006). Another study showed that neurofibromin can be phosphorylated on serine residues when IgM is crossed-linked. However, the precise kinase that is responsible for the IgM cross-linked mediated serine phosphorylations is unknown (Boyer et al., 1994).

On the other hand, evidence for negative regulation of neurofibromin has been presented. Neurofibromin can be degraded by the proteasome when cells were stimulated with growth factors that activate both G protein-coupling receptors and receptor tyrosine kinases. Although neurofibromin is ubiquitinated and degraded, the precise ubiquitin-related enzyme that is responsible for this degradation remains to be identified (Cichowski et al., 2003). Taken together, these findings suggest that neurofibromin is controlled by both protein kinases and ubiquintin-related proteins.   Therefore, identifying new protein candidates that regulate neurofibromin is crucial to advancing the understanding of NF1.

1.7 Summary

Given the remarkable conservation of neurofibromin between yeast and humans, I utilized yeast system as a genetic model to screen for genes that regulate Ira2. In addition, I utilized a proteomic approaches to identify candidate genes that interact with and directly regulate Ira2/neurofibromin functions in yeast and human cells. Ira2 and neurofibromin are large proteins with many unknown functions. Therefore, I hypothesized that identifying the associated proteins that interact with Ira2 and neurofibromin will lead to a clear understanding of neurofibromin functions.

This dissertation summarizes the results of my graduate studies. Chapter 3 summarized the genetic screen I performed to identify novel proteins regulating Ira functions. I identified the small RasGTPase Ypt7/Rab7 as a potential candidate that positively regulates Ira2/neurofibromin. However, I found that Ypt7/Rab7 regulate Ira2/neurofibromin in an indirect mechanism, possibly by induced up-regulation of upstream pathways of Ira2/neurofibromin. Chapter 4-6 described an unbiased proteomic approach I carried out to identify direct protein interacting with Ira2/neurofibromin. I showed the ubiquitin-associated proteins negatively regulate the RasGAP proteins Ira2 and neurofibromin. In yeast, Gpb1 negatively regulates and promotes Ira2 proteasomal degradation. I demonstrated that Gpb1 is required for the Rpn1 proteasome base subunit to trigger Ira2 proteolysis. In addition, I showed the deubiquitination enzyme Ubp6 interacts with Ira2 and antagonizes Gpb1-mediated degradation of Ira2. Futhermore, I found that the serine/threonine kinase CK2 binds and phosphorylates Ira2, preventing Ira2 from protein degradation. Similarly, I identified ETEA as a human ubiquitin-associated protein that negatively regulates neurofibromin levels. RNAi targeting of ETEA expression causes an upregulation of neurofibromin levels, reduces Ras activities, and

downregulates both the ERK and AKT pathways. Therefore, these data reveal critical conserved

ubiquitination pathways that regulate the RasGAP proteins Ira2 in yeast and neurofibromin in
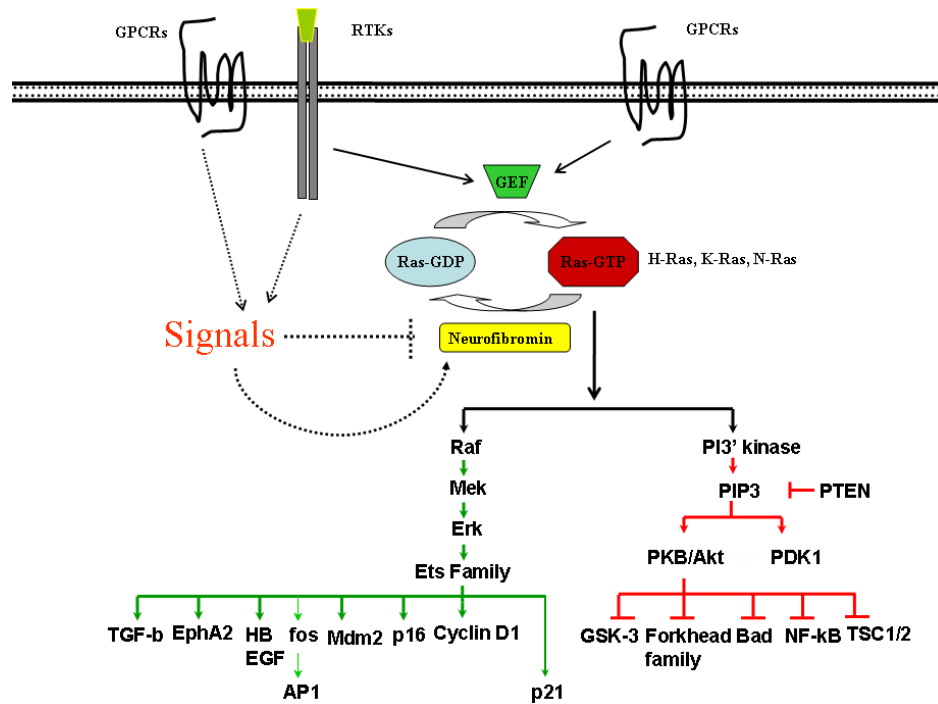
humans.

Figure 1: Neurofibromin controls Ras activity. Neurofibromin is a RasGAP protein that accelerates the hydrolysis of active RasGTP to inactive RasGDP. Mutations in the *NF1* gene lead to tumor formations in humans and in genetic models of NF1. When activated by ligands, either the receptor tyrosine kinases (RTKs) or G-coupling protein receptors (GPCRs) recruit GEFs to the plasma membranes to activate Ras proteins. RasGTP induces activation of downstream effectors, including Erk and Akt pathways that control cell division, proliferation, and growth. Neurofibromin, one of the GAP proteins, down-regulates the active RasGTP by accelerating the hydrolysis of RasGTP to RasGDP. Therefore, mutations of the NF1 gene result in constitutive activation of Ras which leads to formation of tumors in humans. Identification of molecular signals that regulate neurofibromin will be beneficial in designing new therapeutic treatments for NF1 patients (Cichowski and Jacks, 2001; Rodriguez-Viciana and McCormick, 2005b; Schubbert et al., 2007).

A.
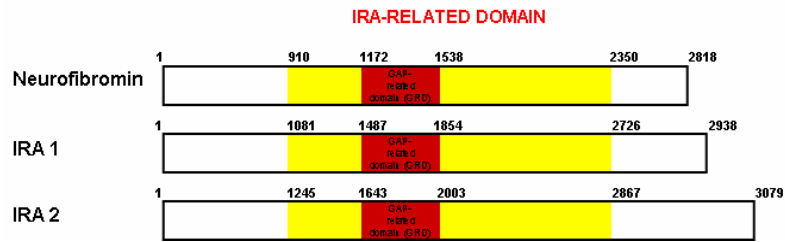
B.
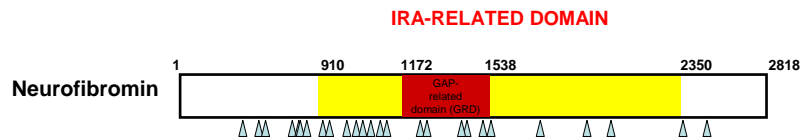
Figure 1.2: Amino acid sequences are conserved between neurofibromin, Ira1 and Ira2 proteins. (A). Neurofibromin is a RasGAP protein in human cells and Ira1 and Ira2 are the RasGAP proteins in yeast. Ira2 shares approximately 22% amino acid sequence homology to neurofibromin (Ira-related domains, yellow boxes). Importantly, the neurofibromin GAP domain consists of only 10% of the protein sequences but are conserved in the yeast Ira proteins. Furthermore, the Ras-induced phenotypes in yeast can be rescued when the neurofibromin GAP domain is introduced in the *ira*-deletion yeast mutants, suggesting that the GAP activity of these proteins is conserved (B). Mutations have been detected in humans with NF1. Triangles represent mutations in the mRNA of the *NF1* gene that lead to early mRNA gene terminations, and loss of neurofibromin function. This figure is adopted from previous publications (Cichowski and Jacks, 2001; Serra et al., 2001)

Chapter 2: Materials and Methods

2.1 Strains and Plasmids

All of the yeast strains were derived from W303a (ade2-1 ura3-1 his3-115 trp1-1 leu2-3 121can-100) except the TAP-tagged strains which were purchased from the TAP-tagged library (Open Biosystems) (Ghaemmaghami et al., 2003). The double epitope-tagged strains described in this manuscript were generated from the TAP-tagged parental strains and the second gene was epitope-tagged using the FLAG-tagged PCR based techniques previously described (Longtine et al., 1998). All plasmid constructs used in this article were generated by standard PCR-targeting techniques and cloned into GATEWAY Entry and Destination vectors (Invitrogen, Table 2.1).

2.2 Preparation of yeast and 293T whole cell extracts

Yeast cells were grown in YPD at 30°C to an OD600 of 1.0. Cells were pelleted by centrifugation and washed twice with cold 1xPBS buffer. The pellet was suspended in 500ml of lysis buffer containing 20 mM Tris-HCl, pH 7.5, 500 mM NaCl, 0.1% NP40, 50 mM NaF, 1 mM DTT, 1 mMNa3VO4 and a protease inhibitor cocktail, Complete Mini (Roche). Acid-washed glass beads were added, vortexed and disrupted in a Bead-Beater twice (2min) at 4°C. Lysates were clarified by centrifugation at 14,000 rpm in a microfuge at 4°C. Protein concentrations were determined by Bradford assay using BSA as a standard. Normalized lysates were used for Istern blotting and immunoprecipitation.

For mammalian experiments, 293T cells seeded in 6-Well dishes 24hrs prior to transiently transfection with 4μg total plasmids DNA and 10ul of Lipofectamine Reagent (Invitrogen). Cells were lysed with lysis buffer 20 mM Tris-HCl, pH 7.5, 500 mM NaCl, 0.1% NP40, 50 mM

NaF, 1 mM DTT, 1 mMNa3VO4 and a protease inhibitor cocktail, Complete Mini (Roche) and protein concentrations were determined as described above.

2.3 Yeast transformation

Yeast cells were grown in YPD at 30°C to an OD600 of 1.0. Cells were pelleted by centrifugation and washed twice with 1xPBS buffer and 2x with 0.1M LiAc. Cells were re-suspended in .1M LiAc. About 70ul of cells were added 10 μl of carrier Salmon testis DNA (20μg) pre-added with1μg of the transforming DNA plasmid. (For genomic library screen, 1ul of genomic library DNA was added 10 μl of carrier Salmon testis DNA). Samples were placed on shaker at 30^0C for 30min and heat shock at 42^0C for 20min. Cells were washed 2x with 0.1M LiAc and plated on selected medium plates. Colonies were scored three to four days later for positive transformation.

2.4 Heat shock assay

Yeast colonies were selected individually and plated onto either rich media or selected medium plates. Cells were grown in a 30^0C chamber for three to four days before being replica-plated. Relica plates were exposed to higher temperature chamber at 55^0C at various time points indicated in a given experiments. After heat exposure, plates were being removed from heat chamber and were allowed to cool down at room temperature for 30min. After cooling, the heat exposed and control plates were grown in a 30^0C chamber for three to four days before being scored for heat resistant colonies. Pictures were taken using BioRad imager.

2.5 cAMP measurement assay

cAMP assays were performed using the HitHunter cAMP detection kit purchased from DiscoverX. Yeast cells were grown in YPD at 30°C to an OD600 of 1.0. Cells were pelleted by centrifugation and washed twice with 1xPBS. Cells were disrupted by vortexing with glass beads. Proteins from samples were prepared and protein concentrations normalized. 10ug of proteins from each sample was plated in a 96-Well plate. For standard cAMP measurement, samples were diluted to generate CAMP standard curve according to manufacture procedure. Appropriate reagents provided with HitHunter cAMP kit were added into the samples for cAMP competitive binding as outlined in the assay procedure. Samples were incubated for 30-60min that would allow the color to develop. Florescent activities were detected using a florescent microreader and the amount of CAMP in each sample was calculated from the cAMP standard curve. cAMP activities were measured from four different experiments.

2.6 Chronological life span Assay

Chronological life span of either wild-type or mutant cells incubated in minimal medium containing glucose (SDC) was measured as described previously (Fabrizio et al., 2005; Fabrizio and Longo, 2003). Briefly, cells were grown in SDC containing 2% glucose with supplemented amino acids, including adenine, histidine, tryptophan, and leucine. Overnight culture was OD600 at 1.0 and diluted (1:200) into fresh SDC medium with a final volume of 20 ml. Cells were maintained at 30°C with shaking (200 rpm) to ensure proper aeration. Chronological life span was monitored in expired SDC medium by measuring colony-forming units every three

days. The number of colony-forming units at day 10 was considered to be the initial survival and used to compare to day 10 post-diauxic phase (100% survival).

2.7 DNA Micro array Analysis

Log phase cultures of wild-type or mutant cells were used to extract total RNA according to the acid phenol method. Equal total RNA concentration samples from independent cultures of each strain were used as template to synthesize complementary RNA. Protocols for generating yeast array chips were obtained from (Chu et al., 1998; DeRisi et al., 1997). cDNA samples were generated from RNA samples and the resuspended cDNA pellet from each samples were added into dried aliquot of Cy3 or Cy5 dye and mixed thoroughly. The combined Cy3 and Cy5 samples were hybridized onto pre-processed array chips obtained from Dr. DeRisi's Laboratory. The arrays were placed in a sealed, humidified, hybridization chamber. The hybridization process was carried out for 10hr in a 62°C water bath. Experiments were done over night, and the next morning arrays were washed immediately with the appropriate buffer as described (Lashkari et al., 1997). Array images were scanned on scanning laser fluorescence microscope provided by the UCSF Cancer Center Core facility. Scanned image with fluorescent spots was over-fitted onto a pre-bounding box, fitted to the size of the DNA spots on the arrays with the corresponding genes. Changes in gene expressions between samples were calculated by the provided software from UCSF Cancer Core facility and a gene list was generated for further analysis.

2.8 2-D DIGE

2-D DIGE (2-dimensional differential in gel electrophoresis) experimental services were provided by Applied Biomics (http://www.appliedbiomics.com). In brief, samples of the wild-type, ypt7- or *ypt7-/ira1*-deletion yeast strains were grown over night in rich media and were OD600 at 1.0. Cells were washed 3x with 1xPBS plus 2xH20 and sent to Applied Biomics for 2-D DIGE proteomic analysis. Protein samples with equal concentration were labeled with charge-matched, spectrally resolvable CyDye™. The three samples were labeled with the three different dyes and the proteins were resolved using one 2-D gel electrophoresis. After the 2D electrophoresis, the gel was scanned using the highly sensitive Typhoon imager. DeCyder software was used to locate the desired protein spots for mass spectrometry analysis. Changes in protein expressions between the experimental samples were detected and the protein spots of interest were excised from the gel using a fully automated Ettan Spot Picker (Applied Biomics). Protein samples were determined using LC-MS/MS mass spectrometry and the protein ID from each sample was compared to the protein data bases. The mass spectrometry analysis studies were provided as collaborations with the UCSF Mass Spectrometry Facility (http://ms-facility.ucsf.edu/).

2.9 Tandem-affinity Purification and Mass Spectrometry

Yeast cells endogenously expressing either *IRA2-TAP* or *GPB1-TAP* or 293T cells expressing the TAP-NF1 fragments (fragments 4 and 5) were used for the tandem-affinity purification experiments. The purification scheme was adapted from (Ghaemmaghami et al., 2003; Iacovides et al., 2007; Rodriguez-Viciana et al., 2006). Briefly, either yeast cell extracts from 6-10 litters

of cells grown in log phase expressing Ira2-TAP or Gpb1-TAP or total lysates from 293T stably-expressed NF1-TAP fragments (fragments 4 and 5) were incubated at 4°C with 500μl of packed IgG-conjugated glutathione resin (Amersham, Piscataway, NJ). The binding complexes were allowed to rotate at 4°C for greater then 2hrs or overnight. Resin beads were washed with washing buffer IPP150 three times. The protein complexes were cleaved with 50 units of TEV protease (Invitrogen) and 1ml of in calmodulin binding buffer. The reaction were carried out for 2hrs at room temperature and allowed to elute into a second column by gravity flow. The second round of affinity purification was performed using 400μl of calmodulin resin. The protein complexes were eluted from the IgG resin in to a second column with packed Calmodulin beads (Amersham) and contained 5ul of 1M CaCl2. At this step, samples were washed three times with calmodulin binding buffer. Protein complexes were eluted from the calmodulin resin with the calmodulin eluting buffer sequentially for seven times with 200ul the eluting buffer. Protein complexes were precipitated with DOC at a final concentration of 0.015% and TCA at 10% of final concentration. The precipitated samples were incubated on ice for 30min followed by centrifugation and protein pellets were suspended in 25ul of 1xSDS loading buffer. Protein complexes were separated by pre-cast NuPAGE gel electrophoresis (Invitrogen). After protein complexes were separated, gels were stained with SimpleBlue SafeStain Coomasie staining solution (Invitrogen) and washed with ddH20. Gels were washed overnight with ddH20 and 20% (w/v) NaCL solution. Separated protein bands were excised and digested with trypsin. Protein complexes were subjected to mass spectrometry analysis (provided by the Mass Spectrometry Core Facility at UCSF). Identified amino acid sequences were analyzed for matched protein sequences against protein database. Experimental methods for protein band sequencing analysis were described previously (Iacovides et al., 2007; Rodriguez-Viciana et al., 2006)

The following buffer solutions were adopted and modified from The Séraphin Group.

(http://www.cgm.cnrs-gif.fr/epissage/index.html)

IPP150: 10mM Tris-Cl pH8.0, 150mM NaCl, 0.1% NP40 (100mL H2O final volume)

IPP150 Calmodulin binding buffer: In 100mL H2O of IPP150 buffer, add 1mM Mg-acetate,

1mM imidazole, 2mM CaCl2, and 10mM b-mercaptoethanol.

IPP150 Calmodulin elution buffer: In 100mL H2O of IPP150 buffer, add

1mM Mg-acetate, 1mM imidazole, 2mM EGTA.

2.10 Immunoprecipitation and Immunoblotting Analysis

Total cell lysates (either yeast or 293T) were prepared in cell lysis buffer 20 mM Tris-HCl, pH

7.5, 500 mM NaCl, 0.1% NP40, 50 mM NaF, 1 mM DTT, 1 mMNa3VO4 and a protease

inhibitor cocktail, Complete Mini (Roche). After normalized protein concentrations,

approximately 300-500μg of total protein samples was immunoprecipitated with the indicated

antibodies. Sample mixtures were rotated at 4°C for 2hr. After three washes in washing buffer

buffer 20 mM Tris-HCl, pH 7.5, 500 mM NaCl, 0.1% NP40, 50 mM NaF, 1 mM DTT, 1

mMNa3VO4 and a protease inhibitor cocktail, Complete Mini (Roche), the proteins bound to

beads were released by boiling in 40μl of 1× SDS-PAGE sample buffer for 10 min. The samples

were then resolved by pre-cast NuPAGE gel electrophoresis (Invitrogen) followed by

immunoblotting analysis using the indicated antibodies.

2.11 In vitro translation

The TNT® Quick Coupled Transcription/Translation System (Promega) was used to detect *in vitro* protein-protein interactions. All experiments described here were done according to the manufacturer's instructions. The p*DEST-IRA2-V5* (fragment) and p*DEST-GPB1-GFP,* pGST-NF1 GRD, pcDNA-ETEA-V5 (wild-type or mutants) plasmids were constructed using the Invitrogen Gateway® Technology. *In vitro* [35S]methionine-labeled reactions were terminated by adding 500ul pull-down buffer 20 mM Tris-HCl, pH 7.5, 500 mM NaCl, 0.1% NP40, 50 mM NaF, 1 mM DTT, 1 mMNa3VO4 and a protease inhibitor cocktail, Complete Mini (Roche). Anti-bodies and conjugated-beads were added to the radioactive proteins matrix and immunoprecipitation was performed. The beads were washed with 1 ml of pull-down buffer for four times. The proteins bound to beads were released by boiling in 50μl of 1× SDS-PAGE sample buffer for 10min. The samples were then resolved by pre-cast PAGE electrophoresis (Invitrogen) followed by visualization with the Storm860 PhosphoImager.

2.12 In Vitro Ubiquitination of Ira2 and Neurofibromin GRD

Gpb1-TAP complexes were purified as described previously in the Tandem-affinity purification method except that the final calmodulin-binding step was omitted from the Gpb1 complex preparation**.** Ira2-Flag purification was performed similar to the immunoprecipitation steps except extra washes were performed to clear possible binding partners from Ira2. The reactions were carried out at 30°C for 1.5hrs in 50μl reaction buffer (40 mM Tris-HCl, pH 7.5, 2 mM DTT, 5 mM $MgCl_2$) containing the following components: 2 or 4μg of ubiquitin (Boston Biochem, #U-100) or 4ug of mutant ubiquitin (ubiØ), 5 mM ATP, activated 1.5ug/ml E1 and

21

20ug/ml UbcH5 complex, purified Flag-Ira2 and 200ug of TAP-cleaved Gpb1 purified protein complex as E3 sources. The reactions were terminated by adding 500ul pull-down buffer 20 mM Tris-HCl, pH 7.5, 500 mM NaCl, 0.1% NP40, 50 mM NaF, 1 mM DTT, 1 mMNa3VO4 and a protease inhibitor cocktail, Complete Mini (Roche).   After addition of 20 μl of M2 Flag agarose-conjugated beads (Sigma), the samples were rotated at 4°C for 2hrs. The beads were washed with 1 ml of pull-down buffer for four times followed by 1x PBS for three times. The proteins bound to flag-beads were released by boiling in 50ul of 1× SDS-PAGE sample buffer for 10min. The samples were then resolved by pre-cast PAGE electrophoresis (Invitrogen) followed by immunoblotting analysis using anti-His or anti-Flag antibodies.

For ubiquitin assay of neurofibromin-GRD, in vitro [35S]methionine-labeled neurofibromin-GRD was immunoprecipitated with gluthidione conjugated-sephorose beads and used as substrates. The reactions were carried out at 30°C for 1.5hrs in 50μl reaction buffer (40 mM Tris-HCl, pH 7.5, 2 mM DTT, 5 mM MgCl$_2$) containing the following components: 10μg of ubiquitin (Boston Biochem, #U-100), 5 mM ATP, activated 1.5ug/ml E1 and 20ug/ml UbcH5 complex, and 100ug of purified GFP-GST, ETEA-GFP or ETEA ΔUBX protein complex as E3 sources. The reactions were terminated by adding 500ul pull-down buffer 20 mM Tris-HCl, pH 7.5, 500 mM NaCl, 0.1% NP40, 50 mM NaF, 1 mM DTT, 1 mMNa3VO4 and a protease inhibitor cocktail, Complete Mini (Roche). Samples were immunoprecipitated with sepharose conjugated glutathione beads at 4°C for 2hrs. The beads were washed with 1 ml of buffer for four times followed by 1x PBS for three times. The [35S]methionine-labeled neurofibromin-GRD complexes were released by boiling in 50μl of 1× SDS-PAGE sample buffer for 10min. The samples were resolved by pre-cast PAGE electrophoresis (Invitrogen), followed by visualizition by Storm860 PhosphoImager after 24hrs of exposures.

2.13 Cycloheximide Chase Experiments

To examine the effect of Gpb1 on Ira2 stability, exponentially growing wild-type or *gpb1*-deleted (*GPB1Δ*) yeast strains were treated with cycloheximide at a final concentration of 50 mg/ml to inhibit *de novo* protein synthesis. At the time points indicated, cells were collected and washed. Total cell extracts were prepared and protein concentration was determined. Samples with equal protein concentration (20ug/sample) were analyzed by immunoblotting (WB) for Ira2 and Gpb1 with anti-Flag or anti-TAP antibodies. To examine the effect of ETEA or ETEA ΔUBX on neurofibromin stability, 293T cells were treated with cycloheximide at a final concentration of 150ug/ml. Samples were terminated at 0, 4, 8, 12, 15 hr time points as indicated. Protein concentration was normalized and 10ug of total protein from each sample were immunoblotted with anti-neurofibromin, anti-GFP, anti-V5, and anti-actin antibodies.

2.14 ShRNA Stable Cell Lines

293T or BT459 cells seeded in 6-Well dishes 24hrs prior to transiently transfection with 4μg of total ShRNA DNA plasmids with 10ul of Lipofectamine Reagent (Invitrogen). The three human pSM2 retroviral shRNAmir plasmids targeting *ETEA* (Clone ID: V2HS_80576, V2HS_80578, V2HS_80580) were purchased from Open Biosystems. In order to generate stable cell lines expressing the shRNA plasmids, 48-72hrs after transfections, cells were replated in DMEM (10%FBS) plus 1μg/ml puromycin for +10days for drug selection to kwell off cells that did not receive the shRNA plasmids. Cells line designated CP (control plasmid), Sh576 (V2HS_80576), Sh578 (V2HS_80578), and Sh580 (V2HS_80580) were generated and used for experiments described in this article.

2.15 RasGTP Detection

Total cellular extracts with equal protein concentration were prepared and used for immunoprecipitation with the GST-fused Ras binding domain conjugated glutathione resin (the GST-fused Ras binding domain is from the Raf1 kinase that preferentially binds to RasGTP). Experimental procedures were previously described (Rodriguez-Viciana et al., 2006). For yeast RasGTP pull-down experiments, membranes were immunoblotted with anti-Ras2 antibody (Santa Cruz Biotechnologies). For RasGTP pull-downed experiments in 293T cells, the panRAS antibody was used to determine RasGTP levels (BD Biosciences).

2.16 Reagents and Antibodies

MG132 was from Calbiochem; Anti-Flag M2 (unconjugated) and anti-Flag M2 conjugated beads were from Sigma; Anti- Ydj1 (sc-23749), anti-NF1 (sc-67), anti-GFP (sc-8334), anti-HA (sc-805), anti-p120GAP, anti-acting, and anti-RAS2 were from Santa Cruz Biotechnology; anti-ubiquitin antibodies were either from Zymed or Abcam; anti-V5 was from Abcam; anti-Ras (panRas) and anti-p120GAP were from BD Biosciences; anti-ERK , anti-phospho-ERK, anti-AKT, anti-phospho-AKT, anit-phospho SER/Thre were from Cell Signaling Technologies. Recombinant ubiquitin proteins were from Boston Biochem.

Table 2.1 List of Gateway Entry/Destination and shRNA Vectors

Gateway® entry vectors		ORFs
pDONR™221		Gpb1
pDONR™221		Gpb1 AB
pDONR™221		Gpb1 BC
pDONR™221		Gpb1 A
pDONR™221		Gpb1 B
pDONR™221		GPb1 C
pDONR™221		Gpb2
pDONR™221		Ira2-C
pDONR™221		CK2
pDONR™221		CK2R165A
pDONR™221		CK2D166A
pDONR™221		CK2K169A
pDONR™221		Rpn1L830A
pDONR™221		Rpn1L831A
pDONR™221		Rpn1R832A
pDONR™221		Rpn1
pDONR™221		Upb6
pDONR™221		Upb15
pDONR™221		ETEA (UBXD8)
pDONR™221		ETEA Fragments
pENTR3C		NF1 Fragments (1-8)
pENTR3C		RAB7 WT
pENTR3C		RAB7 DN
pENTR3C		RAB7 L
Gateway® destination vec	**Promote**	**Epitope-Tagged**
pYES2-DEST52	GAL1	V5-6xHIS
pET-DEST42	T7	6xHIS
pcDNA-DEST47	CMV; T7	GFP
pDEST™24.	T7	GST
	CMV	Flag
	CMV	GFP
	CMV	TAP
	CMV	HA
UXBD8 ShRNA plasmids		Sh576
		Sh578
		Sh580

The entry vectors (pDONR221 and pENTR3C) were purchased from Invitrogen. I cloned the ORFs of the understudied genes into the entry vectors by utilizing PCR based technology and the BP Gateway cloning kits (Invitrogen). After BP ligations, plasmids were digested with restriction enzymes and gene sequencing to identify non-mutated clones. The corrected clones were recombined into destination vectors that contained the appropriate epitope-tagged for gene expressions. All the cloning experimental procedures were adapted from Invitogen cloning manual protocols.

Tandem Affinity Purification (TAP) strategy
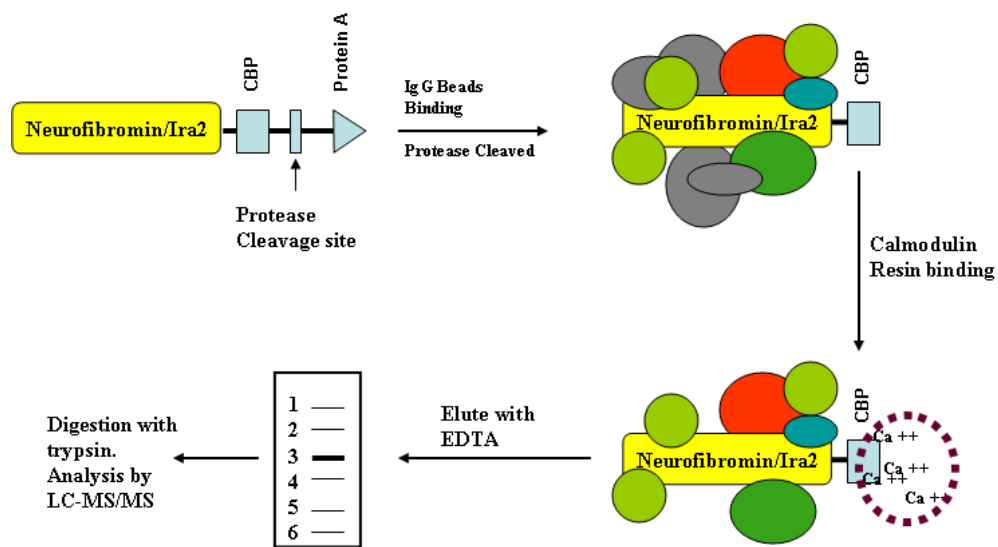
Figure 2.1: Identification of the Neurofibromin/Ira2 and Gpb1 protein complexes. The
Ira2-TAP or Gpb1-TAP protein complexes were purified from the *IRA2-TAP* yeast strain.
Neurofibromin fragments were cloned into the NTAP-gateway vector and the neurofibromin-
TAP complexes were purified from 293T cells. The experimental procedures and figures were
adapted from previous publications (Angers et al., 2006; Iacovides et al., 2007)

Chapter 3: Identify Candidate Genes Regulate Ira2 Functions

3.1 Background

Neurofibromin is a large protein with many unknown functions. The GAP domain represents approximately10% of the neurofibromin protein. In addition, mutations flanking the GAP domain have been detected in patients with NF1 (Serra et al., 2001). Patients with NF1 suffered diverse genetic diseases, and in many cases, involved Ras dysregulations. However, Ras-independent pathways have been suggested to cause disease development in humans with NF1, and in genetic models of NF1.

In the yeast *S. cerevisae*, there are two neurofibromin-like genes, *IRA1* and *IRA2*, which encode Ira1 and Ira2 proteins, respectively. Similar to human neurofibromin, Ira proteins are negative regulators of Ras1 and Ras2 proteins in yeast. The Ras proteins in *S. cerevisae* were first identified as components of the cAMP pathway (Toda et al., 1985). Loss of Ras activity in yeast causes cell arrest at G0 of the cell cycle caused by reduction of adenylyl cyclase activity. Inactivation of Ira proteins or expression of activated *RAS* alleles causes hyper-activation of the cAMP/PKA pathway (Figure 3.1). The *Ira*-deletion yeast strains suffer heat shock sensitivity caused by hyperactive Ras. Surprisingly, the neurofibromin GAP domain can rescue the deficiency of Ira activity in yeast (Ballester et al., 1990; Xu et al., 1990a; Xu et al., 1990b).

Given the conservation between neurofibromin in humans and Ira2 in yeast cells, I utilized yeast genetics to identify new gene candidates that can upregulate Ira2 activity. I employed a genetic screen to identify genes that when transformed into an *ira1*-deletion mutant strain (*ira1Δ IRA2*) can rescue its temperature sensitive phenotype. Working on the hypothesis that Ira senses other molecular signals to down-regulate Ras, I wished to identify gene candidates that can upregulate Ira2 activity to down-regulate Ras.

3.2 Objectives

Neurofibromatosis type 1 gene encodes the tumor suppressor protein, neurofibromin. Neurofibromin negatively regulates Ras signaling pathways by accelerating the hydrolysis of the active form, RasGTP, to the inactive form, RasGDP. Thus, loss of neurofibromin results in hyperactive Ras signaling. However, neurofibromin is a large protein with few known functions. Studies that seek to understand the molecular functions of neurofibromin are important in the prevention and treatment of this disease.

In a genetic study to identify genes that when over-expressed interact with Ira2 protein, a yeast homolog of neurofibromin, to suppress hyperactive Ras2 activity, I have isolated the Ypt7 protein as a candidate that acts upstream of the Ras2 signaling pathways. Over-expression of Ypt7 suppresses Ras2 activity in an ira-deletion yeast strains. Ypt7 over-expression fails to rescue heat shock phenotype of mutant yeast strains that have permanent constitutive activation of Ras (*Ras2^{V19}, ira1Δ ira2Δ*), or constitutive activation of adenylyl cyclase (*ras1Δ ras2Δ cyr1*mut). These observations suggest that Ypt7 acts upstream of Ira proteins and is able to suppress Ras activity in an *ira*-dependent mechanisms. This chapter explains the steps taken to identify Ypt7 as a candidate that positively regulates Ira2 functions in yeast and neurofibromin in human cells.

3.3 Results

Ypt7 functions upstream of Ras

I designed a genetic screen to identify genes that when overexpressed in the haploid yeast strain *ira1Δ IRA2* can suppress hyperactive Ras2 activity (Figure 3.2). I have systematically screened more than 5000 independent yeast colonies from a genomic yeast library and identified more than 200 heat shock resistant colonies. These positive colonies contained genes that might act either in the Ras signaling pathway or in parallel to suppress hyperactive Ras2 signaling. Among these are known genes that have been reported in the literature to signal downstream of Ras. Further epistasis genetic and genomic sequencing experiments reveal that about 5% of the 200 positive colonies (~0.2% of total colonies screened) contain genes that might function upstream of Ras by upregulating Ira2 activity (Figure 3.2).

I found that the heat resistant clone #11 contains the *YPT7* gene that potentially of an interest for further analysis (Figure 3.3). Ypt7 is a small GTPase protein that regulates protein localization. I observed that Ypt7 over-expression results in suppression of heat shock sensitivity in the *ira1Δ* or the *ira2Δ* yeast strains (Figure 3.4). Over-expression of Ypt7 suppresses the heat shock phenotypes of the *ira1Δ* or *ira2Δ* mutant strains but does not suppress the heat shock phenotype of the double mutant *ira1Δ ira2Δ* strain. This suggests that Ypt7 functions upstream of Ira proteins. Furthermore, epistasis genetic studies suggest that Ypt7 acts upstream of Ira to regulate Ras activity. If Ypt7 acts down-stream of Ras, then over-expression of Ypt7 in the *ira1Δ ira2Δ* mutant strain would interfere with adenylyl cyclase activity. This would rescue the temperature sensitive phenotype in the *ira1Δ ira2Δ* mutant strain. However, I found that over-expression of Ypt7 rescues both the *ira1Δ IRA2* and *IRA1 ira2Δ* yeast strains but not *ira1Δ ira2Δ*, hyperactive Ras^{V19}, or hyperactive adenylyl cyclase

mutant yeast strains (Figure 3.4). These data suggest that Ypt7 is signaling upstream of Ira and Ras signaling and positively regulates Ira1 and Ira2 activities.

Ypt7 over-expression suppresses Ras activity

The Ras2/PKA signaling pathway has been shown to regulate longevity in yeast. Increase life span in yeast is achieved by the suppression of Ras2/PKA pathway. Cells that have decreased Ras2 or the adenylyl cyclase activity double their life spans when compared to wild type cells (Fabrizio and Longo, 2003; Fabrizio et al., 2001). These mutant cells have activation in pathways that induce resistance to stress environments such as starvation, severe temperature environments and oxidative damages. Since over-expression of Ypt7 increases Ira2 activity, I hypothesized that over-expression of Ypt7 will suppress Ras activity and increases cell survival in yeast.

The Ras2/PKA signaling pathway is involved in nutrient signaling in yeast. Hyperactive Ras signaling in yeast results in failure to store glycogen as an energy source. When yeast cells are grown in limited nutrient medium, they will either enter a high metabolism post-diauxic phase or a low metabolism stationary phase (Fabrizio and Longo, 2003). Yeast cells with hyperactive Ras will fail to arrest at G1 when entering diauxic phase and thus will have an increase in mortality.

To determine whether increased Ypt7 activity will activate Ira2, and down-regulates Ras activity, I utilized the longevity assay as a read-out. This assay has been previously described (Fabrizio and Longo, 2003). I observed that Ypt7 over-expression in wild type yeast strain increases its life span when compared to wild strain received the control plasmid (Figure 3.6). Over-expression of the plasmid #11 (obtained from the genetic screen), or Ira1 in wild-type cells

31

caused an increase in mortality. In contrast, the *ypt7*-deletion strain has decreased mortality comparable to that of the wild-type or the *CYR1^{mut}* mutant, which has an active adenylyl cyclase gene. As expected, the *ira1*-deletion yeast strain has a decreased life span, greater than both the wild-type and *ypt7*-deletion strains. These data suggest that decreased mortality is dependent on activation of the Ras similar to previously reported by Fabrizio et al. (Fabrizio et al., 2001). Furthermore, *ypt7*-deletion strain has similar life span to wild type yeast strain. This result is inconsistent with previous observations that both the cAMP and RasGTP levels were very high in these mutants. I was expected to observe that the *ypt7*-deletion strain would die quicker when compared to *ira1*-deletion strain. However, I did not observe such results. This data suggest that the *ypt7*-deletion strain might cause activation in pathways that were able to suppress Ras signaling.

Rab7 over-expression increases neurofibromin protein levels

Ypt7 is a member of the Ras super-family of small GTPases and is known to regulate vesicle transport of late endosomes and lysosomes (Echard et al., 1998; Haas et al., 1995; Wichmann et al., 1992). From the genetic screen, I have observed that over-expression of Ypt7 rescues the hyperactive Ras2-induced heat shock phenotype in yeast cells. To investigate whether over-expression of the ypt7 mammalian homolog, Rab7, would increase neurofibromin levels, I cloned and over-expressed Rab7 in 293T cells. Western blotting analysis was performed to determine the neurofibromin protein levels.

Figure 3.11 shows increased neurofibromin protein levels when Rab7 is over-expressed in 293T cells. This increase is specifically for neurofibromin and not p120RasGAP, which is known to

down-regulate RasGTP activity similar to neurofibromin. Furthermore, I did not detect any changes in the neurofibromin 2 levels as well as changes in total Ras. Previous study by Cichowski et al has shown that neurofibromin is regulated via an unknown proteolysis pathway when cells are stimulated with EGF, PDGF or G-coupling protein receptor ligands. (Cichowski et al., 2003). To test whether EGF could change the dynamic of Rab7-induced neurofibromin up-regulation, I over-expressed Rab7 in 293T cells and stimulated the cells with EGF. Figure 3.8 shows that EGF stimulation further increases neurofibromin levels compared to Rab7 over-expression alone. Importantly, EGF stimulation did not result in down regulation of neurofibromin levels as observed previously (Cichowski et al., 2003). From these observations, I conclude that over-expression of Rab7 results in increased neurofibromin protein levels. This is what I also observed in yeast, where Ypt7 over-expression suppresses the heat shock sensitive phenotype in yeast by increasing Ira2 protein levels (Figure 3.5).

To investigate whether siRNA oligos targeting *RAB7* expression could activate Ras, 293T cells were transfected with siRNA to knockdown *RAB7*. Cells were transfected with control or siRNA oligos targeting *RAB7*. After 24hrs or 48hrs of oligos transfections, cells were collected to detect Ras and Erk activities (Figure 3.12). For controls, cells were plated in serum free MEM media and stimulated with 5% FBS to detect Ras and Erk activities as indicated. I found that targeted knock-down of *RAB7*expresssion resulted in an increase of RasGTP and phosphor-ERK levels. Although I failed to observed neurofibromin protein levels due to technical difficulty, the data from the previous experiments suggested that Rab7 acts upstream of Ras to regulate Ras activity.

Loss of Ypt7 function results in activation of Ras

Over-expression of Ypt7 decreases hyperactive Ras levels in *ira*-deletion yeast strains, I hypothesized that deletion of YPT7 in these strains would further increase the temperature sensitive phenotypes. To characterize the epistasis relationships of *YPT7* and *IRA*, I performed *YPT7* gene deletion in the *ira1Δ, ira2Δ, or ira1Δ ira2Δ* yeast strains to map out the genetic relationships between *YPT7*, *IRA2* and *RAS*.

If Ypt7 interact with Ira to regulate Ras2, then deletion of YPT7 alone might have an effect on Ras2. This mutant strain should be heat shock sensitive with similar phenotypes to the Ira-deletion strains. Interestingly, I found that deletion of ypt7 alone does not induced heat shock sensitivity. Figure 3.4 shows that the *ypt7Δ* mutant does not have heat shock phenotype compared to wild-type control or the *ira1Δ* and *ira2Δ* mutants. The *ira1Δ ypt7Δ* mutant cells were more heat sensitive when compared to the *ira1Δ* mutant cells. Furthermore, mutant cells that have either *ira1Δ ypt7Δ IRA2* or *ira2Δ ypt7Δ IRA1* genotypes are more heat sensitive compare to the *ypt7Δ* mutant or wild-type control.

If over-expression of Ypt7 up-regulate Ira levels, then loss of Ypt7 will result in increased RasGTP levels. To test whether the *ypt7Δ* mutant activate Ras signaling, I performed RasGTP pull-down assays to measure active Ras protein levels in these mutant yeast strains. I utilized the GST-Ras-Binding-Domain of Raf to immunoprecipitate Ras2-GTP as previously described (Rodriguez-Viciana and McCormick, 2005a). Western blot analysis of the different yeast strains shows that Ras2-GTP levels were increased in the *ypt7Δ* mutant (Figure 3.8). I found that deletion of *ypt7* greatly increases Ras activity compared to either *ira1*- or *ira2*-deletion strains alone. Furthermore, the double mutant *ira1Δ ypt7Δ* and *ira2Δ ypt7Δ* have greater RasGTP levels

compared to the *ira1Δ* and *ira2Δ* mutants. Surprisingly, the triple mutant *ira1Δ ira2Δ ypt7Δ*

shows further increased in RasGTP levels. These data suggest that *ypt7*-deletion strain has

dysregulation in Ras signaling that might be synergized with the Ras dysregulation in the *ira1*-

and *ira2*-deleted strains (Figure 3.8, lanes 7, 8 and 9).

In yeast cells, Ras2 activation causes increased cAMP levels, which activates PKA pathway. To

investigate whether *ypt7Δ* deletion in yeast strains would increase cAMP levels, I measured

cAMP concentrations in the different mutant strains described in Figure 3.4. Protein lysates

from different mutant strains were normalized and subjected to cAMP measurements as

described in the experimental procedures (Chapter 2). I found that the *ypt7Δ* has elevated cAMP

levels, interestingly, with greater cAMP levels compared to the *ira1Δ ira2* double mutant. These

data are inconsistent with the RasGTP levels measured in these two strains described in Figure

3.4, lanes 8 and 9. Furthermore, the cAMP levels in the double *ira2Δ ypt7Δ* mutant were much

greater when compared to the cAMP levels in the *CYR1^{mut}* mutant, which has an active adenylyl

cyclase gene. Loss of *YPT7* in yeast results in increasing Ras2GTP levels. However, *ypt7*-

deletion strain is not heat shock sensitive. One explanation is that *ypt7*-deletion results in

activation of stress responsive genes, which suppresses Ras2GTP induced heat shock phenotype.

Increases in stress responsive genes will result in heat shock resistant in cells. However, this

stressed suppression is overcome when one or both of the *IRA* genes are deleted (Figure 3.4).

Ras signaling pathways in mammalian cells are complex and involved multiple downstream

pathways. Different signaling can be achieved by increasing amounts of RasGTP levels as well

as binding of different Ras effectors to the active RasGTP to facilitate downstream signals. Thus,

the same mechanism of Ras activations can be achieved in yeast.   Depending on the levels of

Ras2GTP activations or which upstream signals Ras2GTP has received its signals from, or which effectors the Ras2GTP binds to, will a particular downstream pathway get activated. Supporting this argument is the observation that activation of Ras2 pathways through the PHO36 membrane receptor results in necrosis and cell death, as well as activation of genes that are known to induce stress resistance (Narasimhan et al., 2005).

Since *ypt7*-deletion strain has hyperactive Ras and heat-resistant phenotype, I hypothesized that the *ypt7*-deletion induced stress resistant genes to suppress heat shock phenotype. To test this hypothesis, I transformed the hyperactive $RAS2^{v19}$ plasmid into *ypt7*-deletion yeast strain and determined whether this mutant strain could suppress $RAS2^{v19}$-induced heat shock phenotype. Previous experiments have shown that wild type yeast strains when transformed with the mutant $RAS2^{v19}$ are heat shock sensitive (Toda et al., 1985).

As expected, wild-type cells transformed with the mutant $RAS2^{v19}$ results in heat shock sensitivity (Figure 3.10, Lane 3). However, *ypt7*-deletion yeast strain was resistant to $RAS2^{v19}$–induced heat shock phenotype (Figure 3.10, Lanes 1 and 2). This result supports the hypothesis that Ras activation in the *ypt7*-deletion yeast strain activates pathways that are able to suppress the heat shock response causes by loss of ypt7 function activation.

ypt7-deletion induces activation of aomplex signaling pathways

To investigate mechanisms that control *ypt7*-deletion yeast strain resistant to hyperactive Ras-induced heat shock phenotype, I utilized micro array and proteomic approaches to compare gene changes between wild-type and ypt7-deleted strains.

Figure 3.13 shows genomic analysis of changes in gene expressions of wild-type and *ypt7Δ* yeast strains. I compared the total cDNA samples from wild-type (green) and *ypt7Δ* (red) using the pre-processed micro array chips obtained from Dr. DeRisi (DeRisi et al., 1997). Red spots represent gene populations that were only expressed in the mutant cells. Green spots represent gene populations that were only expressed in wild-type cells. Yellow spots represent gene populations that were expressed in both strains. I used the accompanied software provided by the UCSF Core Facility to analyze the gene expression changes.

In addition to micro array analysis, I also utilized proteomic approach to analyze changes in protein expressions of the wild-type and *ypt7Δ*, or wild-type and *ypt7Δ ira1Δ* yeast strains. To obtain the final changes in the protein identification, protein samples with equal concentration were pre-mixed with the different dyes wild-type (green), *ypt7Δ* (red), or *ypt7Δ ira1Δ* (red). Samples were analyzed on 2D gel electrophoresis and protein spots were compared to detect changes in protein expressions (Figure 3.14). I was interested in protein spots that were up-regulated in ypt7-deleted cells (red spots) or down-regulated (green spots). I excluded any yellow spots because these are proteins that expressed equally in both strains. The picked protein spots of interests were subjected to mass spectrometry analysis (2D protein labeling and spots picking were performed by J. Shen (Applied Biomics). Mass Spectrometry analysis was performed at the UCSF Mass Spectrometry core facility). The results from Figure 3.13 and 3.14 showed complex protein changes in the *ypt7*-deleted yeast strain. Table 3.1 summarized protein candidates that were upregulated or downregulated in the *ypt7*-deleted yeast strain. Based on the results, I concluded that Ypt7 likely regulates Ira2 activity in an indirect pathway.

3.4 Discussion

I have utilized genetic approaches to identify genes that regulate Ira2 and neurofirbomin. I have identified Ypt7 as a candidate that regulates Ira proteins. Ypt7 is a Ras-related GTPase that belongs to the Ras super-family (Bourne et al., 1991; Colicelli, 2004; Houlden et al., 2004). This protein is highly conserved between mammalian and yeast cells (65% homology between yeast Ypt7 and human Rab7). Over-expression of Ypt7 in the *ira1Δ IRA2* yeast strain rescues its temperature sensitive phenotype. Further epistatic genetic experiments suggest that Ypt7 acts upstream of Ira and Ras proteins. Ypt7 is known to be involved in vesicle transport between late endosomes and lysomomes. However, its roles in cellular functions are not fully understood. Recently, Edinger and coworkers have suggested that dominant-negative Rab7 (Rab7T22N) can regulate nutrient receptors turn over in mammalian cells. Furthermore, Rab7T22N can cooperate with E1A to promote transformation in p53 null mouse embryonic fibroblasts (Edinger et al., 2003). Mutations in Rab7 have been identified in patients suffering from neuropathy diseases (Houlden et al., 2004; Verhoeven et al., 2003). Genetic studies in yeast suggest that *YPT7* is a non-essential gene, although there might be redundancy of the *YPT* gene family functions in yeast (Echard et al., 1998; Haas et al., 1995; Wichmann et al., 1992). Based on the remarkable degree of conservation between Ypt7 and Rab7, it seems likely that this protein has important roles in regulating cellular signaling.

I found that over-expression of Ypt7 upregulates Ira2 function. Ypt7 expression suppresses the heat shock phenotypes of the *ira1*- and *ira2*-deletion yeast strains. However, further functional studies suggested that Ypt7 positive regulation of Ira2 might be resulted from many complex and indirect mechanisms. Although we found expression of Ypt7 increases Ira2 protein levels, and expression of Rab7 increases neurofibromin levels, deletion of Ypt7 resulted in an increase of

RasGTP levels but *ypt7*-deletion cells does not have heat shock phenotype. Further genetic and proteomic data analysis showed that the *ypt7*-deletion mutants have many changes in gene expressions when compared to wild-type cells. These observations fit with the hypothesis that deletion of ypt7 results in complex gene changes and might not fit with the previously predicted one gene-one pathway hypothesis. *Ypt7*-deletion results in changes in a wide range of gene classifications, including membrane proteins, proteasomal proteins and transcription factors (Table 3.1 and Figure 3.14). Undoubtedly, dysregulation of pathways that required the functions of these proteins would result in complex signaling pathway activation, including pathways that were able to suppress the mutant Ras^{V19}-induced heat shock phenotype observed in Figure 3.10. Therefore, I decided to discontinue Ypt7 functional studies in association with Ira2 because of the indirect activity. Instead, I utilized the TAP-tagged purification approach to identify protein candidates that directly interact with Ira2 and neurofibromin to study their functional interactions.
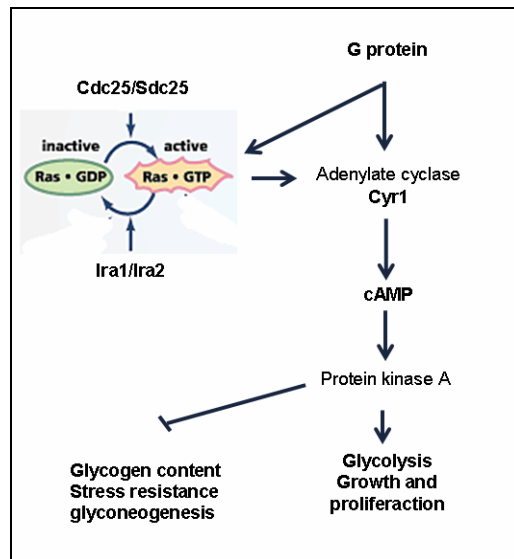
Figure 3.1: **A model of Ras2p signaling in yeast.** RasGTPase signals down-stream of the yeast nutrient pathway, including the G-coupling protein receptor Gpr1. The GEF protein Cdc25 converts RasGDP for RasGTP. Ira1 and Ira2 proteins are GAPs proteins that accelerate the hydrolysis of active RasGTP or RasGDP. Loss of functions of Ira1 and Ira2 proteins result in activation of the Ras2 pathway. Ras2 activates andenylyl cyclase, increases cAMP concentration and activates the PKA protein kinase (Thevelein and de Winde, 1999).
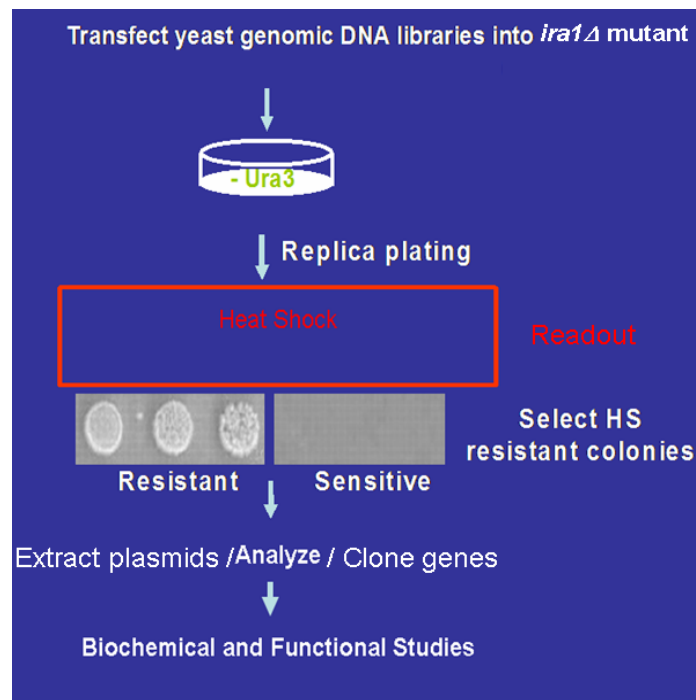
Figure 3.2: A flowchart demonstrates the steps that were taken to select positive clones containing potential candidate genes that positively regulate Ira2 activity. (Step 1): A yeast genomic library was introduced into a haploid *ira1*-deletion yeast strain (*ira1Δ IRA2*). This mutant yeast strain does not survive the high temperature environment that caused by hyperactive Ras2. I hypothesized that over-expression of candidate genes in the library will provide clones that should upregulate Ira2 activity to reverse the heat shock phenotype in the *ira1Δ IRA2* mutant. (Step2): To select for genes that function upstream of Ira2, plasmids from the heat shock resistant colonies from (Step1) will be cloned, and re-expressed in the double *ira1Δ ira2Δ* mutant to determent the Ira2-dependent mechanism. Potential and interesting heat resistant genes that passed the Step2 screen will further be investigated and studied.
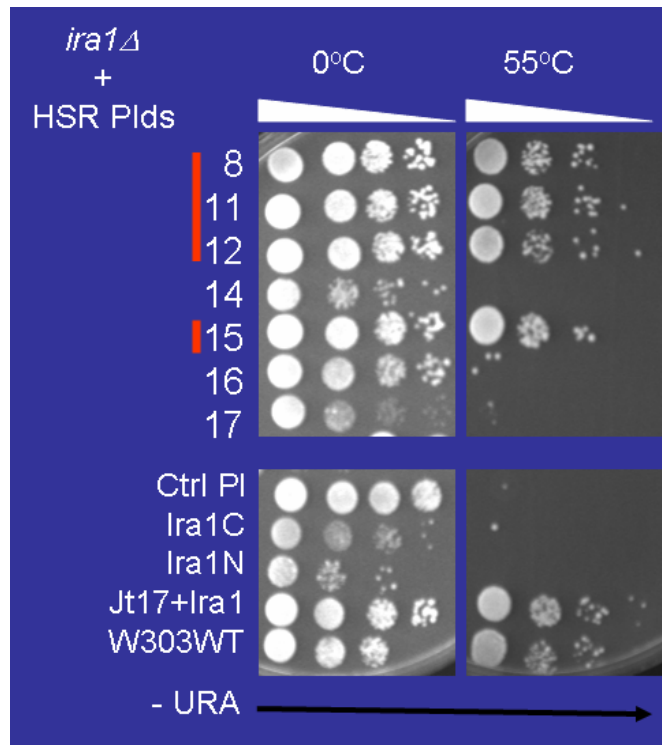
Figure 3.3: Photograph of scored positive colonies that are resistant to heat shock experiments. Colonies numbered 8, 11, 12 and 15 likely contained genes of interest. Colonies have been selected and subjected to a second screen. Yeast cells were plated in serial dilutions 1:1000 and either un-exposed or exposed in a 55°C chamber for 75 minutes. Controls are shown on the bottom half of the figure.

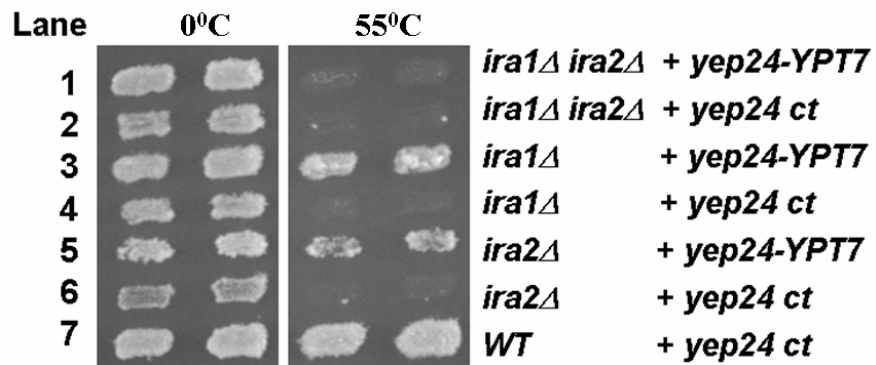| Lane	0°C	55°C	
1			*ira1Δ ira2Δ* + yep24-YPT7
2			*ira1Δ ira2Δ* + yep24 ct
3			*ira1Δ* + yep24-YPT7
4			*ira1Δ* + yep24 ct
5			*ira2Δ* + yep24-YPT7
6			*ira2Δ* + yep24 ct
7			WT + yep24 ct

Figure 3.4: Ypt7 over-expression suppressed the *ira1Δ* and the *ira2Δ* mutant heat shock phenotypes. Either yep24 control (CT) or yep24-*YPT7* plasmids were transformed in the *ira1Δ ira2Δ, ira1Δ, ira2Δ* yeast strains. Single colonies were spotted onto –URA3 plates and replica plated before being exposed to 55°C heat chamber at the different time points indicated. After the heat shock assays, cells were growing at 30°C for 2-3days. Over-expression of Ypt7 suppresses the heat shock phenotypes of the *ira1Δ* or *ira2Δ* mutant strains but does not suppress the heat shock phenotype of the double mutant *ira1Δ ira2Δ* strain. This suggests that Ypt7 functions upstream of Ira proteins.
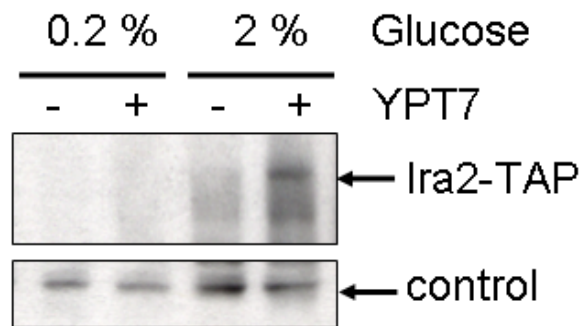
Figure 3.5: Over-expression of Ypt7 increases Ira2 protein levels in yeast cells. Cells were grown overnight with control or Ypt7 plasmids and total lysates with equal concentration were subjected to western blotting. Over-expression of Ypt7 increases Ira2 protein levels at 2% glucose concentration. Ira2 protein levels could not be detected at low glucose concentration (.2%). Membranes were immunoblotted with anti-TAP antibody and loading controls were blotted with anti-Ras2 antibody (control).
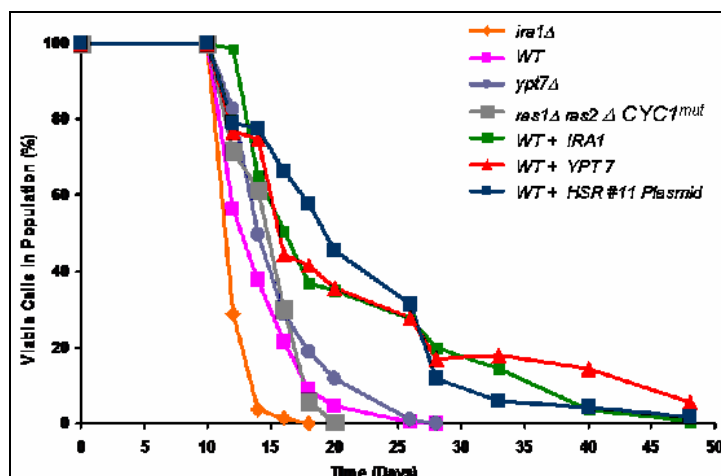
Figure 3.6: Ypt7 over expression increases longevity in yeast. The different yeast strains were grown in synthetic complete (SC) medium in the presence of glucose as previously described (Fabrizio and Longo, 2003). The experiments were performed in the same SC medium to eliminate any possible variation in cell growth condition. For each indicated time point, the same volume of cells was taken out from the population and grew in rich agar medium plates (-URA3) to recover survival cells. Colonies were counted three days after the recovery period and the percentage of viable cells were calculated and compared to day 10 post-diauxic phases (100% viable cells).
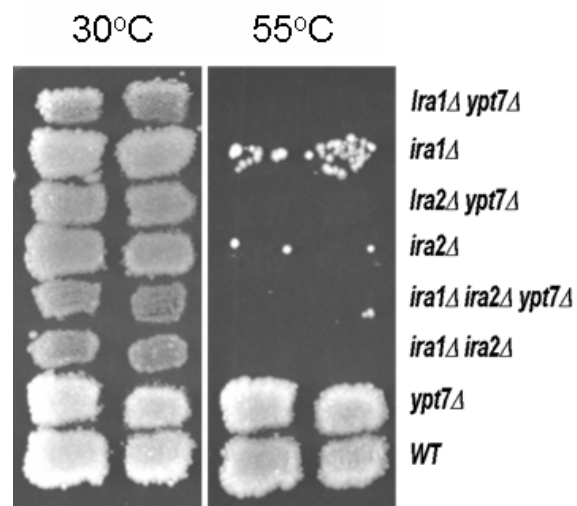
Figure 3.7: Heat shock assays of the different mutant yeast strains: *ira1Δ ypt7Δ, ira1Δ, ira2Δ ypt7Δ, ira2Δ, ira1Δ ira2Δ ypt7Δ, ira1Δ ira2Δ, ypt7Δ* or wild-type (WT). Cells were plated and replica plated on rich medium plates and exposed to 55°C at different time points indicated. After heat shock assays, cells were growing at 30°C for 2-3days. Interestingly, the *ypt7Δ* mutant strain does not have the heat shock phenotype. The *ira1Δ ypt7Δ* cells were more heat sensitive when compared to the *ira1Δ* mutant cells.
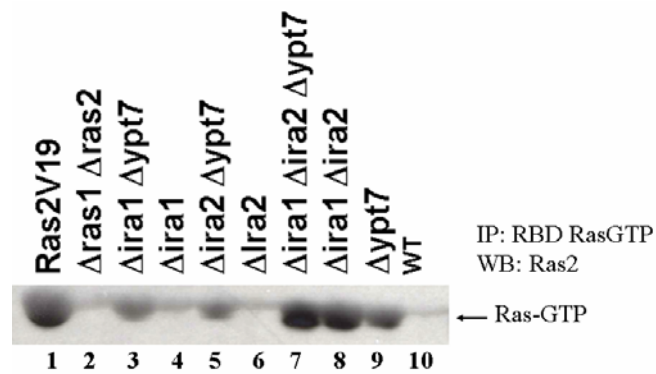
Figure 3.8: Western blot analysis of the different yeast strains was performed to determine the Ras2-GTP levels. The active Ras mutant, *RAS2^{v19}* was used as a positive control. This mutant strain has constitutively activation of Ras2. The F1D, which has both RAS1 and RAS2 genes deleted, was used as negative control. RasGTP was immunoprecipitated (IP) from total protein lysates with equal concentration. Membrane was immunoblotted (WB) with anti-Ras2 antibody.
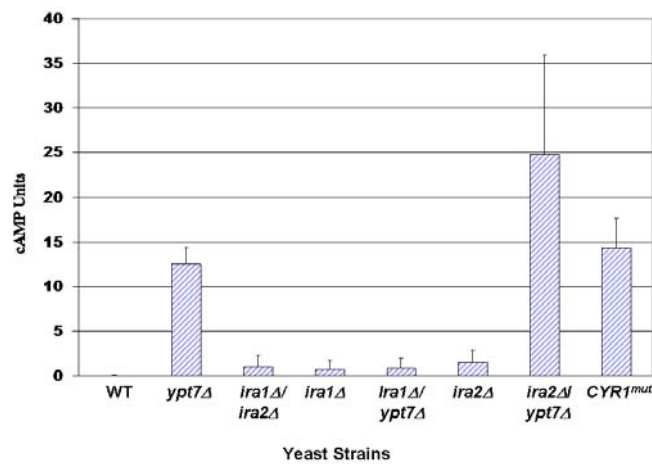
Figure 3.9: cAMP levels were measured in either wild-type or mutant yeast strains as indicated. Yp7-deletion yeast strain has elevated cAMP levels, interestingly, with greater cAMP levels compared to the *ira1Δ ira2* double mutant. Furthermore, the cAMP levels in the double *ira2Δ ypt7Δ* mutant were greater to the cAMP levels in the *ira7Δ, ira1Δ ira2, ira1Δ, ira1 ypt7Δ,* and *ira1Δ* mutants. The *CYR1^{mut}* is a mutant that has an active adenylyl cyclase gene.

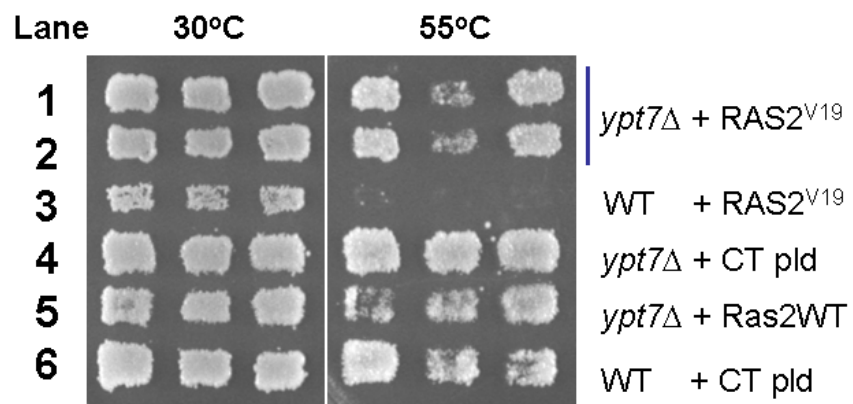| Lane	30°C			55°C			
1							*ypt7Δ* + RAS2^{V19}
2							
3							WT + RAS2^{V19}
4							*ypt7Δ* + CT pld
5							*ypt7Δ* + Ras2WT
6							WT + CT pld

Figure 3.10: *YPT7* deletion suppressed mutant RasV19 heat-shock phenotype. The heat shock phenotype of the *ira1Δ ira2Δ ypt7Δ* and the *ira1Δ ira2* mutant yeast strains are similar after a short exposure to 55°C.
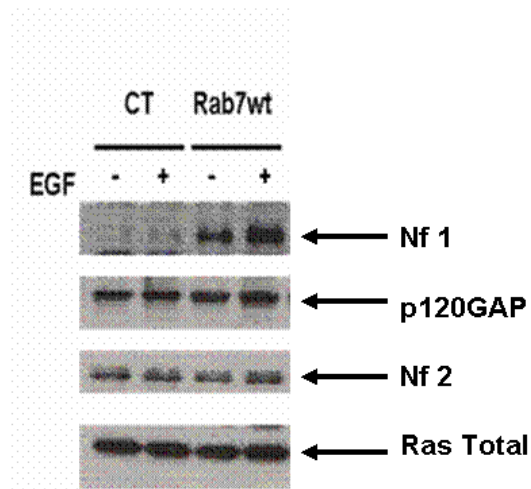
Figure 3.11: Rab7 over-expression in 293T cells increased neurofibromin protein levels.
Western blotting analysis shows over-expression of Rab7 in 293T cells increases neurofibromin levels. 293T cells were transfected with control or wild-type Rab7 plasmids. Cells were plated in serum free MEM media overnight and stimulated with either PBS or EGF for 10 minutes. Over-expression of Rab7 increased neurofibromin protein levels. EGF stimulation further increased neurofibromin levels.
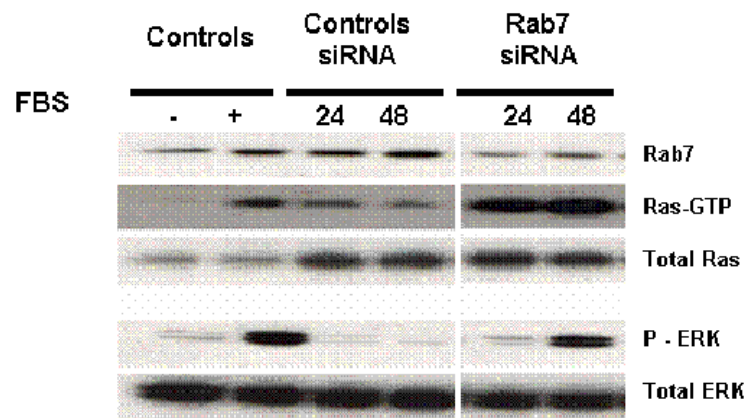
Figure 3.12: siRNA targets *RAB7* expression in 293T cells. Cells were transfected with control siRNA, or *RAB7* siRNA oligos targeting *RAB7*expression. After 24hrs or 48hrs of oligos transfections, cells were collected to detect Ras and Erk activities. For controls, cells were plated in serum free MEM media and stimulated with 5% FBS to detect Ras and Erk activities as indicated. Targeted knock-down of *RAB7*expresssion results in upregulation of RasGTP and phosphor-ERK levels.
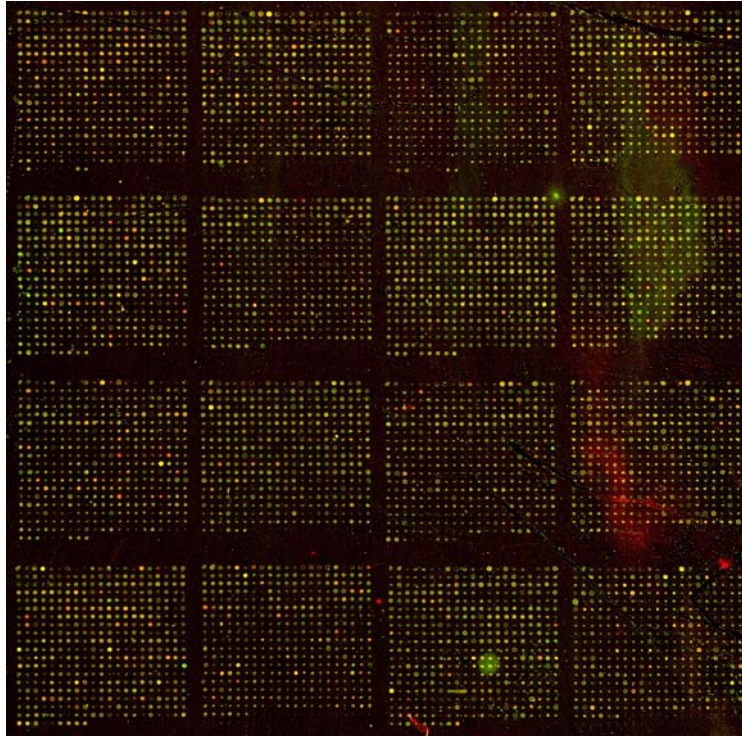
Figure 3.13: Genomic micro array analysis of wild-type and *ypt7Δ* yeast strains. Total cDNA samples with equal concentration were pre-mixed with the different dyes, wild-type (green) and *ypt7Δ* (red), and were hybridized on pre-processed micro array chips obtained from Dr. DeRisi (DeRisi et al., 1997). The red spots represent gene populations that were only expressed in the mutant cells. The green spots represent gene populations that were only expressed in wild-type cells. The yellow spots represent gene populations that were expressed in both strains. Analysis of gene changes was analyzed using the accompanied software (UCSF Core Facility) and targeted genes were further examined using gene deletion techniques.
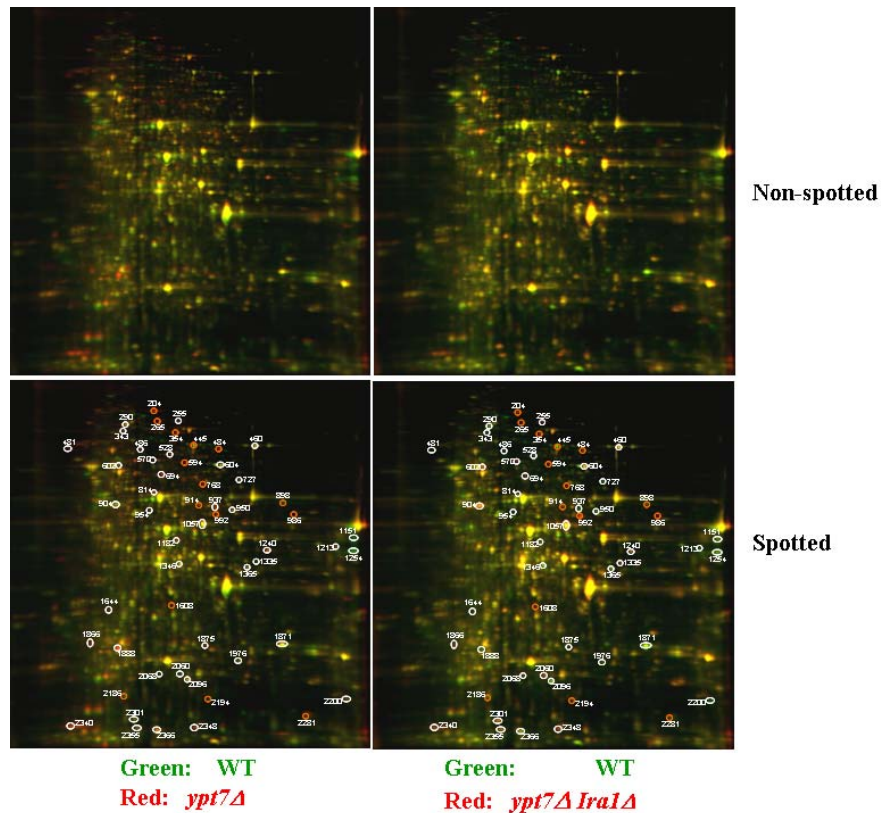
Figure 3.14: 2D gel proteomic analysis of wild-type and *ypt7Δ*, or wild-type and *ypt7Δ ira1Δ* yeast strains. Protein samples with equal concentration Ire pre-mixed with the different dyes wild-type (green), *ypt7Δ* (red), or *ypt7Δ ira1Δ* (red) and ran on 2D gel to compare changes in protein expressions. The red spots represent protein populations that Ire only expressed in the mutant and not wild-type cells. The green spots represent protein populations that Ire only expressed in wild-type cells. The yellow spots represent populations that Ire expressed in both strains. Either red or green protein spots Ire labeled and picked for further proteomic analysis (spotted). Upper panel represents 2D gel of protein samples before the spots Ire chosen to be picked (non-spotted).

Gene ID	NAME	Log Ratio		Gene ID	NAME	Log Ratio
YBR098W	MMS4	16.61		YEL016C	NPP2	-3.907
YLR368W	MDM30	16.61		YGR017W		-3.585
YAR040C	YAR040C	16.61		YML013C-A	YML013C-A	-3.585
YAL041W	CDC24	16.61		YNL074C	MLF3	-3.459
YOR360C	PDE2	16.61		YGL063W	PUS2	-2.807
YBR234C	ARC40	16.61		YDR183W	PLP1	-2.663
YBL039C	URA7	16.61		YER131W	RPS26B	-2.661
YIR013C	GAT4	5.392		YKL021C	MAK11	-2.115
YPR145W	ASN1	4.075		YBL091C	MAP2	-2.222
YCR017C	CWH43	4.392		YJL138C	TIF2	-2.043
YDR536W	STL1	3.209				
YLR384C	IKI3	3.585				
YPR077C		3.585				
YPR043W	RPL43A	3.773				
YOR036W	PEP12	3.138				
YPR130C		3.115				
YFR034C	PHO4	3.17				
YAL044C	GCV3	3.954				
YDL113C	ATG20	3.322				
YDR227W	SIR4	3.248				
YOR056C	NOB1	3.585				
YOR011W	AUS1	3.585				
YBR129C	OPY1	3.907				
YBR127C	VMA2	3.459				

Table 3.1: Micro array analysis. Changes in gene expressions obtained from micro array analysis, comparing wild-type and *ypt7*-deletion yeast strains. Red-labeled gene names represent up-regulation in gene expressions on the ypt7-deletion strain. Green-labeled gene names represent down-regulation in gene expressions of the ypt7-deletion strain.

Chapter 4: Gpb1 is a negative regulator of Ira2

4.1 Introduction

The yeast *Saccharomyces cerevisiae* has two RasGAP proteins, Ira1 and Ira2, with conserved amino acid sequences to the mammalian RasGAP protein neurofibromin, including the GTPase related domain (GRD) (Bollag and McCormick, 1991; Cichowski and Jacks, 2001). Neurofibronin is a large protein with many unknown functions. Furthermore, the NF1 gene is highly mutated and many approaches have been taken in cloning the full-length cDNA with little success. Therefore, I utilized yeast as a genetic model to study neurofibromin functions. Ira2 has approximately 22% amino acid sequences homology to neurofibromin. Furthermore, the *IRA2-TAP* yeast strain was previously generated with the TAP fusion protein tagged to the N-terminus of Ira2 (Ghaemmaghami et al., 2003).

To better understand the molecular mechanisms underlying Ira2 function and regulation, I utilized the tandem-affinity purification strategy coupled with mass spectrometry to identity protein complexes that directly interact with Ira2 in yeast cells (Figure 2.1). I identified many previously unknown proteins interact with and regulate Ira2 functions. Of interests is the Gpb1 Kelch-repeat protein. I found that the Ira2 protein is negatively regulated by Gpb1. Gpb1 promotes proteolysis of Ira2 and induces Ira2 degradation. Furthermore, the data suggests that Gpb1 and Gpb2 are functionally different proteins. Whereas Gpb1 negatively regulates Ira2, Gpb2 might have a positive role in regulating Ira2. This chapter shows functional studies of Gpb1 association with Ira2 in yeast cells.

4.2 Results

Analysis of Ira-TAP fusion protein and purification of Ira2 binding partners

To identify protein complexes that bind to Ira2, I performed a tandem-affinity purification (TAP) of Ira2 in yeast cells where the *IRA2-TAP* gene is expressed endogenously under its promoter. I first characterized the *IRA2-TAP* yeast strain (Ghaemmaghami et al., 2003) to determine whether the Ira2-TAP protein was functional. Western blotting analysis showed endogenously expressed Ira2-TAP fusion protein (Figure 4.1A). Loss of Ira2 activates Ras and as a result, *ira2*-deletion mutant cells are sensitive to heat (Tanaka et al., 1990a; Tanaka et al., 1990b). To examine whether loss of the Ira2-TAP protein results in heat shock sensitivity, I deleted the *IRA2-TAP* open reading frame to generate an ira2 mutant strain (*ira2-TAPΔ*) and compared its heat sensitivity to *IRA2-TAP* or non-tagged wild type strains. (Figure 4.1B) shows the *ira2-TAPΔ* yeast strain is more heat sensitive compared to wild type (lanes 2 and 4). Thus, our data show that the Ira2-TAP protein is functional in the *IRA2-TAP* yeast strain, and that the TAP-tagged fusion protein does not impair Ira2 activities.

IRA2-TAP cells grown to mid log phase were spun down and cell extracts were isolated as described (Ghaemmaghami et al., 2003), and after two rounds of affinity purification, protein complexes bound to the Ira2 were separated by gel electrophoresis, digested with trypsin and analyzed by liquid chromatography-tandem-mass spectrometry (LC-MS/MS). The data reveal both the previously known and novel binding partners of Ira2. The analysis represents two independent pull-down experiments (Figure 4.2 and Table 4.1). I found both Ira1 and Ira2 in the mass spectrometry analysis as well as the chaperone MSI3 that had previously been reported to bind to Ira2. Rim15, a component of the Ras/cAMP pathway, was also bound to Ira2 (Pedruzzi

et al., 2000; Reinders et al., 1998; Shirayama et al., 1993; Thevelein and de Winde, 1999; Vidan and Mitchell, 1997). Proteins involved with glycolysis and the production of ATPs, including pyruvate kinase, phosphoglycerate kinase, ATP synthase beta subunit, as well as ADP/ATP carrier protein 2, were found in the Ira2-bound complex. Interestingly, I found Ira2 binds to prohibitin, an evolutionarily conserved protein required for Ras-induced c-Raf activation in mammalian cells (Rajalingam et al., 2005). Furthermore, GBLP, a yeast homolog of human RACK1 which contains WD40 repeats, also binds to Ira2. PKC has been shown to regulate neurofibromin and Ras signaling in mammalian systems (Mangoura et al., 2006). Of interest is the G-beta mimic kelch-repeat protein 1 (Gpb1) which I found to be abundantly bound to Ira2 on the mass spectrometry analysis.

Gpb1 has 34% homology to another kelch-repeat protein, Gpb2. Both Gpb1 and Gpb2 proteins share strikingly similar amino acid sequences at their carboxyl terminus, including the β-propeller kelch-repeat domain (Harashima and Heitman, 2002). However, the two proteins contain unique amino acid sequences at their N-terminal domains, suggesting that the two N-terminal domains may possess different biological activities. Recently, both Gpb1 and Gpb2 were shown to associate with the Ira1 and Ira2 proteins in yeast, and positively regulate Ira1 and Ira2 activity (Harashima et al., 2006; Niranjan et al., 2007)

To investigate endogenous protein interactions between Ira2 and Gpb1, I utilized the *GPB1-TAP* yeast strain and doubly tagged the *IRA2* gene with *3FLAG* cDNA to generate the *IRA2-3FLAG/GPB1-TAP* yeast strain. I verified integration by PCR and protein expression by immunoblotting (WB) analysis (Figure 4.3). I confirmed Ira2 and Gpb1 interactions by performing immunoprecipitation (IP) and immunoblotting (WB) experiments (Figure 4.4A). Ira2 and Gpb1 association was further investigated by *in vitro* translation and

58

immunoprecipitation experiments. I cloned the ORFs of *GPB1* and the C-terminal domain of

IRA2 into destination vectors (see the experimental procedures), *in vitro* translated and

immunoprecipitated with anti-V5 monoclonal antibody. I found Ira2 efficiently interacts with

Gpb1 in the *in vitro* translation and binding experiments (Figure 4.4B). Taken together, the

results confirm that Ira2 interaction with Gpb1 is direct.

Gpb1 Negatively Regulates Ira2

Gpb1 and Gpb2 have been reported recently to interact with Ira1 and Ira2, and to positively

regulate Ira protein levels when over-expressed in yeast cells (Harashima et al., 2006). However,

I observed different results in our experimental systems. I found that deletion of *GPB1-TAP*

ORF in the *IRA2-3FLAG/GPB1-TAP* yeast strain caused Ira2 to increase approximately three to

four fold compared to the wild type strain (Figure 4.5). Since our results were contrary to

previously reported data, I repeated our genetic deletions of the *GPB1-TAP* ORF and obtained

two independent yeast strains that have deletions in the *GPB1* allele. Again, I found that *gpb1Δ*

mutants possessed higher Ira2 protein levels compared to wild type cells. Figure 4.5 shows two

independent results of the *IRA2-3FLAG/gpb1-TAPΔ* yeast strains (numbered 7 and 10). To

further investigate the biological activity of Gpb1 in the Ira2/Ras signaling pathway, I cloned

GPB1 into the p*DEST52* destination vector that contains the *GAL1* promoter. I reasoned that if

Gpb1 is truly a negative regulator of Ira2 then over-expression of Gpb1 would down regulate

Ira2 and activate Ras. The p*GAL1-GPB1-V5* construct was expressed transiently in the *gpb1Δ*

mutant strain to eliminate any endogenous Gpb1 interference activity. After 4hrs of galactose

stimulation, I found over-expression of Gpb1-V5 extensively reduced Ira2 protein levels (Figure 4.6). Furthermore, overexpression of Gpb1 results in an increase in RasGTP levels (Figure 4.6).

To further examine Gpb1 activity *in vivo*, I constructed mutant yeast strains in which the ORFs of *IRA1, IRA2 or IRA1/IRA2* are deleted. I over-expressed Gpb1 in these mutant strains and examined their sensitivity to high temperatures in a heat shock assay. I found that induced GPB1-V5 expression increased heat sensitivity in the *ira1Δ/IRA2* yeast strain when compared to control plasmid (Figure 4.7). Although I could not assess the level of heat sensitivity in the *ira2Δ/IRA1* mutant strain, the results in the *ira1Δ/IRA2* strain confirmed the hypothesis that Gpb1 directly down regulates Ira2, activates Ras signaling, and inactivates heat shock response genes which results in heat sensitivity. Therefore, the data strongly suggest that Gpb1 is a negative regulator of Ira2.

Gpb1 controls Ira2 stability during glucose stimulations

In yeast, glucose stimulation activates the G protein coupling receptor Grp1, which induces Ras and adenylyl cyclase activity. Glucose-induced activation of Grp1 stimulates pathways that are critical for cell metabolism and growth (Kraakman et al., 1999). Since Ira2 negatively regulates Ras activity, I hypothesized that in the event of rapid Ras activation induced by nutrient stimulation such as glucose, the Ira2 protein levels would be tightly regulated. As demonstrated by Cichowski and co-workers, neurofibromin is rapidly degraded upon growth factor stimulation via the ubiquitin-proteasome pathway in mammalian cells (Cichowski et al., 2003).

I therefore investigated whether Ira2 is down-regulated by glucose stimulation. I treated *IRA2-3FLAG/GPB1-TAP* cells with 5uM glucose and the Ira2 levels were assessed by immunoblotting

analysis. Glucose stimulation triggered Ira2 down-regulation within 10 min and a further

decrease was seen at 15 min. Moreover, glucose-induced down-regulation of Ira2 is

accompanied by a gradual elevation of Gpb1 protein levels (Figure 4.8). This data is consistent

with the earlier observations that Gpb1 is a negative regulator of Ira2 (Figure 4.6).

Because glucose stimulation or over-expression of Gpb1 down-regulated Ira2 endogenous levels,

I hypothesize that Ira2 might be ubiquitin-modified for rapid Ras activation and that Gpb1 is

responsible for Ira2 stability. To investigate whether Ira2 is a target of the ubiquitination

machinery, I treated *IRA2-3FLAG/GPB1-TAP* cells with the proteasome inhibitor MG132 and

the Ira2 protein was immunoprecipitated and immunoblotted with an anti-ubiquitin antibody. I

detected Ira2 ubiquitination after 4hrs of MG132 treatment (Figure 4.9). To test the role of

Gpb1 in Ira2 stability, I examined the steady-state turnover of Ira2 levels in the *gpb1Δ* mutant

when compared to wild-type yeast cells. The half-life of endogenous Ira2 was rapidly degraded

in cycloheximide-treated wild-type cells while Ira2 was stabilized in *gpb1Δ* mutant cells (Figure

4.10). These results suggest that glucose stimulation induced down-regulation of Ira2, possibly

by triggering Gpb1-mediated Ira2 ubiquitination and degradation.

Gpb1 is required for Ira2 ubiquitination and degradation

Gpb1 has a unique N-terminal domain (amino acids 1-220) with similar amino acid sequences to

the ubiquitin-associated domain (UBA) at amino acids 1-31, and a seven β-propeller kelch-

repeat domain at its C-terminus (amino acids 292-816). Previous reports suggest that UBL-UBA

proteins can bind to and deliver ubiquitinated proteins to the proteasome for protein degradation.

In addition, the kelch-repeat domain has similar structure to the WD40 repeat domain, which is

involved in substrate recognition for ubiquitin ligase complexes (He et al., 2006; Minella et al., 2005; Welcker and Clurman, 2008). A recent finding also showed the Kelch protein, KLHL12, binding to Cullin-3 ubiquitin ligase to negatively regulate the Wnt-β-catenin pathway (Angers et al., 2006). To examine the role of Gpb1 in ubiquitination of Ira2 *in vivo*, I generated galactose inducible plasmids containing either *GPB1* full-length (WT) or *KELCH-* (KelchΔ) or *UBA-* deleted fragments (UBAΔ) and expressed these plasmids in the *IRA2-3FLAG/gpb1Δ* yeast strain. At different time points post galactose induction, I collected cells for immunoprecipitating and immunoblotting assays. Figure 4.11B shows the galactose-induced expression of full-length Gpb1in the *IRA2-3FLAG/gpb1Δ* yeast strain caused an increase of Ira2 ubiquitination in a Gpb1-dose dependent manner (WT, Figure 4.10B, first panel). Surprisingly, neither the KelchΔ nor UBAΔ fragments promote Ira2 ubiquitination (KelchΔ or UBAΔ, Figure 4.11B, second panel) even though the wild-type, KelchΔ and UBAΔ Gpb1 fragments do efficiently bind to Ira2 (Figure 4.11B). These results suggest that only the full-length Gpb1 is required for Ira2 ubiquitination.

To determine whether Gpb1 can efficiently conjugate ubiquitin to Ira2 *in vitro*, I purified Ira2-Flag and Gpb1-TAP fusion protein complexes from the *IRA2-3FLAG/Δgpb1* and *Δira2/GPB1-TAP* mutant strains, respectively, and performed *in vitro* ubiquitin-conjugation experiments. I used extensively washed immuno-purified Ira2-Flag as the substrate and purified TEV-cleaved Gpb1 as the ubiquitin-conjugating enzyme complex. After incubation with either recombinant His-ubiquitin or recombinant His-ubiquitin mutant with all the lysine residues deleted (KØ) (Chapter 2, Experimental Methods), Ira2-Flag was immunoprecipitated and immunoblotted with anti-His antibody to detect Ira2-conjugated His-ubiquitin chains. I found the purified TEV-cleaved Gpb1 complex can readily promote Ira2 polyubiquitination *in vitro* in a ubiquitin dose-

dependent manner (Figure 4.12). Taken together, I conclude that Gpb1 complex ubiquitinates Ira2 *in vivo* and *in vitro*.

Gpb2 is functionally different from Gpb1 in regulating Ira2

Previous reports suggested that Gpb1 and Gpb2 positively regulate Ira proteins in yeast (Harashima et al., 2006; Harashima and Heitman, 2002). However, I observed that Gpb1 negatively regulates endogenous Ira2 protein levels when overexpressed in cells (Figure 4.6), and that Ira2 is upregulated in *gpb1* mutant cells (Figure 4.5). Therefore, I hypothesized that Gpb2 and Gpb1 have opposite roles in regulating Ira2. Gpb1 and Gpb2 possess a similar kelch-repeat domain at their C-terminus (35% homology), but contain unique N-terminal domains. Therefore, it is possible that Gpb2 positively regulates Ira2, while Gpb1 is a negative regulator of Ira2. To test the hypothesis that Gpb2 is a positive regulator of Ira2, I cloned *GPB2-V5* and *GPB1-V5* under the control of the GAL1 promoter. I over-expressed p*GAL1-GPB1-V5* and p*GAL1-GPB2-V5* in the *IRA2-3FLAG* yeast strain and performed western blots to determine the Ira2 protein levels. I found that Gpb2 over-expression modestly increases Ira2 levels, while over-expression of Gpb1 down-regulates Ira2 (Figure 4.13). To further investigate the differences between Gpb1 and Gpb2 *in vivo*, I over-expressed a control, p*GAL1-GPB1-V5* or p*GAL1-GPB2-V5* plasmid in the wild type strain or *ira2Δ/IRA1, ira1Δ/IRA2* and *ira1Δ ira2Δ* strains, and assessed heat sensitivity. As expected, I found that over-expression of Gpb1 increases heat sensitivity, whereas over-expression of Gpb2 causes heat resistance in *ira2Δ/IRA1* cells (Figure 4.14). Therefore, I conclude that Gpb2 positively regulates, whereas Gpb1 negatively regulates Ira2.

4.3 Discussion

I generated and utilized the *IRA2-FLAG* yeast strain to investigate the biological activities of the

Ira2. Based on the abundance of the Gpb1 protein association with Ira2 in our proteamic

analysis, I focused on functional characterization of Gpb1 and Ira2. I found that overexpression

of Gpb1 resulted in downregulation of Ira2 (Figures 4.6 and 4.7), whereas the overexpression of

Gpb2 resulted in similar activities as previously described (Harashima et al., 2006). These

observations are in contrast to previous reports where Harashima and coworkers showed

overexpression of the Gpb1 and Gpb2 ketch-repeat proteins positively regulate Ira1 and Ira2

activity (Harashima et al., 2006). In this study, I overexpressed Gpb1 and directly examined the

endogenous FLAG-tagged Ira2 levels (Ira2-Flag; Figure 4.6) instead of determining Ira2 levels

by immunoprecipitation (Harashima et al., 2006; Figure 4B and 4D). Determining endogenous

Ira2-Flag levels by immunoblotting experiments affords an advantage over immunoprecipitation

because immunoprecipitation experiments can result in saturation of the Ira2-Flag levels. Since

Gpb1 and Gpb2 possess similar kelch-repeat domains with differences in amino acid sequences

at the N-terminal domain, I focused on the N-terminal regions of Gpb1 and Gpb2 to identify

differences in the biological functions of the two proteins. Based on our analysis of the amino

acid sequences, I suggest that Gpb1 possesses a ubiquitin-associated domain (UBA) from amino

acids 1 to 31 (Figure 4.11). Importantly, these amino acids lie within the N-terminal domain of

Gpb1 and are not conserved in Gpb2. I further demonstrate that overexpression of wild-type

Gpb1 is critical and sufficient for Ira2 downregulation and Ras activation (Figure 4.6), by

promoting ubiquitination of Ira2 (Figure 4.8). In contrast to Gpb1, I found that Gpb2 positively

regulate Ira2. Overexpression of Gpb2 modestly increased Ira2 levels whereas overexpression of

Gpb1 had a negative effect on Ira2 (Figure 4.12). I further confirmed the differences between

Gpb1 and Gpb2 by utilizing genetic analysis to show that overexpression of Gpb2 upregulates Ira2 activity by inhibiting the heat shock phenotype usually accompanied by loss of Ira function in the *ira1Δ* or *ira2Δ* single gene deletion strains. Importantly, overexpression of Gpb1 resulted in heat shock sensitivity in these mutant yeast strains under the same experimental conditions. Taken together, the data demonstrate that Gpb1 and Gpb2 possess different biological functions.

There are several possible explanations for the differences in Gpb1 and Gpb2 functions. One possibility is that Gpb1 and Gpb2 might have two completely different functions but share similar kelch-repeat domains. Many proteins have been identified which share similar domain structures but also have different functions, including the small GTPase family of proteins (Colicelli, 2004). The yeast *Saccharomyces cerevisiae* has two RasGAP proteins, Ira1 and Ira2. In addition to their biological redundancy in regulating Ras, previous reports have pointed out that Ira1 and Ira2 can independently regulate different biological pathways (Magherini et al., 2006; Park et al., 2005; Tanaka et al., 1990b). It is also possible that Gpb2 has lost its UBA domain function and is unable to negatively regulate Ira proteins. Therefore, overexpression of Gpb2 could inhibit Gpb1-mediated degradation of Ira2 by competing with Gpb1 for binding to Ira2 through the kelch-repeat domain interaction. Furthermore, proteomic experiments have shown that Gpb1 and Gpb2 bind to different intracellular protein partners, suggesting that these proteins mediate independent signaling pathways (Collins et al., 2007). Thus, deletion of Gpb1 or Gpb2 might result in different genetic changes that result in completely different activation or deactivation of downstream effectors. Therefore, it is possible that deletions of Gpb1 or Gpb2 (or both Gpb1 and Gpb2) might result in different genetic and molecular signaling consequences as observed in previous findings.

Previous reports suggest that Gpb1 and Gpb2 function as downstream effectors of the G beta-subunit Gpa2 to negatively regulate Gpr1 glucose receptor signaling, similar to Gbeta-subunit inhibiting G protein signaling by sequestering the GDP-bound Gbeta-subunit, thereby inhibiting the downstream signaling cascades (Harashima and Heitman, 2002; Peeters et al., 2006). These conclusions are based on the findings that *gpb1/2Δ* cells have increased Gpa2 activity and as a result these mutant cells have invasive and pseudohyphal growth, as Well as an inablilty to store glycogen due to activation of PKA (Harashima and Heitman, 2002). Interestingly, it was also demonstrated that the double mutant *gpb1Δ gpa2Δ* or *gpb2Δ gpa2Δ* do not have the pseudohyphal growth phenotype and the triple deletion mutant *gpb1/2Δ gpa2Δ* has less pseudohyphal and invasive growth phenotypes as Well as decreased *FLO11* expression when compared to the *gpb1/2Δ* strain (Harashima and Heitman, 2002). Although the current work does not directly address these pseudohyphal growth phenotypic differences between the *gpb1Δ* and *gpb1Δ* strains and the effects these two kelch-repeat proteins have on Gpa2 signaling, I speculate that Gpb1 might negatively regulate components of the Gpa2 signaling cascades by inhibiting activation of Gpa2 similar to the Gpb1 negative regulation of Ira2 as described in this report. Therefore, it is possible that deletion of Gpb1 results in failure to initiate degradation of important regulatory proteins that are necessary for controlling Gpa2 activity, thereby constitutively activating Gpa2 (Harashima and Heitman, 2002). Supporting this argument is the recent finding which showed Gpa2 mutants that failed to bind Gpb2 (Krh1p) are constitutively active (Niranjan et al., 2007). Here, Niranjan and coworkers proposed that Gpb2 might have unique interactions with Gpa2 (Niranjan et al., 2007), in contrast to previously proposed models (Harashima et al., 2006). Further experiments are needed to fully address these differences

between Gpb1 and Gpb2 in loss of function experiments and their direct effects on Gpa2 signaling pathways.

In yeast and mammalian cells, GPCR senses signals from the cell environment to direct intracellular communications. In yeast, in addition to the Well characterized GPCR pheromone signaling pathway (Bourne, 1997; Dohlman and Thorner, 2001; Sprang, 1997), the recently identified G coupling receptor protein Gpr1 recognizes nutrients (including high glucose concentrations) from the cellular environment and mediates Gpa2 activation of the Ras/cAMP/PKA pathway (Kraakman et al., 1999; Lorenz et al., 2000; Thevelein and de Winde, 1999). Gpa2 has similar structure and function to the Gα subunit of GPCR proteins. However, instead of forming a heterotrimeric G protein complex with the Well characterized Gαβ subunits Ste4/18, Gpa2 binds to two Gβ like kelch-repeat proteins, Gpb1 and Gpb2 (Harashima and Heitman, 2002, 2005; Peeters et al., 2006). Both Gpb1 and Gpb2 proteins contain a seven kelch-repeat domain at its C-terminus and a unique N-terminal domain (Gettemans et al., 2003; Harashima and Heitman, 2002). The kelch-repeat domain is predicted to have a similar protein folding structure to the WD40 repeat domain that is commonly found in the GPCR Gβ subunits, TAFII transcription factor, and E3 ubiquitin ligase (Gettemans et al., 2003; Jin et al., 2006; Petroski and Deshaies, 2005). Our data demonstrate for the first time that the Gpb1 kelch-repeat protein directly binds and mediates Ira2 degradation. I have also found that Gpb1 binds to the base subunit Rpn1 of the proteasome, which further supports our conclusion that Gpb1 is responsible for mediating Ira2 degradation (data not shown). I suggest that Gpb1, similar to the WD40 domain family of proteins, belongs to a new class of ubiquitin ligase complexes that possess kelch-repeat domains to mediate protein-protein interactions and ubiquitination of the targeted substrates for proteasomal degradation. Similar to the widely studied WD40 repeat

proteins and their proposed roles in protein scaffolding and mediating protein interactions, the Kelch-like 12 protein has only recently been demonstrated to bind to the Cullin3 E3 ligase to promote degradation of the Dishevelled protein (Angers et al., 2006). Proteomic analysis from the same study identified protein complex binding to Dishevelled-2, including WD repeat protein 6, Kelch-like 12, Galpha2 and Galpha4, as well as other proteins (Angers et al., 2006). Therefore, it is likely that mammalian cells employ the same regulatory mechanisms involving kelch-repeat proteins to directly regulate G proteins signaling in a manner found in yeast cells. Interestingly, a different Kelch-like 10 protein, Klhl10, has recently been identified as part of the Cullin3 ubiquitin ligase complex that regulates spermatid development in *Drosophila* (Wang et al., 2006). Currently, the human homologues of Gpb1 and Gpb2 have not been identified. In mammalian systems, kelch-repeat proteins represent diverse sets of proteins with unknown functions. Future studies are needed to address their functions in human disease.

Our working model is supported by previous findings that show the human RasGAP protein neurofibromin is negatively regulated by the ubiquitin machinery when cells are stimulated with various growth factors (Cichowski et al., 2003). It was postulated that an E3 ligase is responsible for targeting neurofibromin degradation for the rapid activation of Ras. Although the E3 ligase targeting neurifibromin for protein degradation was not identified, amino acid sequences adjacent to the GAP-related domain (GRD) of neurofibromin have been identified and demonstrated to be critical sites for neurofibromin degradation (Cichowski et al., 2003). In yeast, glucose signaling results in activation of the glucose receptor Gpr1 and the Ras/PKA pathways (Colombo et al., 1998; Lemaire et al., 2004). Here, I show that glucose stimulation triggered downregulation of the yeast RasGAP protein Ira2 (Figure 4.7), similar to neurofibromin downregulation in response to growth factor stimulation in mammalian cells.

More importantly, I show that Gpb1 directly interacts with and ubiquitinates Ira2 (Figure 4.12)

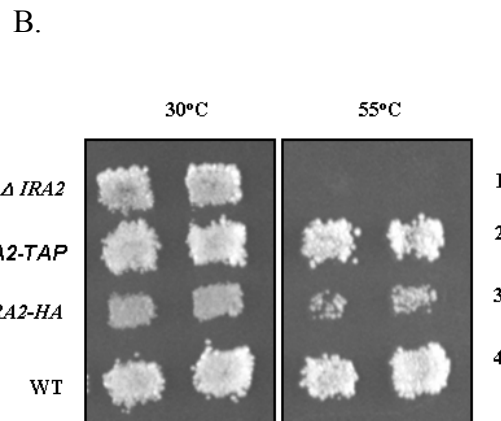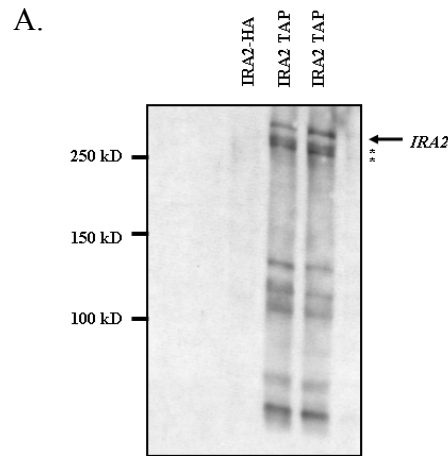whereas loss of Gpb1 function stabilized Ira2 levels (Figure 4.5).

Figure 4.1: Characterization of the *IRA2-TAP* yeast strain. A) Soluble extracts from cells expressing the indicated Ira2-HA or Ira2-TAP fusion proteins were immunoblotted for TAP fusion protein with anti-TAP antibody. Asterisk represents three isoforms of Ira-TAP with the predicted molecular weight. B) Heat shock experiments were performed on yeast strains as indicated. Cells were grown at $30^{o}C$ for three days, replaca plated, and either exposed to a chamber preheated at $55^{o}C$ or unexposed ($30^{o}C$) as controls. Photographs were taken three days after heat exposure. The Ira2-TAP protein is expressed under its endogenous promoter, lane 1) a strain with the *IRA2* deleted by genetic homologous recombination, lane 2) wild type strain expressing the Ira2-TAP fusion protein, lane 3) wild type strain expressing the Ira2-HA fusion protein, and lane 4) wild type strain that is not ira2-tagged.
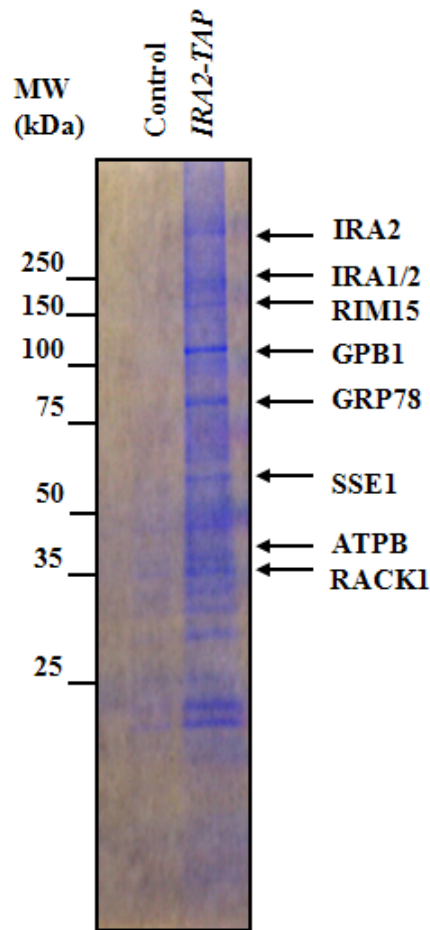
70

Figure 4.2: Identification of Gpb1 kelch-repeat protein as a negative regulator of Ira2.
TAP-tagged Ira2 purification identified protein binding partners for Ira2 in yeast cells. Ira2-TAP
fusion protein is expressed endogenously under the *IRA2* promoter. Ira2-TAP co-purified
protein complexes were resolved by NuPAGE gel electrophoresis (Invitrogen) and identified by
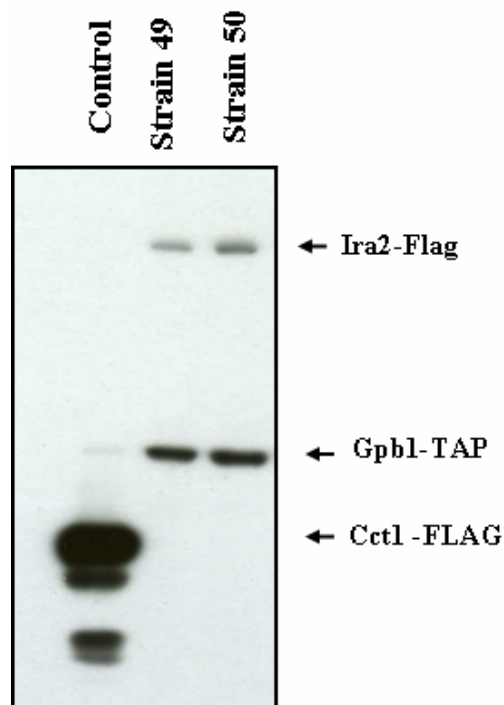mass spectrometry. Control sample was from wild-type yeast cells that are not tagged (Control).

Figure 4.3: Yeast strains doubly expressed endogenous Ira2-Flag and Gpb1-TAP fusion proteins. Western blots showed either control strain expressing Cct1-Flag or two different strains expressing Gpb1-TAP/Ira2-Flag. The *GPB1-TAP* yeast strain was used to create double-tagged *GPB1-TAP/IRA2-3FLAG* strains, 49 and 50. We generated *CCT1-3FLAG* strain for control. Genetic integration experiments were performed using plasmids from previously described publications.
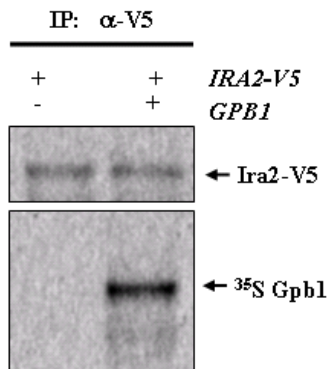
A.
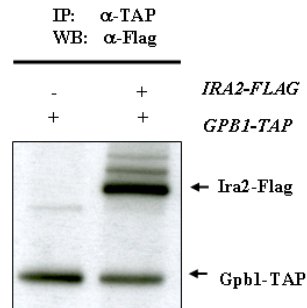
B.

Figure 4.4: Gpb1 and Ira2 endogenously interact *in vivo* and *in vivo*. (A) Yeast cells endogenously expressed Gpb1-TAP and Ira2-Flag fusion proteins were immunoprecipitated (IP) with IgG-conjugated glutathione beads, followed by Western blotting analysis (WB) with anti-TAP and anti-Flag antibodies as indicated to the right. (B) Ira2 and Gpb1 interaction *in vitro*. Ira2-V5 and Gpb1-GFP were translated *in vitro* (Experimental Procedures) and subjected to immonoprecipitation (IP) with anti-V5 antibody and visualized by Storm860 PhosphoImager.
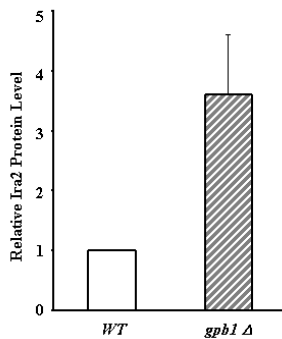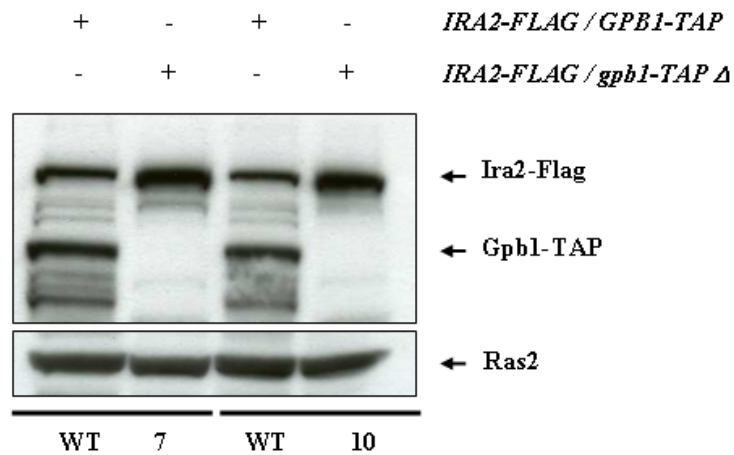
Figure 4.5: Gpb1 deletion ncreases Ira2 levels. Lysates from either wild type (WT) or *gpb1-*deletion mutant (7 and 10) yeast extracts were normalized and subjected to Western blotting analysis with anti-Flag or anti-TAP antibodies. Membrane was blotted using anti-Ras2 antibody to control for equal protein loading. Protein levels of Ira2 were quantified from three independent experiments of either wild type (WT) or *gpb1*-deletion mutants (*ΔGPB1*) and showed with the standard error of the mean.
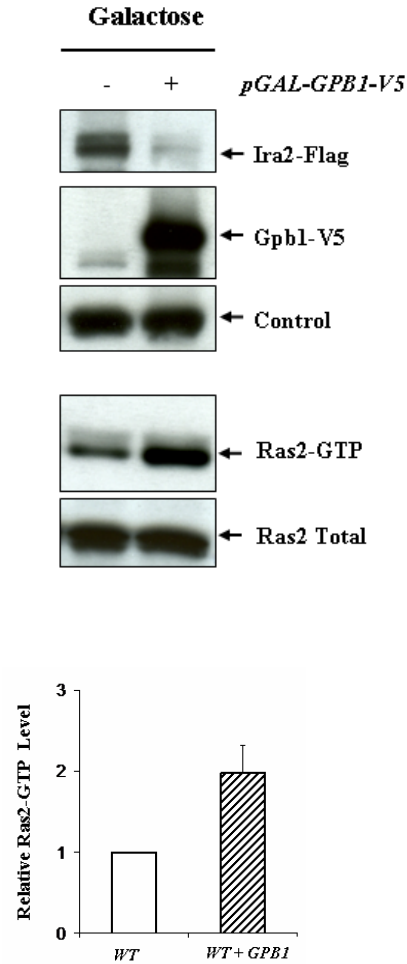
Figure 4.6: Gpb1 overe-xpression decreases Ira2 stability and activates Ras signaling. The p*GAL-GPB1-V5* plasmid was transformed into wild-type yeast cells endogenously expressing Ira2-flag. Cells were induced with galactose for 3hrs and subjected to immunoblotting with anti-Flag and anti-V5 antibodies to determine protein levels. Lower panel showed Ras2-GTP levels in cells overexpressing Gpb1-V5. Ras2-GTP was purified from lysates with equal protein concentrations. RasGTP pull-downed samples were diluted three folds and then subjected to immunoblotting with anti-Ras2 antibody. Total Ras2 levels were Western blotted for comparison. Quantified Ras2-GTP levels from either wild-type (WT) or wild-type with Gpb1 overexpression (WT + Gpb1) were shown on the right from three independent experiments with the standard error of the mean.
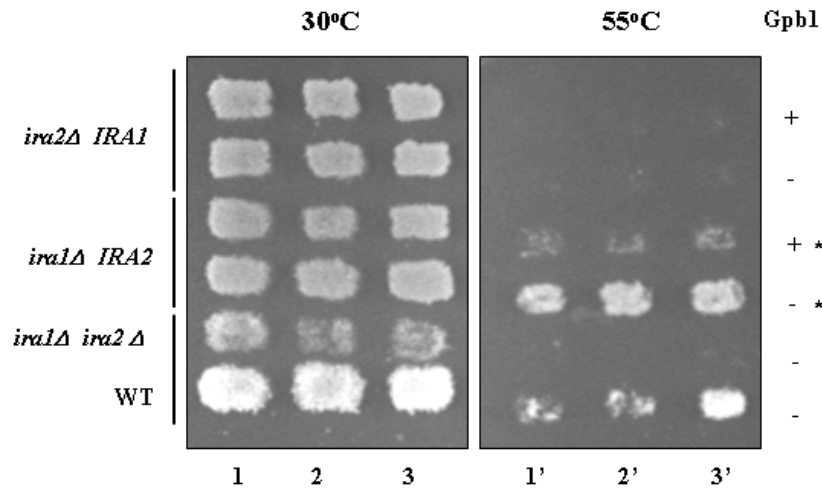
Figure 4.7: Over-expression of Gpb1-V5 in *ira1Δ/IRA2* mutant yeast strain causes heat sensitivity. Galactose induced expression of Gpb1 causes heat sensitivity in *ira1Δ/IRA2* yeast cells that have a functional *IRA2* allele (+ *) when compared to cells that received an empty plasmid (- *). We could not assess heat sensitivity in *ira2Δ/IRA1* mutant strain. To assay for heat shock sensitivity, cells were replica plated onto GAL/-Ura3 plates and exposed to a high temperature chamber (55^0C) for 60 minutes or unexposed to heat chamber (30^0C). Plates were then cooled down at room temperature for 30 minutes, incubated at 30^0C for 3-7days before pictures were taken.

Total Lysate

| 0 | 10 | 15 | 30 | (Min) | + Glucose |

← Ira2-Flag

← Gpb1-TAP
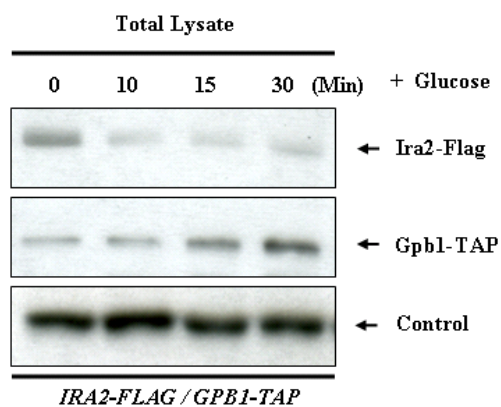
← Control

IRA2-FLAG / GPB1-TAP

Figure 4.8: Ira2 is down-regulated in response to glucose stimulation. *IRA2-FLAG/GPB1-TAP* cells were grown to log phase in rich medium over night and switched to glucose-free medium for 4-6hrs before 5% glucose stimulation. Ira2 and Gpb1 protein levels were detected by immunoblotting using anti-Flag and anti-TAP antibodies. Membrane was blotted using anti-Ydj1 antibody for equal protein loading control. (Ydj1 is an Hsp40 protein in yeast).
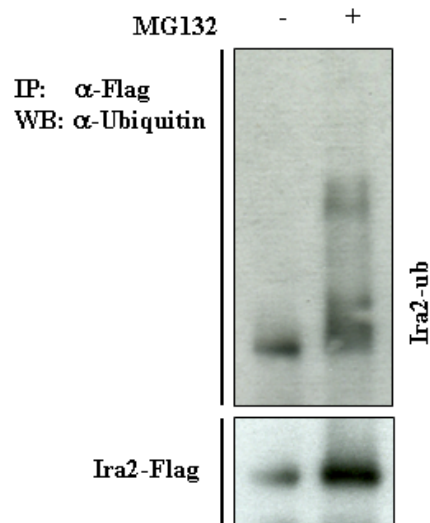
Figure 4.9: Ubiquitination assay of endogenous Ira2-Flag. *IRA2-FLAG/GPB1-TAP* cells were grown to log phase then either untreated (DMSO) or treated with the proteasome inhibitor MG132 (10uM) for 3hrs. Immunoprecipitation assay (IP) was performed on cell lysates with equal protein concentrations using anti-Flag antibody and immunoblotted (WB) with either anti-ubiquitin or anti-Flag antibodies.
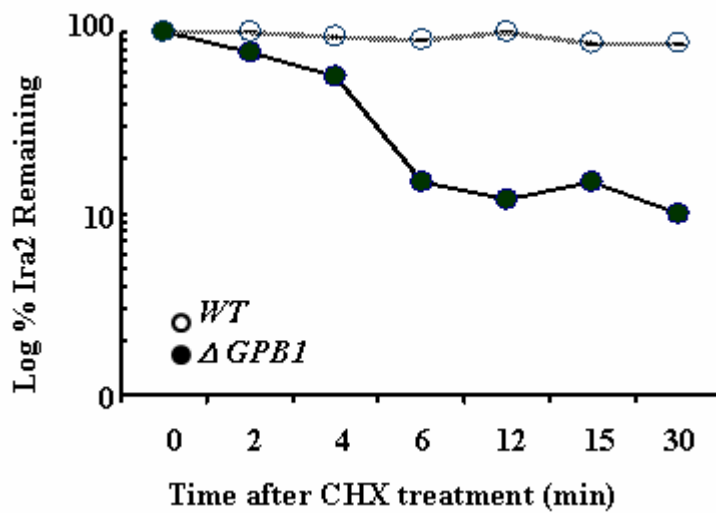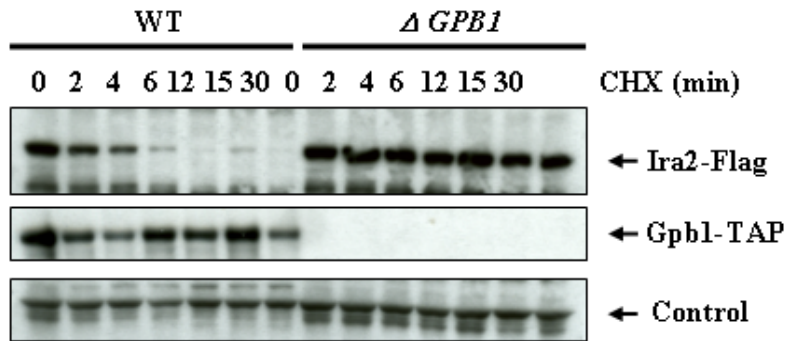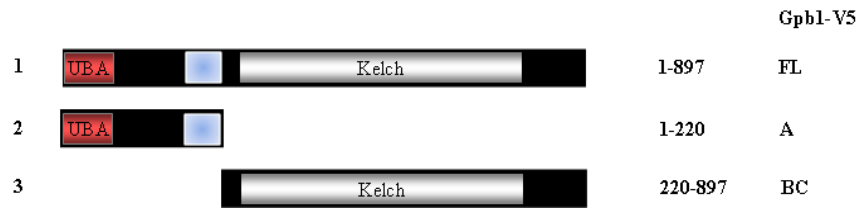
Figure 4.10: Cycloheximide chase assay of Ira2 in wild type (WT) and *gpb1Δ* yeast strains.
Ira2 and Gpb1 protein levels were detected by immunoblotting using anti-Flag and anti-TAP antibodies. Membrane was immunoblotted with anti-Ras2 antibody for equal protein loading control.

A.

B.
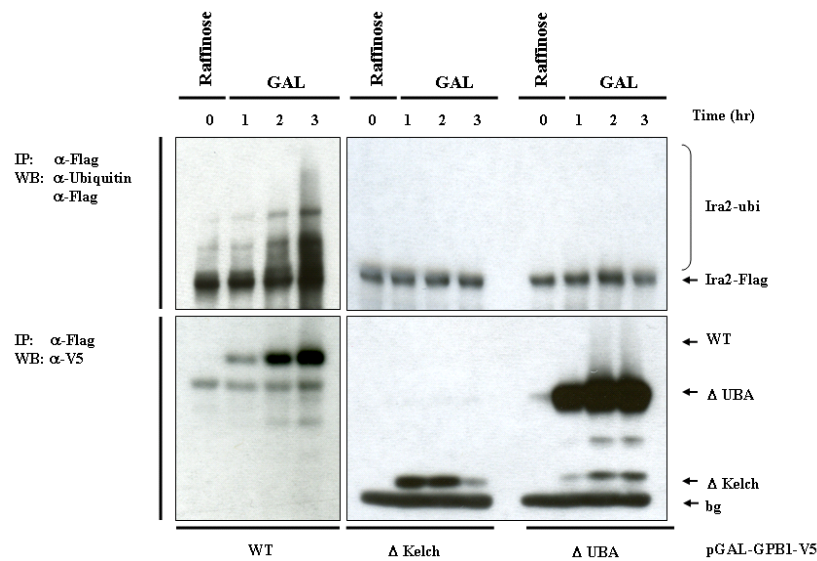
Figure 4.11: Full-length Gpb1 targets Ira2 for protein degradation. (**A**). Domain structure of Gpb1 contains a UBA domain at the N-terminus and a kelch-repeat domain at the C-terminus. Amino acid positions of the individual domain are shown to the right with corresponding numbers and notations. (**B**) Gpb1 wild-type targets Ira2 for ubiquitination. Overexpression of Gpb1-V5 wild-type (left panel), ΔKelch C-terminal deletion (middle panel), or ΔUBA N-terminal deletion (right panel) were performed in the *IRA2-FLAG* yeast strain by treating cells with galactose at different time points as indicated (0-3hrs). Lysates were collected at different time points and subjected to immunoprecipitation (IP) with anti-flag and immunoblotted with anti-ubiquitin, anti-flag and anti-V5 antibodies. Only Gpb1 wild-type can ubiquitinate Ira2. Gpb1-WT, ΔKelch or ΔUBA fragments can efficiently bind to Ira2.
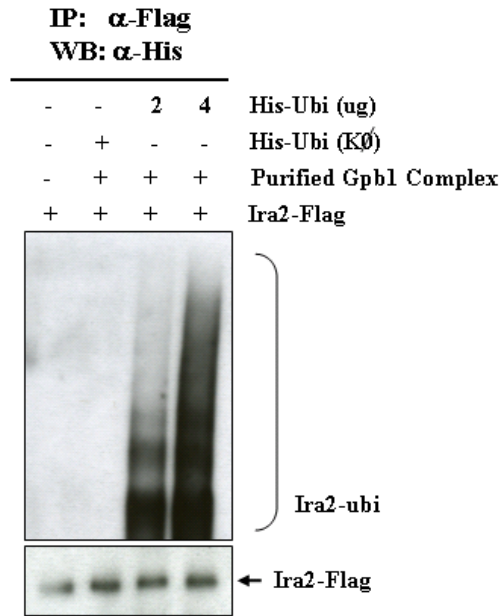
Figure 4.11: Gpb1 ubiquitinates Ira2 *in vitro*. Ira2-Flag and Gpb1-TAP complexes were purified from *IRA2-FLAG Δgpb1* and *GPB1-TAP Δira2* yeast strains respectively and subjected to *in vitro* ubiquitination assays (Experimental Procedure). Gpb1 ubiquitination activity was observed in reactions containing recombinant wild-type His-ubiquitin (His-ubi), but not with untreated or mutant His-uniquitin, where all the lysine amino acids were mutated (KØ). Reactions were incubated for 1hr, immunoprecipitated (IP) with anti-Flag antibody and immunoblotting (WB) with anti-His or anti-Flag antibodies.
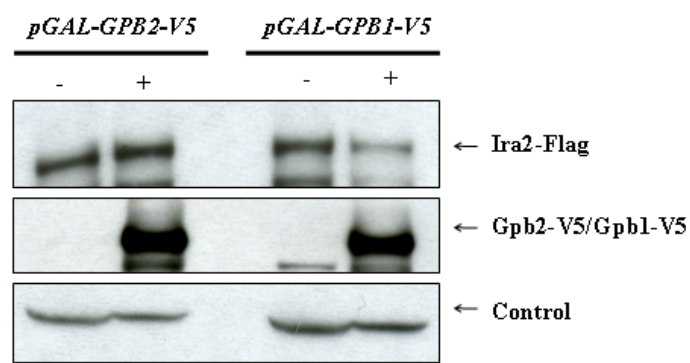
Figure 4.12: Gpb1 and Gpb2 have opposite functions. Overexpression of Gpb2 positively regulates Ira2 activity. p*GAL-Gpb2-V5* (lane 2) or p*GAL-Gpb1-V5* (lane 4) was overexpressed in the *IRA2-FLAG* yeast strain and cell lysates were subjected to immunoblotting analysis (WB) with anti-Flag or anti-V5 antibodies to detect Ira2, Gpb2 or Gpb1 protein levels. Membrane was blotted using anti-Ydj1 antibodies to control for equal protein loading. (Ydj1 is an Hsp40 protein in yeast).
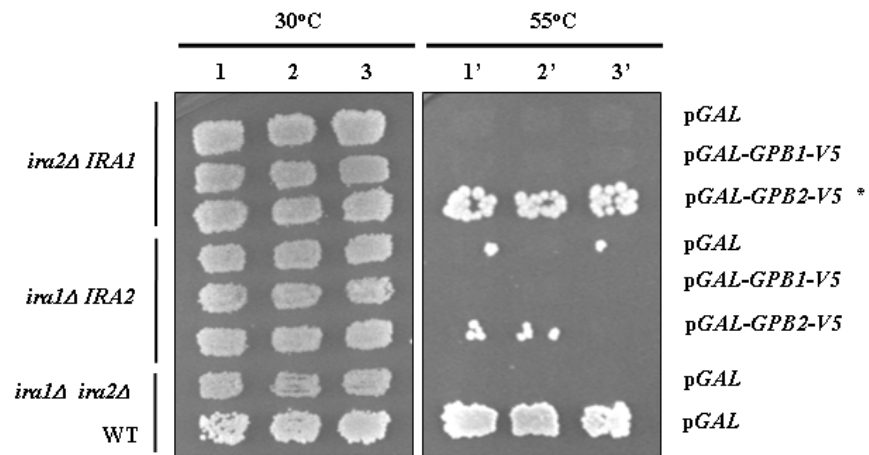
Figure 4.13: Overexpression of Gpb2-V5 in *ira2Δ IRA1* mutant yeast strain causes heat shock resistance. Galactose-induced expression of Gpb2 causes heat shock resistance in *ira2Δ IRA1* mutant yeast strain when compared to Gpb1-V5. To assay for heat shock sensitivity, cells were replica plated onto GAL/-Ura3 plates and exposed to a high temperature chamber for 60 minutes (55^0C) or unexposed to heat (30^0C). Plates were then cooled down at room temperature for 30 minutes, incubated at 30^0C for 3-7days before pictures were taken. Controls cells were either from the double *ira1Δ ira2Δ* mutant and wild type cells.

Table 1: Supplementary report for Mass Spectrometry data for IRA2 protein complexes		
S. cerevisiae Protein Identified	**% Sequence Coverage**	***Homo sapiens*** **putative orthologues**
Heat shock protein YG100	48%	HSPA8
Phosphoglycerate kinase	36%	PGK1
Inhibitory regulator protein IRA2	32%	NF1
ORF YOR371c	28%	Unknown
Pyruvate kinase 1	28%	PKM2
Mannose-1-phosphate guanyltransferase	25%	GMPPA
prion protein RNQ1	23%	Unknown
Prohibitin	21%	PHB
Enolase	20%	ENO1
GBLP	19%	RACK1
Fructose-bisphosphate aldolase	18%	ALDOC
ATP synthase beta chain	17%	ATPB
ADP,ATP carrier protein 2	16%	SLC25A5
Chaperone protein MSI3	14%	HSPH1
GRP 78	13%	HSPA5
Glycyl-tRNA synthetase	12%	GARS
V-ATPase A subunit	10%	ATPA
URA1	9%	CPS1
Inhibitory regulator protein IRA1	8%	NF1

Table 4.1: Table shows a list of proteins that were identified from two independent Mass Spectrometry experiments using Ira2-TAP fusion protein as baits.

Chapter 5: Upb6 and CK2 Positively Regulate Ira2 Activity

5.1 Background

In chapter 4, I utilized the TAP-tagged strategy to identity proteins that directly interact with Ira2 to regulate its activity. To further determine the mechanism underlying the molecular signaling pathways that control Gpb1-induced down-regulation of Ira2, I wished to investigate the protein complex that binds to Gpb1. Again, I utilized the tandem-affinity purification strategy coupled with mass spectrometry to identity protein complexes that interact with Gpb1.

I identified previously unknown proteins interacting with Gpb1 to regulate Ira2. I found the CK2 kinase binds and phosphorylates Ira2, thereby preventing Gpb1-induced Ira2 proteolysis. Consistent with the proposal that Ira2 is a target of the ubiquitination machinery, I found that the de-ubiquitination enzyme Ubp6 binds and positively controls Ira2 levels. This chapter describes the functional studies of Gpb1- and Ira2-associated proteins and their molecular activity in yeast cells.

5.2 Results

Identification of Gpb1 Binding Partners

Since Gpb1 negatively regulates Ira2 protein degradation, I want to identify novel protein complexes that associate with Gpb1 to better understand the underlying molecular networks connecting Gpb1 and Ira2. Since Gpb1 has a kelch repeat domain spanning its C-terminus and an UBA domain at the N-terminus, I hypothesize that Gpb1 could bind to a network of proteins that regulate Ira2 depending on signals received from the cellular environment. I therefore performed the TAP-pull down experiment using Gpb1-TAP as a bait (Figure 5.1 and Table 5.1).

Rack1, which was identified as an Ira2 binding partner by this approach, was also found in the mass spectrometry analysis. The COP1-beta subunit that has a WD40 repeat domain similar to Rack1 is also present. Of interest is the protein Rpn1, a subunit of the proteasome which previously has been shown to be responsible for delivering ubiquitin-conjugated substrates to the proteasome for protein degradation. Interestingly, I also found the deubiquinating enzymes Upb15 and Rpn11 were also found to bind to Gpb1. Previous publications have revealed that deubiquitinating enzymes can bind to Ira2, including Upb15, Rpn11 and Upb6 (Collins et al., 2007). The casein kinase 2-alpha, an ubiquitously expressed serine/threonine kinase that was previously found to bind to G protein beta subunits, also co-purified with Gpb1. A full list of proteins that were in our mass spectrometry analysis is presented in the Supplementary Figure 5.1 and Table 5.1.

I then sought to determine whether any of these putative Gpb1-binding partners is required for mediating Gpb1's effects on Ira2. Therefore, I cloned all of the ORFs corresponding to encoding proteins that were identified in our Gpb1-pull down experiment, including Cob1-beta, CK2-alpha, Rpn1, the deubiquitination enzymes Ubp15 and Ubp6. I expressed these genes in the *IRA2-3FLAG/GPB1-TAP* or *IRA2-3FLAG/gpb1Δ* mutant strain and assessed the Ira2 activity.

Binding of Rpn1 to Ira2 is mediated by Gpb1 and promotes Ira2 degradation

Gpb1 is a negative regulator of Ira2 and is necessary for Ira2 degradation. Rpn1 is a component of the proteasome base subunit and is responsible for recognizing and delivering ubiquitin-conjugated substrates to the proteasome for protein degradation (Elsasser et al., 2002). The mass spectrometry analysis identifies Rpn1 as a binding partner for Gpb1, therefore I

hypothesize that Rpn1 could promote Ira2 degradation.   To test our hypothesis, I cloned *RPN1*

ORF into the GAL1 promoter plasmid *(pDEST52)* and determined whether overexpression of

Rpn1 leads to Ira2 degradation. p*GAL1-RPN1-V5* overexpression promotes degradation of Ira2

after 2hrs, indicating its important role in regulating Ira2.

In the TAP-tagged pull-down experiments, Rpn1 co-purifies with Gpb1, but not with Ira1. I

hypothesized that Gpb1 first interacts with Ira2 and promotes the conjugation of ubiquitin chains

to Ira2. After interacting with Ira2, Gpb1 recruits the modified ubiquitin-conjugated Ira2 to the

proteosome by interacting with Rpn1. Therefore, I examined whether Gpb1 is required for Ira2

binding to Rpn1. Rpn1 is expressed in either *IRA2-3FLAG/GPB1-TAP* or *IRA2-3FLAG/gpb1Δ*

strain and immunoprecipitation experiments were performed. I found that Ira2 associates with

Rpn1 only in the presence of Gpb1 (Figure 5.3). This data is consistent with the finding that

expression of Rpn1 fails to promote Ira2 proteolysis in *IRA2-3FLAG/Δgpb1* mutant (data not

shown). Therefore, I conclude that Gpb1 targets Ira2 for proteasomal degradation by interacting

with the proteasome base subunit Rpn1.

Deubiquitinating enzyme Ubp6 is required for Ira2 deubiquitination

While ubiquitin-mediated degradation of proteins is a critical mechanism regulating cellular

signaling processes, recent studies report the role of deubiquitinating enzymes in regulating

physiological protein levels at the proteasome (Hanna et al., 2006; Hanna et al., 2007). In this

system, I have identified Gpb1 as a critical negative regulator of Ira2 by promoting Ira2

proteolysis. I further show that some Gpb1 binding partners are components of the proteasome.

In particular, I show that Gpb1 is required for Rpn1-mediated proteolysis of Ira2. Through our

pull-down experiments I have identified two binding partners of Gpb1 that are known to be deubiquitinating enzymes. The Rpn11 protein has previously been shown as the deubiquitinating enzyme that is important for processing and recycling ubiquitin while delivering the substrates to the proteasome core for protein degradation (Guterman and Glickman, 2004; Verma et al., 2002). In contrast, Upb15 has not been studied extensively. In addition, ubp6 is a deubiquitinating enzyme that has recently been reported to bind to Gpb1 and Ira2 in system wide proteomic study (Collins et al., 2007), However, the functional role of the Ubp6-Ira2 interaction has not been investigated.

Furthermore, Ubp6 can bind Rpn1 or ubiquitin-conjugated proteins that are argeted for proteasomal proteolysis. Similar to Rpn1, Ubp6 possesses a ubiquitin-like (Ubl) domain at its N-terminus and has previously been shown to associate with the proteasome by binding to Rpn1 (Wyndham et al., 1999). Recently, Upb6 functionality studies have revealed its critical roles in delaying proteasomal activities to gradually deubiquitinating ubiquitin-conjugated substrates at the proteasome (Hanna et al., 2007).

To examine the potential role of Ubp6 as a deubiquitinating enzyme for Ira2, I expressed Ubp6-HA in the *IRA2-3FLAG/GPB1-TAP* strain and Ira2 protein levels were assessed. Figure 5.4 shows over-expression of Ubp6 causes an increase in Ira2 protein levels. I found Gpb1 association with Ira2 is greatly reduced when Ubp6 is expressed, suggesting a competing role for Ubp6 and Gpb1 in regulating Ira2 protein stability (Figure 5.5). Interestingly, I found Ubp6 directly binds to Ira2 independent of Gpb1 (Figure 5.5) which is in contrast to Rpn1 association with Ira2 where Gpb1 is required.

Finally, I confirmed Ubp6 as the deubiquitinating enzyme for Ira2 by treating yeast cells with MG132 and investigated whether expression of Ubp6 can reduce the accumulation of

unibiquitinated Ira2 isoforms. I found inhibiting the proteasome activity with MG132 greatly

increases polyubiquitination of Ira2. However, Ubp6 expression reduced the Ira2

polyubiquitination levels (Figure 5.6), possibly by removing conjugated-ubiquitin from Ira2 and

therefore reduced Ira2 protein degradation level. Taken together, I have discovered that Ira2 is a

substrate for the deubiquitinating enzyme Ubp6 and that over-expression of Ubp6 can increase

Ira2 protein levels and stability.

CK2 phosphorylates and stabilizes Ira2

In addition to the proteasome machinery targeting neurofibromin for protein degradation,

according to the current model, neurofibromin is also a target of protein kinases, including PKA,

PKC and other unknown serine/threonine kinases (Boyer et al., 1994; Cichowski et al., 2003;

Izawa et al., 1996; Mangoura et al., 2006). In the mass spectrometry analysis of the Gpb1-TAP

pull-down, I have identified the catalytic α-subunit of casein kinase 2 (CK2) as a binding partner

of Gpb1. CK2 is an evolutionarily conserved serine/threonine protein kinase with roles in cell

growth, proliferation and inhibition of apoptosis (Ahmed et al., 2002).

Therefore, I investigated whether CK2 can directly regulate Ira2. First, I performed

immunoprecipitation experiments to examine whether Gpb1 can bind to CK2. I used the same

protein-tagged strategy described above to endogenously tag the *GPB1* ORF with *3FLAG* in the

CK2-TAP yeast strain and tested their interactions in vivo. I found that CK2 can readily bind to

Gpb1 (Figure 5.7). Since neurofibromin has been previously shown to be phosphorylated on

serine residues, I hypothesize that CK2 could phosphorylate and directly regulate Ira2 function.

To test this hypothesis, I overexpressed CK2 in *IRA2-3FLAG/GPB1-TAP* or *IRA2-*

3FLAG/gpb1Δ yeast strains and performed immunoprecipitation experiments with anti-Flag antibody. Interestingly, I found Ira2 can interact with CK2 independently of Gpb1 (Figure 5.8). Previous studies have demonstrated that expression of CK2 resulted in deactivation of MEK/Erk/MAPK signaling pathway. Therefore, I investigated whether expression of CK2 has any effect on Ira2. I induced p*GAL1-CK2-V5* expression in the *IRA2-3FLAG/GPB1-TAP* strain and monitored Ira2 protein levels at increasing CK2 concentrations by treating cells with galactose at different time points. Surprisingly, I found that CK2 overexpression increases both Gpb1 and Ira2 protein levels (Figure 5.9). Although I do not know the precise mechanism that causes upregulation of Gpb1 when CK2 is over expressed, I can only speculate that when forced CK2 expression increases Ira2 stability and thus down regulation of Ras, cells might activate a positive feedback pathway in an attempt to down regulate Ira2 to physiological concentration, therefore causing an increase in Gpb1protein levels. Further studies are needed to address this possibility.

The data obtained in Figure 5.9 lead us to hypothesize that overexpression of CK2 might modify Ira2, therefore inhibiting Gpb1 from interacting with Ira2. To address this possibility, I expressed CK2 and immunoprecipitated Ira2 and Gpb1protein complexes. Figure 5.10 reveals the dissociation of Gpb1from Ira2, or Ira2 from Gpb1 complexes while both Gpb1 and Ira2 protein levels were increased under the same condition in the total lysate analysis. Since CK2 can directly bind and positively regulate Ira2 protein levels, I tested whether CK2 can phosphorylate Ira2 in vivo by expressing the p*GAL1-CK2-V5* plasmid in the *IRA2-3FLAG/ CK2Δ* mutant strain, where endogenous CK2 is genetically deleted. For comparison, I also generated a catalytically inactive mutant p*GAL1-CK2K169A-V5 (K169A)* which was previously shown to be unable to phosphorylate its substrates (Heriche et al., 1997). Wild type or mutant

K169A was induced with galactose for 3hrs and normalized total lysates were immunoprecipitated for Ira2-Flag and Istern blotted with anti-serine/threonine antibodies. I found that CK2 expression can readily phosphorylate Ira2 but not the control or the inactive mutant K169A (Figure 5.11). Furthermore, only wild type CK2 causes increased Ira2 protein levels but not control or CK2 mutant K169A (Figure 5.11). Therefore, I concluded that CK2 phosphorylates and stabilizes Ira2 protein levels, thereby preventing Gpb1 mediated protein degradation.

Finally, I addressed whether CK2 phosphorylation could restore Ira2 activity *in vivo* by performing heat shock experiments. Single deletion *ira1Δ* and *ira2Δ* or the double deletion *ira1Δ/ira2Δ* mutant strains were transformed with the p*GAL1-CK2-V5* plasmid and their heat shock sensitivities were examined. I found CK2 overexpression increases Ira2 activity and causes *ira1Δ/IRA2* to be resistant to higher temperatures, indicating CK2 can restore Ira2 activity in vivo. Similar to our previous heat shock experiments, the *ira2Δ*/IRA1 mutant is less responsive under our experimental conditions, possibly due to the specificity of Gpb1 toward Ira2 rather than Ira1 (Figure 5.12).

5.5 Discussion

The observation that Gpb1 negatively regulates Ira2 led us to further investigate novel proteins association with Ira2. I demonstrated that the ubiquitinating enzyme Ubp6 and the serine/threonine kinase CK2 can interact and positively regulate Ira2 function. Here, I showed CK2 overexpression results in increased Ira2 activity. CK2 is a constitutively active serine/threonine kinase enzyme and is up regulated in different types of human cancers (Ahmad

et al., 2005; Issinger, 1993; Pinna, 1997). CK2 can phosphorylate many substrates responsible for cell survival, stress response, and growth signaling pathways (Ahmed et al., 2002). Although I found here that overexpression of CK2 can phosphorylate Ira2 and prevent Gpb1-mediated degradation of Ira2 (Figure 5.10), I also believe CK2 inhibition of the heat shock sensitivity in the *ira1* or *ira2Δ* mutant strains (Figure 6F) were also indirect by having CK2 phosphorylating many different substrates (Meggio and Pinna, 2003). CK2 overexpression has previously been shown to downregulate Ras-induced oncogenic cell transformation (Heriche et al., 1997), possibly by targeting the RAF/MAPK pathway downstream of Ras (Lebrin et al., 1999). Here I provided evidence to further support the molecular connection between CK2 and the Ras signaling pathway. Previous studies have shown neurofibromin is targeted for proteasomal degradation in response to growth factor stimulation (Cichowski et al., 2003). Whether CK2 can directly phosphorylate neurofibromin to prevent proteasomal degradation is unknown. Therefore the next logical step is to investigate whether CK2 can directly phosphorylate neurofibromin in human cells and whether treating cells with RNAi or inhibitors targeting CK2 activity will alter neurofibromin stability.

The observations that Upb6 can positively regulate Ira2 by promoting deubiquitination of Ira2 (Figure 5.4) further supports the current working model that Ira2 is targeted for ubiquitin-conjugation and protein degradation at the proteasome. Upb6 and Rpn11 are the two known deubiquitination- associated proteins at the proteasome in yeast responsible for deubiquitinating ubiquitin-conjugated substrates (Guterman and Glickman, 2004; Leggett et al., 2002; Verma et al., 2002; Yao and Cohen, 2002). Although I found both Rpn11 and Ubp6 binding to Ira2, I was more interested on characterizing Ubp6 activity toward Ira2 because Ubp6 has been previously reported to bind to Rpn1 at the base of the proteasome (Leggett et al., 2002). The results show

Rpn1 negatively regulates Ira2 in a Gpb1-dependent mechanism. In contrary, Upb6 positive regulation of Ira2 does not depend on the presence of Gpb1, further support the data that Gpb1 is responsible for Ira2 proteolysis as well as delivering the ubiquintin-conjugated Ira2 to the proteasome. An example of multiple E3 ligases involved in substrate modifications is the ubiquitinating mechanisms regulating p53 function in mammalian cells (Hirano and Ronai, 2006; Salmena and Pandolfi, 2007). The data also raise several questions regarding deubiquitinating enzymes and their regulatory roles in regulating neurofibromin. Clearly, more studies are needed in order to address the role of deubiquinating enzymes in association with neurofibromin in mammalian cells.
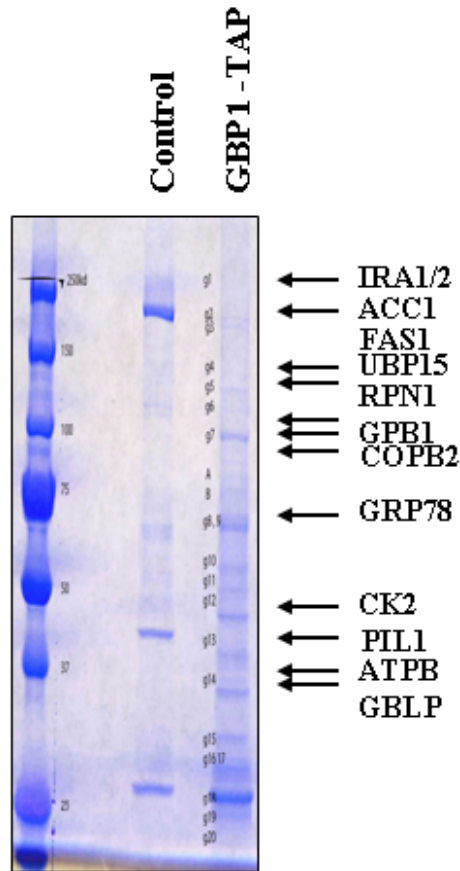
Figure 5.1: TAP purification of Gpb1 protein binding partners in yeast cells. Gpb1-TAP fusion protein is expressed endogenously. Yeast strain was purchased from TAP library generated by Ghaemmaghami and coworkers (Ghaemmaghami et al., 2003). Gpb1-TAP co-purified protein complexes were resolved by NuPAGE gel electrophoresis and identified by mass spectrometry (experiment procedure). Control sample was from wild-type yeast cells expressing a TAP-tagged protein fragment unrelated to GPB1 signaling (Control). Mass spectrometry protein analysis of protein bands were compared between Gpb1 and control samples. All positive hits were included in Supplementary Table 2.
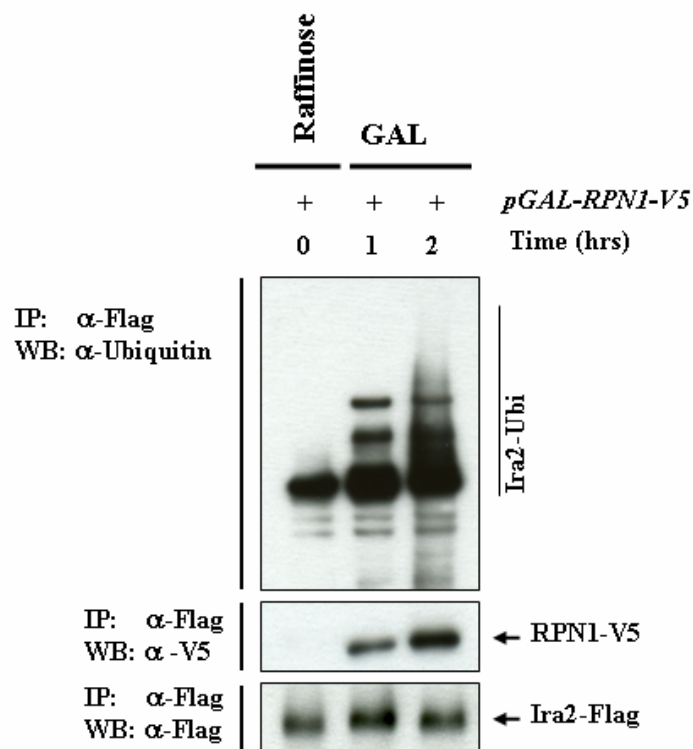
Figure 5.2: Rpn1 promotes Ira2 proteolysis is dependent on Gpb1. (A) Over-expression of *RPN1-V5* was performed in Ira2-Flag yeast strain to assess Ira2 ubiquitination activities. Cells were stimulated with Galactose for Rpn1 induction at different time points as indicated. Immunoprecipitation (IP) of Ira2 was performed with anti-Flag and immunoblotting (WB) with anti-ubiquitin antibodies. The membranes were immunoblotted with anti-V5 and anti-Flag antibodies to determine Rpn1 binding to Ira2 protein.
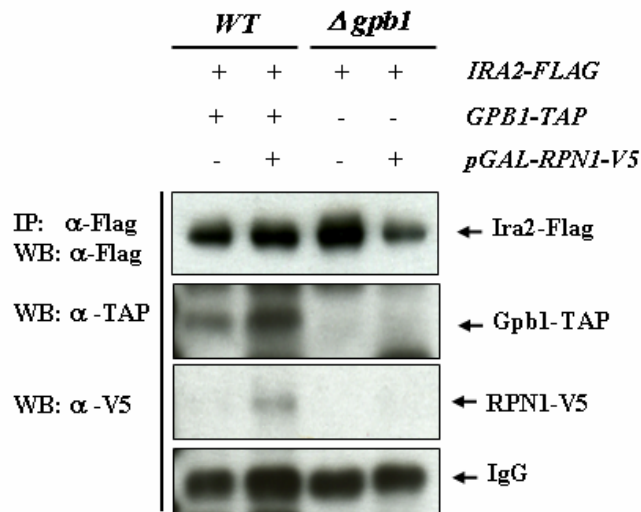
	WT		Δgpb1		
	+	+	+	+	*IRA2-FLAG*
	+	+	-	-	*GPB1-TAP*
	-	+	-	+	*pGAL-RPN1-V5*

IP: α-Flag
WB: α-Flag   ← Ira2-Flag

WB: α-TAP   ← Gpb1-TAP

WB: α-V5   ← RPN1-V5

← IgG

Figure 5.3: Rpn1 promotes Ira2 proteolysis is dependent on Gpb1. Rpn1 binding to Ira2 is dependent on Gpb1. *IRA2-3FLAG/GPB1-TAP* (WT) and *IRA2-3FLAG/gpb1Δ (Δgpb1)* were grown in log phase and immunoprecipitated (IP) with anti-Flag antibodies. Membranes were subjected to immunoblotting (WB) with anti-Flag, anti-V5, and anti-TAP antibodies as indicated to the right. IgG showed in the lower panel to serve as control for equal protein loading.
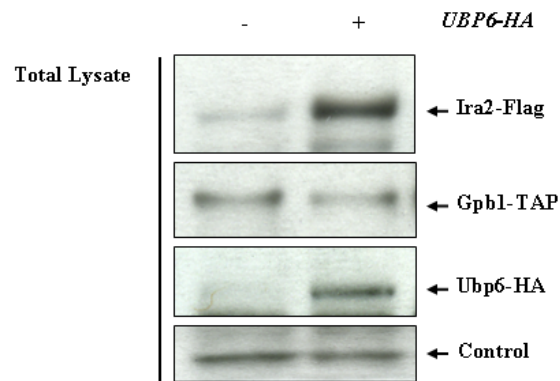
Figure 5.4: Upb6 deubiquitination of ubiquitin-conjugated Ira2. Overexpression of the deubiquitinating enzyme HA-Ubp6 causes an increase in Ira2 protein level. Lysates were normalized and subjected to Western blotting with anti-Flag or anti-HA antibodies. Membrane was blotted using anti-Ydj1 antibody to control for equal protein loading.
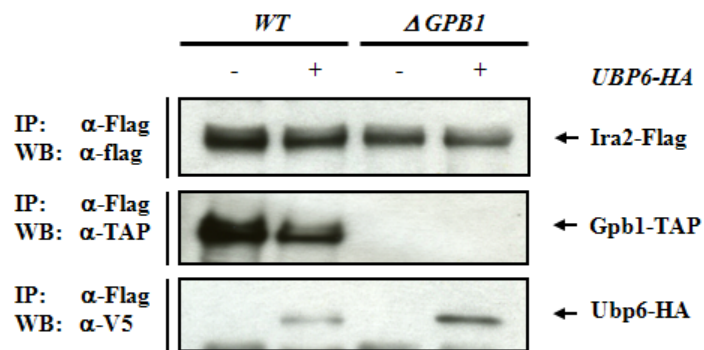
Figure 5.5: Ubp6 binds to Ira2 is Gpb1-independent. HA-Ubp6 was expressed in the *IRA2-3FLAG/GPB1-TAP* (WT) and the *IRA2-3FLAG/gpb1 Δ (Δ GPB1)* the yeast strains and equal protein concentrations were subjected to immunoprecipiation (IP) followed by immunoprecipitation with anti-Flag, anti-TAP or anti-HA antibodies. Ubp6 expression reduces Gpb1 binding to Ira2.
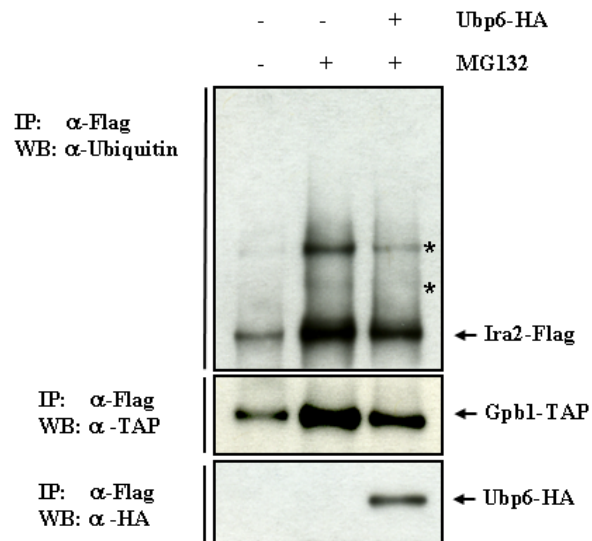
Figure 5.6: Over expression of Ubp6 reduces enriched Ira2 ubiquitination. *IRA2-FLAG* yeast strain received empty or *UPB6-HA* plasmids were treated with either vehicle or 10uM of the proteasome inhibitor MG132 for 12hrs. Total lysates were immunoprecipitated (IP) with anti-Flag and analyzed by Western blotting (WB) with anti-ubiquitin, anti-TAP or anti-HA antibodies.
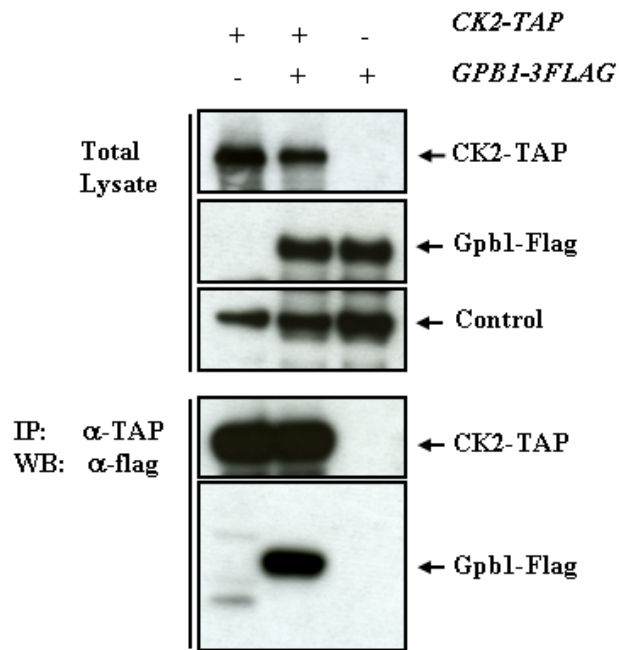
Figure 5.7: CK2 binds to Gpb1. Yeast cells endogenously expressing CK2-TAP, and CK2-TAP /Gpb1-Flag, or Gpb1-Flag fusion proteins were immunoprecipitated (IP) with IgG-conjugated glutathione beads, followed by Western blotting with anti-TAP and anti-Flag antibodies as indicated to the right (lower panel). Total lysates were Western blotted (WB) using anti-TAP and anti-Flag antibodies. Membrane was blotted using anti-Ydj1 antibody (control) for equal protein loading (total lysate, top panel).
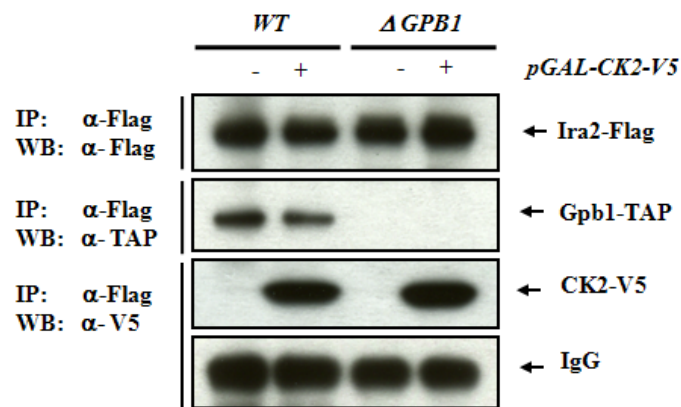
Figure 5.8: CK2 binding to Ira2 is Gpb1- independent. *IRA2-3FLAG/GPB1-TAP* (WT) and *IRA2-3FLAG/gpb1Δ (Δ GPB1)* were grown in log phase and immunoprecipitated (IP) with anti-Flag antibodies. Membranes were subjected to Western blotting (WB) with anti-Flag, anti-V5, and anti-TAP antibodies as indicated to the right.
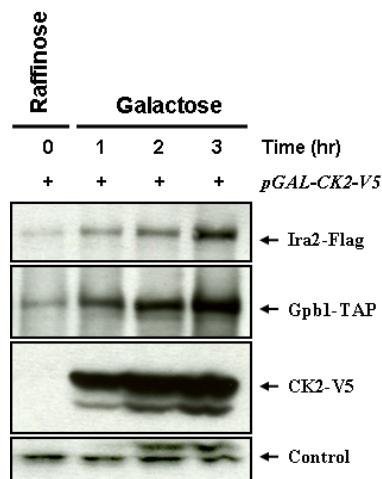
Figure 5.9: Induced CK2 expression increases Ira2 protein levels. p*GAL1-CK2-V5* plasmid was expressed in *IRA2-FLAG/GPB1-TAP* yeast strain and CK2 was induced with galactose at the time points indicated. Total lysates with equal protein concentrations were Western blotted (WB) with anti-Flag, anti-TAP or anti-V5 antibodies as indicated on the right. Membrane was stripped and re-blotted with anti-Ydj1 antibody (control) for equal protein loading.
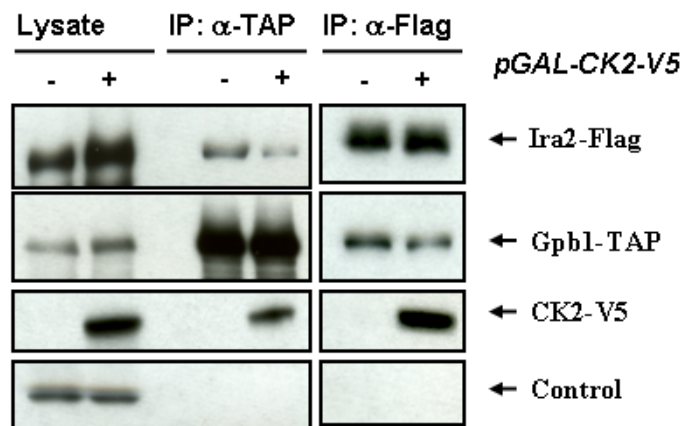
Figure 5.10: CK2 expression reduces Gpb1 binding to Ira2 complex. p*GAL1-CK2-V5*
plasmid was expressed in *IRA2-FLAG/GPB1-TAP* yeast strain. Cells were stimulated with
galactose for 3hrs. Total lysates were normalized, immunoprecipitated (IP) and Western blotted
(WB) with either anti-Flag or anti-TAP antibodies to determine Ira2 and Gpb1 association in the
presence or absence of CK2. Membranes were stripped and re-blotted with anti-Ydj1 antibody
(control) for equal protein loading.

A.

pGAL-CK2-V5

	-	Wt	K169A
Total Lysate			← Ira2-Flag
			← CK2-V5
			← Control

Human CK2α DHEHRKLRLID
Yeast CK2α MHRDVKPQNVMID
                          *

B.

pGAL-CK2-V5

	-	Wt	K169A
IP: α-Flag / WB: α-p-Ser/Thr			← p-Ira2-Flag
IP: α-Flag / WB: α-Flag			← Ira2-Flag
IP: α-Flag / WB: α-V5			← CK2-V5
			← IgG

Figure 5.11: CK2 wild-type, and not the CK2 mutant (K169A), phosphorylates Ira2 *in vivo*. Control (-), p*GAL1-CK2-V5* wild type (WT) and mutant (K169A) plasmids were expressed in *IRA2-FLAG/GPB1-TAP* yeast strain. Sequence alignment of human and yeast CK2 show the conserved K169 amino acid (*) at the catalytic pocket. The mutant plasmid was generated from the p*GAL1-CK2-V5* wild type plasmid by PCR-based site mutagenesis techniques and had previously been characterized (Heriche et al., 1997). Total lysates were Western blotted (WB) with anti-Flag and anti-V5 antibodies to assess Ira2 and CK2 protein levels. Blots were stripped and re-blotted with anti-Ydj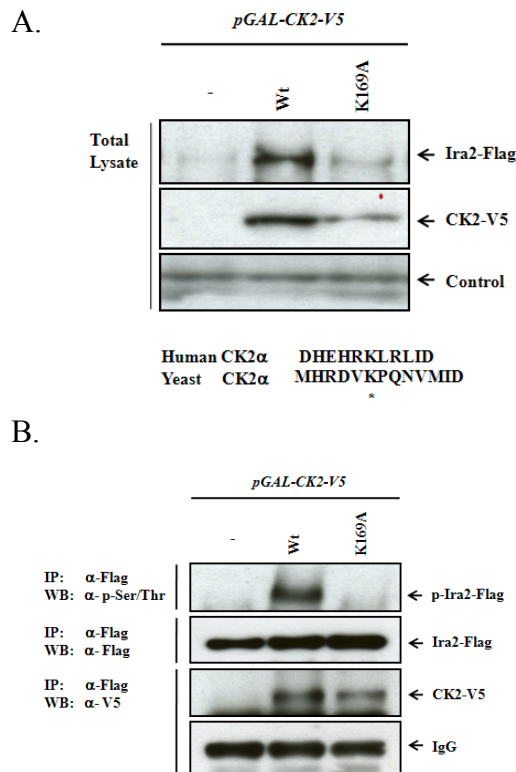1 antibody (control) for equal protein loading (upper panel, total lysate). For direct phosphorylation of serine/threonine residues of Ira2 in vivo, total lysates were normalized and subjected to immunoprecipitation (IP) and Western blotted (WB) with either anti-phospho serine/threonine, anti-Flag or anti-V5 antibodies to access Ira2-phosphorylated levels as well as Ira2 and CK2 protein levels (Lower panel).
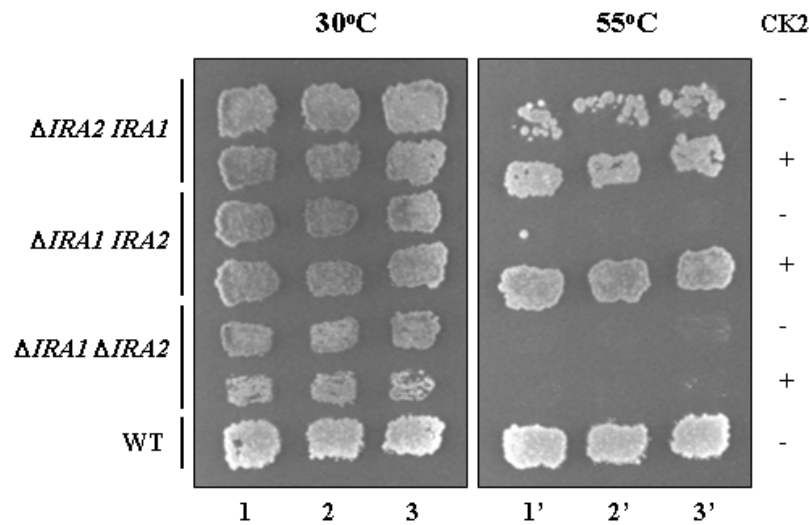
Figure 5.12: CK2 expression increases heat shock resistance in *ira2Δ IRA1* and *ira1Δ IRA2* mutant yeast strains. Galactose induced expression of CK2 causes heat shock resistance in mutant yeast strains when compared to cells that did not receive the plasmid (-). To assay for heat shock sensitivity, cells were replica plated onto GAL/-Ura3 plates and exposed to a high temperature chamber for either 55^0C for 60 minutes or unexposed to heat 30^0C. Plates were cooled down at room temperature for 30 minutes, incubated at 30^0C for 3-7 days before pictures were taken. Control cells were either from the double mutant *ira1Δ ira2Δ* (heat shock sensitive phenotype) and WT (heat shock resistant phenotype).

Table 2: Supplementary Report for Mass Spectrometry data for Gpb1 protein complexes	
S. cerevisiae **Protein Identified**	**% Sequence Coverage**
Gbeta mimic kelch protein 1 GPB1	56%
Receptor of activated protein kinase C 1	54%
Phosphofructokinase 1	30%
Inhibitory regulator protein IRA2	26%
Nuclear localization sequence-binding protein (p67)	26%
Protein BMH1	23%
Inhibitory regulator protein IRA1	19%
Plasma membrane ATPase 1	19%
Putative NADH-cytochrome b5 reductase	17%
Ubiquitin carboxyl-terminal hydrolase 15	14%
Fatty acid synthase subunit beta	13%
26S proteasome regulatory subunit RPN1	11%
Casein kinase II subunit alpha	11%
Acetyl-CoA carboxylase	9%
DEAD box protein 2	8%
Coatomer subunit beta	7%

Table 5.1: Gpb1-TAP fusion protein was used as bait. The table shows a list of proteins that were identified from the Mass Spectrometry experiment.

Chapter 6: ETEA/UBXD8 negatively regulates Neurofibromin

6.1 Introduction

Previous studies have shown that neurofibromin can be targeted for proteasome degradation upon growth factor stimulation (Cichowski et al., 2003). I showed in Chapter 3 that Ira2, the yeast homolog of neurofibromin, is targeted for ubiquitination and proteasomal degradation by Gpb1. Therefore, I hypothesized that there must be a mammalian protein functional equivalent to Gpb1 in human cells that is responsible for neurofibromin ubiquitination and degradation.

To better understand the molecular mechanisms underlying neurofibromin function and regulation, I utilized the tandem-affinity purification strategy coupled with mass spectrometry to identity protein complexes that directly interact with neurofibromin. This chapter describes the functional studies of the proteomic analysis that I carried out to identify ETEA association with neurofibromin.

6.2 Results

ETEA binds and negatively regulates neurofibromin

To identify the human homologue of Gpb1, I cloned neurofibromin into eight different fragments (Figure 6.2) and performed TAP-tagged pull-down experiments of several of these fragments (Fragments 4 and 5). I then analyzed the pull-down candidates using mass spectrometry as described in Experimental Procedures. Of the neurofibromin binding partners in our analysis, I found ETEA (UBXD8) to contain a ubiquitin-associated domain (UBA) at its N-terminus and a ubiquitin-related domain (UBX) at its C-terminus.

ETEA was first cloned in CD3-positive blood cells of patients with atopic dermatitis, an inflammatory skin condition characterized by an elevation of eosinophils due to an inappropriate immune response (Imai et al., 2002). I analyzed the sequence homology between ETEA and Gpb1 and found remarkable amino acid conservation, specifically at the N-terminal domains of Gpb1 and ETEA. Although ETEA lacks the kelch-repeat domain that is present in Gpb1, I found that Gpb1 and ETEA have a high degree of conservation in the amino acids 1 through 31. Therefore, I suggested that Gpb1 contains a UBA domain spanning amino acids 1 through 31 (Figure 4.11). Furthermore, I found that a domain of unknown function in Gpb1, amino acids 189 through 243, is conserved in ETEA (Figure 6.1). In addition, when I excluded the kelch-repeat domain of Gpb1 and compared only the N-terminal domain of Gpb1 to ETEA, I found the two proteins share approximately 18% homology. Importantly, these amino acids are less conserved in Gpb2 when I compared the Gpb2 amino acid sequence to ETEA and Gpb1 (data not shown).

To investigate whether ETEA can directly bind to neurofibromin, I expressed Flag-ETEA in 239T cells and performed immunoprecipitation and immunoblotting experiments. I found ETEA directly binds to endogenous neurofibromin *in vivo* (Figures 6.1). To determine which domain of neurofibromin interacts with ETEA, I co-transfected Flag-tagged neurofibromin fragments (1 through 8) and TAP-ETEA in 293T cells. Immunoprecipitation assays were performed in the total cell lysates (Figures 6.2 and 6.3). I found ETEA directly interacts with three neurofibromin fragments spanning amino acids 372-1552, with the strongest interaction with the fragment expressing amino acids 1176 through 1552 (fragment 4, including the GAP-related domain, GRD, Figure 6.2). This finding is consistent with the previous observations of Cichowski and coworkers in which neurofibromin fragments containing the neurofibromin-GRD were targeted

110

for degradation by the proteasome machinery (Cichowski et al., 2003). Our binding experiments reveal ETEA binds to neurofibromin at amino acids 372 through 1552, with the strongest interaction at amino acids 1176 through 1552. Figure 6.3 shows the protein expression levels of the different NF1 Flag-tagged fragments. To investigate whether ETEA can directly bind to neurofibromin-GRD *in vitro*, I utilized a rabbit reticulocyte-coupled transcription/translation system and performed immunoprecipitation experiments. I found that neurofibromin-GRD directly binds to ETEA (Figure 6.2). Therefore, the interaction between ETEA and neurofibromin is direct, and ETEA interacts with neurofibromin within regions that were previously identified as critical for neurofibromin degradation (Cichowski et al., 2003).

Silencing of ETEA stabilizes neurofibromin and downregulates Ras activity

I next utilized the short hairpin interfering RNA (shRNA) technique to examine whether reducing the expression of ETEA would stabilize neurofibromin as this would be an indication that ETEA is directly responsible for neurofibromin degradation. I generated stable cell lines expressing three different shRNA plasmids targeting the human *ETEA* transcription sequences (Sh576, Sh578 and Sh580, Open Biosystems). When compared to unstransfected or control RNAi samples, reduced *ETEA* expression by RNAi knock-down resulted in an increase in neurofibromin levels (Figure 6.4). The RNAi constructs Sh576 and Sh578 greatly reduced the ETEA levels while the construct Sh580 had a moderate impact on ETEA. Consistently, Sh576 and Sh578 RNAi expression resulted in greater increase in neurofibromin levels while Sh580 moderately induced neurofibromin when compared to control samples.

Neurofibromin is a RasGAP protein and directly regulates Ras signaling. I have demonstrated here that ETEA directly regulates neurofibromin. I next investigated whether RNAi reduction of the ETEA levels would downregulate Ras signaling. I generated stable cell lines expressing Sh578 or an empty vector as control and performed Istern blots to assess ERK phosphorylation or immunoprecipitation to detect active RasGTP levels. As shown in Figure 6B, under nonmitogenic growth conditions (serum concentrations of 0% and 1%), reducing ETEA levels markedly upregulated neurofibromin and as a result greatly reduced the basal levels of Ras and ERK signaling (Figure 6.5, lanes 1-4). At serum concentrations of 5% and 10%, decreased ETEA levels in Sh578 cell cells only modestly reduces ERK basal activity when compared to control samples. However, RasGTP levels were greatly reduced at 5% and 10% serum concentrations when ETEA is decreased (Figure 6.5, lanes 5-8). Neurofibromin loss of function leads to Ras activation and deregulation of both ERK and AKT pathways. I next examined whether targeting ETEA expression could reduce AKT phosphorylation in 293T and BT549 cell lines. Both of these cell lines normally have high basal AKT phosphorylation. I generated 293T and BT549 stable cell lines expressing ShRNA that targeted ETEA expression and performed immunoblots to examine AKT phosphorylation levels. As expected, reducing ETEA in both 293T and BT549 cells resulted in upregulation of neurofibromin and a decrease in AKT phosphorylation (Figure 6.6). Taken together, these results demonstrate that neurofibromin stability is controlled by ETEA and that targeting ETEA activity reduces Ras activity and downregulation of the ERK pathway. Furthemore, the data also demonstrate that in cells that display deregulation of AKT, reduced ETEA expression results in downregulation AKT activity.

The UBX domain of ETEA controls neurofibromin downregulation

Since ETEA has high degree of amino acid conservation when compared to Gpb1 and directly interacts with neurofibromin at amino acid sites that were previously identified responsible for neurofibronin stability (Cichowski et al., 2003), I hypothesize that ETEA targets neurofibromin for ubiquitination and degradation. To investigate this possibility, I expressed ETEA-V5 full-length (WT) in 293T and examined neurofibromin levels. I found overexpression of ETEA causes a decrease in endogenous neurofibromin protein levels when compared to an empty plasmid control (Figure 6.7). ETEA has both UBA and UBX domains, and while UBA has been shown to bind ubiquitinated substrates and deliver them to the proteasome for protein degradation, UBX domain has not been fully characterized. To investigate the mechanism by which ETEA regulates neurofibromin, I generated full-length and mutant constructs in which the UBX domain is deleted and overexpressed these constructs in 293T cells (Figure 6.7). Figure 6.7B shows overexpression of the truncated UBX domain (ETEA ΔUBX) was less affective in reducing neurofibromin levels compared to full-length ETEA (ETEA WT). I found the neurofibromin-GRD fragment can efficiently bind to ETEA (Figure 5D). To examine whether UBX deletion construct could bind to neurofibromin since ETEA ΔUBX failed to downregulate neurofibromin, I performed immunoprecipitation experiments of neurofibromin-GRD coexpressing either the wild-type or UBX-deleted ETEA in a rabbit reticulocyte-coupled transcription/translation system (Experimental Procedures). Figure 6.8 shows neurofibromin-GRD does efficiently bind to both ETEA wild-type and ETEA ΔUBX. These results indicate that ETEA targets neurofibromin for protein degradation. The UBX domain of ETEA is necessary for ETEA-mediated neurofibromin degradation and that deletion of the UBX domain does not hinder the ability of ETEA to bind efficiently to neurofibromin.

I next investigated the steady-state of neurofibromin to confirm that ETEA does indeed regulate neurofibromin degradation. 293T cells expressing control, ETEA WT, or ETEA ΔUBX constructs were treated with cycloheximide to inhibit *de novo* protein translation and neurofibromin levels were detected by immunoblotting at the indicated time of treatement. Overexpression of ETEA resulted in a decrease in neurofibromin levels. Surprisingly, neurofibromin levels were unchanged in control samples under cycloheximide treatment, suggesting that neurofibromin is highly stabilized in cells. In contrast to wild-type ETEA, ETEA ΔUBX did not induce degradation of neurofibromin (Figure 6.9), supporting our previous observations that ETEA ΔUBX failed to downregulate neurofibromin (Figure 6.7).

To examine whether ETEA induced neurofibromin ubiquitination, I purified GFP-control, ETEA-GFP or ETEA ΔUBX-GFP complexes from 293T cells and performed *in vitro* ubiquitination assays in a rabbit reticulocyte-coupled transcription/translation system expressing ^{35}S-labelled neurofibromin-GRD domain. I found wild-type ETEA complex can readily ubiquitinate neurofibromin *in vitro* (Figure 6.10, lane 4). Both GFP-control and ETEA ΔUBX-GFP complexes failed to ubiquitinate neurofibromin-GRD (Figure 6.10, lanes 3 and 5). Taken together, I conclude that ETEA ubiquitinates and targets neurofibromin for degradation and the UBX domain of ETEA is critical in mediating the ubiquitination of neurofibromin.

6.5 Discussion

Based on our finding that Ira2 is targeted for ubiquitination by Gpb1 and previous reports showing that growth factors are able to trigger neurofibromin degradation, I wished to identify the mammalian protein responsible for neurofibromin degradation. I showed here for the first

time the identification and functional analysis of a previously unknown UBA-UBX protein that targets neurofibromin for protein degradation. ETEA has an UBA domain at the N-terminus and a UBX domain at the C-terminus, and is found to be highly upregulated in T-cells and eosinophils of patients with atopic dermatitis, a chronic inflammatory skin disease (Imai et al., 2002). Surprisingly, I found a high level of amino acid conservation between ETEA and Gpb1 (Figure 5A), and loss of function analysis revealed ETEA to be critical for neurofibromin activity.   Neurofibromin is a RasGAP protein that plays pivotal roles in regulating many cell types and tissues. Loss of neurofibromin function results in Ras activation and tumor formation in both human and mouse models of NF1. Importantly, in NF1 mouse models, the heterozygous $Nf1^{+/-}$ mast cells are critical in contributing to tumor formation by infiltrating the distressed Ras-activated Schwann cells that excrete cytokine signals into the tumor microenvironment (Yang et al., 2003; Zhu et al., 2002). Clearly, positive control over neurofibromin function in heterozygous $Nf1^{+/-}$ mast cells and Schwann cells is needed to alleviate the tumor burden in patients with NF1.

Although more studies are needed to fully address the role of ETEA in neurofibromin regulation, these findings indicate that interfering with ETEA function increases neurofibromin levels and activity. Remarkably, reducing ETEA activity is effective at lowering active Ras levels, and downregulating the Ras downstream effectors, ERK and AKT (Figures 6.5 and 6.6). Therefore, future studies are needed to explore targeted ETEA function as a therapeutic strategy to treat NF1 tumors early in the course of or even prior to the onset of tumorigenesis in NF1 patients.
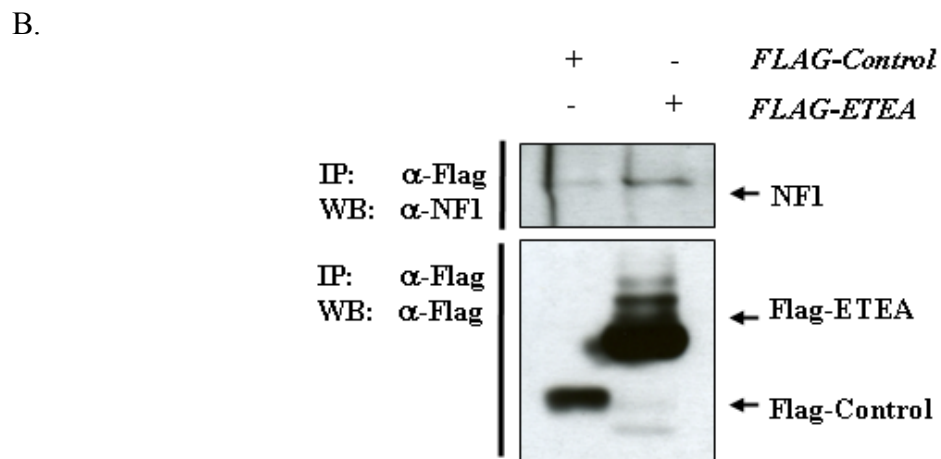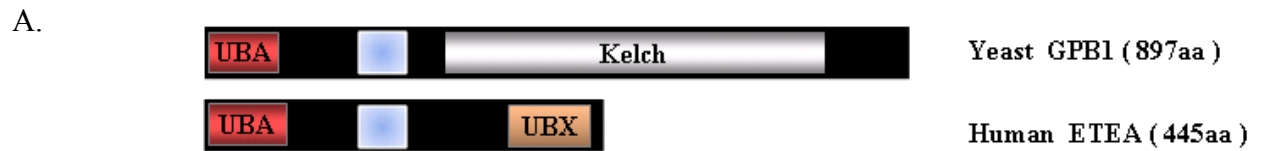
A.

B.

Figure 6.1: Identification of ETEA as a UBA-UBX protein that binds to neurofibromin.
(A) The N-terminal domain alignments of Gpb1 and ETEA. (B) ETEA binds to endogenous neurofibromin. Flag-tagged GFP (Flag-control) or ETEA-Flag were expressed in 293T cells and equal protein concentrations were subjected to immunoprecipitation (IP) followed by immunoprecipitation with anti-Flag and anti-neurofibromin antibodies. ETEA can bind to endogenous neurofibromin *in vivo*.
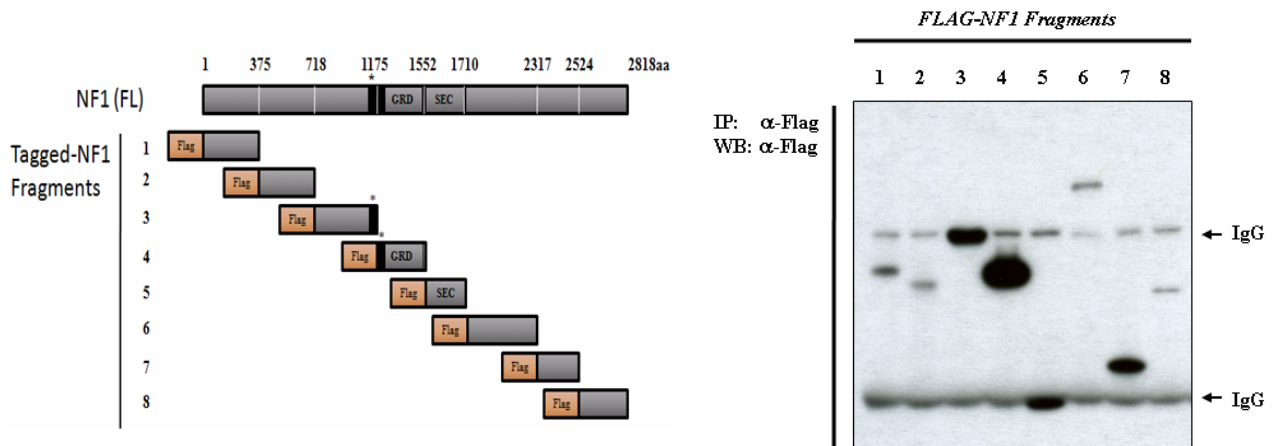
Figure 6.2: Expression of Flag-tagged neurofibromin fragments. Total lysates were immunoprecipitated (IP) with anti-Flag antibody and immunoblotted (WB) with anti-Flag antibody as indicated. Large and small IgG fragments are showed in the background (IgG).
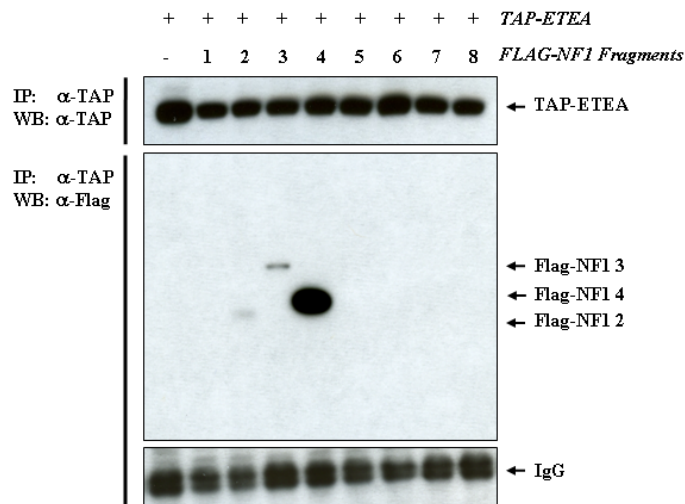
Figure 6.3: Neurofibromin domains bind to ETEA. Flag-tagged NF1 fragments and TAP-tagged ETEA were co-expressed in 293T cells. Total lysates were immunoprecipitated (IP) with anti-TAP antibody and immunoblotted (WB) with anti-Flag or anti-TAP antibodies as indicated to the right. IgG showed in the lower panel as loading control.
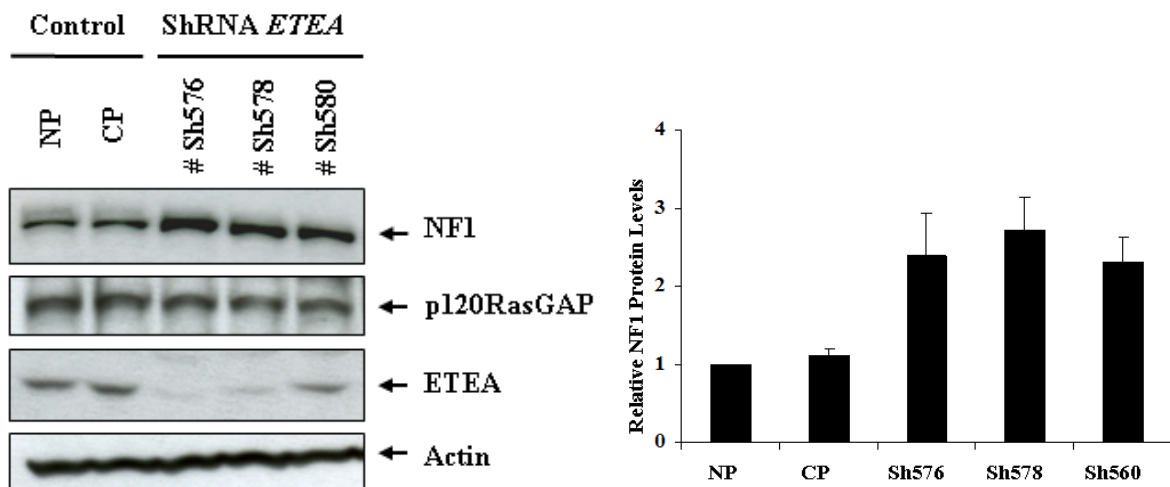
Figure 6.4: ShRNA targeting *ETEA* expression upregulates neurofibromin activity. (A) RNAi targeting *ETEA* transcription increases neurofibromin levels. 293T cells (no plasmid: NP) or 293T stable cell lines expressed control empty (CP) or three different shRNA plasmids (Sh576, Sh578, Sh580) targeting transcript sequences of *ETEA*. Total lysates were immunoblotted (WB) with the indicated antibodies to the right. For controls, membranes were blotted with anti-p120RasGAP or anti-actin antibodies. Quantitative analysis data of neurofibromin levels are presented in the right panel from three different experiments with error of the mean.
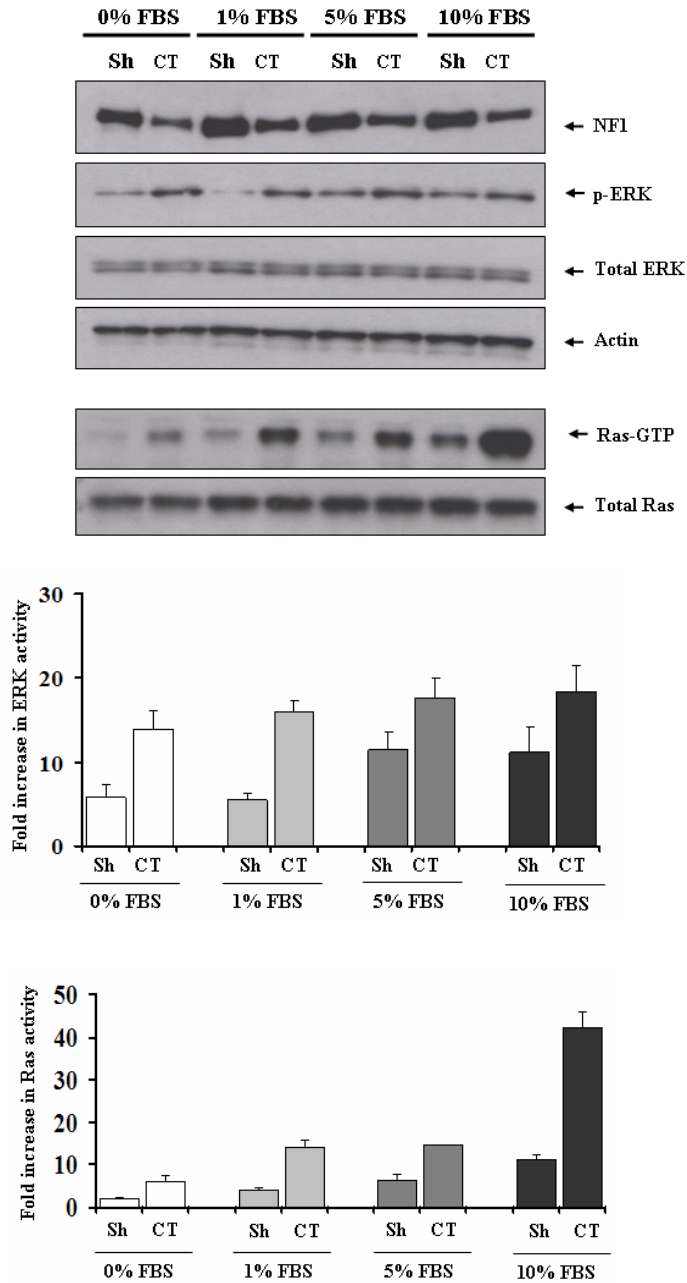
Figure 6.5: RNAi targeting *ETEA* transcription inhibits Ras and ERK activities. 293T stable cell lines expressed control (CT) or sh578 (Sh) plasmids were used to determine Ras and ERK activation at different serum concentrations (0%, 1%, 5% and 10%). Normalized protein levels were subjected to immunoblotting analysis with anti-bodies indicated to the right (left panel). Quantitative analysis data of RasGTP levels and ERK phosphorylation are shown in the right panel from four different experiments with error of the mean.
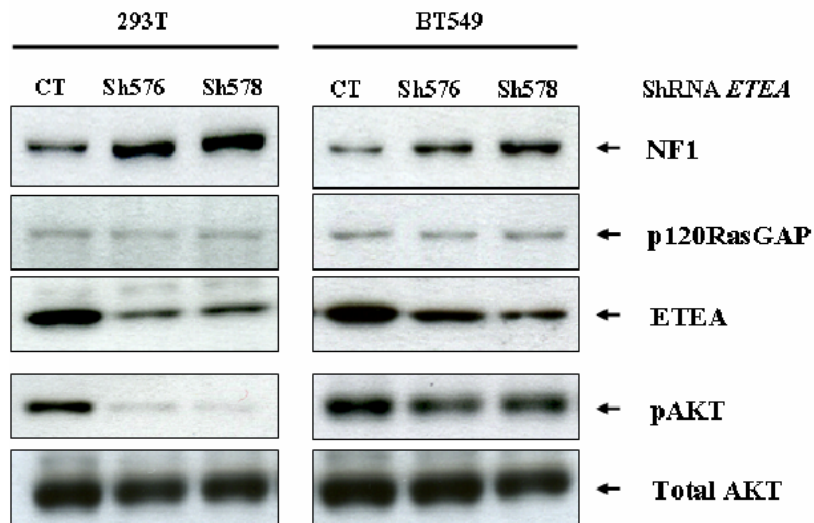
Figure 6.6: RNAi targeting *ETEA* transcription downregulates AKT phosphorylation in 293T and BT549 cell lines. 293T and BT549 stable cell lines expressed control plasmid (CT) or sh576 and sh578 targeting *ETEA* expression were used to determine neurofibromin levels and AKT phosphorylation at 1% serum concentration. Normalized protein concentrations were subjected to Western blotting analysis with anti-bodies indicated to the right (left panel).

A.

B.
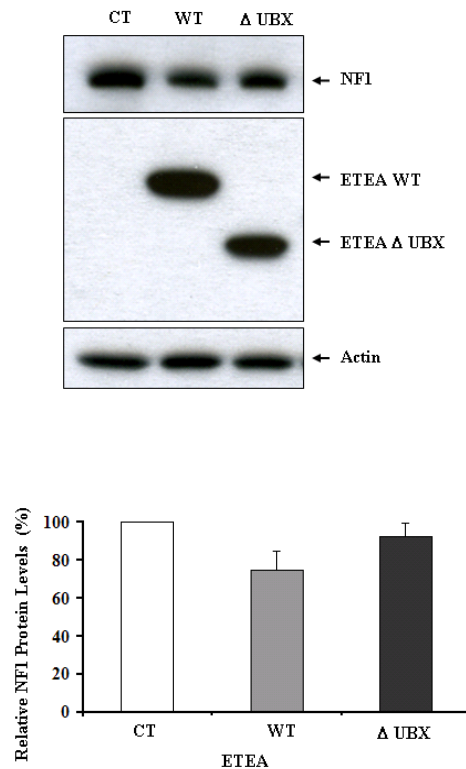
Figure 6.7: Functional analysis of ETEA UBX domain. (A-B) Overexpression of full-length, but not ETEA ΔUBX, reduces neurofibromin levels. Equal protein concentrations from 293T cell lysates expressing an empty control (CT), *ETEA-V5* (WT), or *ETEA ΔUBX-V5* (ΔUBX) plasmids were subjected to immunoblotting analysis (WB) with the indicated antibodies to the right. For control loadings, membranes were immunoblotted (WB) with anti-actin antibody.

+	+	+	*GST-NF1 GRD*
-	+	-	*ETEA-V5 WT*
-	-	+	*ETEA-V5 Δ UBX*

IP: GST

← GST-NF1 GRD

← ETEA WT
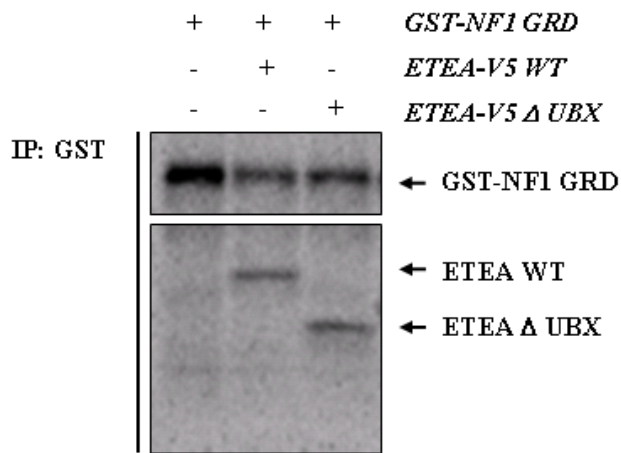
← ETEA Δ UBX

Figure 6.8: Neurofibromin-GRD binds to both ETEA full-length and ETEA ΔUBX *in vitro*.
^{35}S-labelled GST-GRD, ETEA-V5 full-length, and ETEA ΔUBX-V5 were coupled transcripted/translated in rabbit reticulocyte lysates and were co-immunoprecipited (IP) with sepharose conjugated glutathione beads and visualized by Storm860 PhosphoImager.
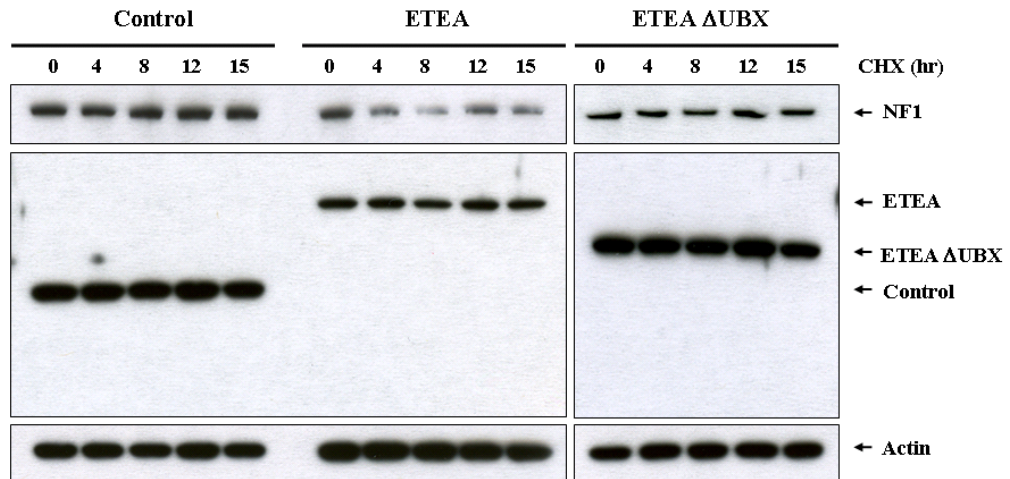
Figure 6.9: The UBX domain of ETEA controls neurofibromin stability. 293T cells were transfected with GST-GFP (CT), ETEA-V5 (WT) or ETEA ΔUBX-V5 (ΔUBX). Twenty-four hours after transfection, cells were treated with cycloheximide (CHX) at the time points indicated, and the half-life of neurofibromin was analyzed by immunoblotting with antibodies as indicated to the right.

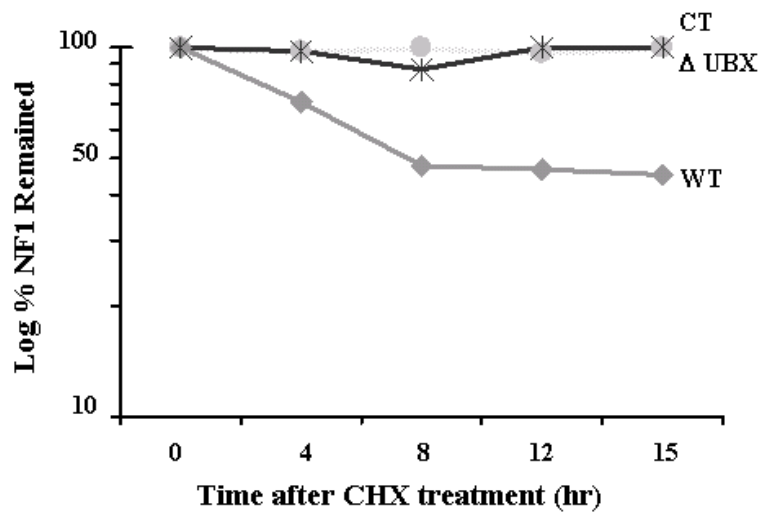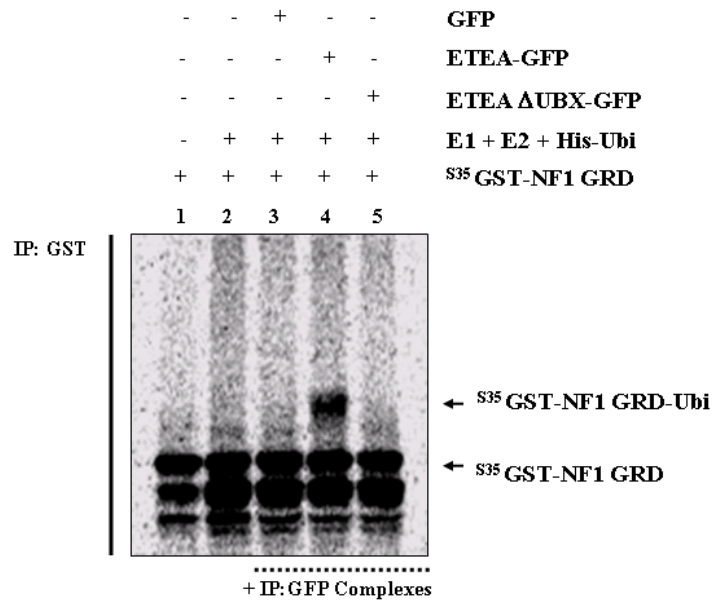**Figure 6.10: ETEA wild-type but not ETEA ΔUBX ubiquitinates neurofibromin *in vitro*.**
Ubiquitin ligation assay of ^{35}S-labelled GST-GRD was conducted *in vitro* in the absence or
presence of GST-GFP control, ETEA-GFP or ETEA ΔUBX-GFP complexes that were purified
from 293T cells. Samples were performed at 30°C for 90min. GST-GRD was co-
immunoprecipited with sepharose conjugated glutathione beads, separated by NuPage gel
electrophoresis and visualized by Storm860 PhosphoImager. ETEA activity was observed in
reactions containing ETEA wild-type (Lane 4) but not GFP-control or ETEA ΔUBX complexes.

Chapter 7: Conclusions and Remarks

The NF1 tumor suppressor gene product, neurofibromin, an important regulator of Ras, is known to be regulated by both protein kinases and ubiquitin-related enzymes. However, many of the proteins that interact with neurofibromin to either positively or negatively regulate its function still remain unknown. The budding yeast *Saccharomyces cerevisiae* has two neurofibromin homologues, Ira1 and Ira2. Similar to neurofibromin, loss of function studies have shown that deletion of Ira proteins result in activation of Ras and GPCR signaling pathways, indicating evolutionarily conserved functions between Ira proteins and neurofibromin.

In this study, I utilized genetic and proteomic approaches to identify proteins that can interact with and regulate Ira2 and neurofibromin. I found the ubiquitin-associated protein Gpb1 targets and ubiquitinates Ira2 for proteasomal degradation. In human cells, I found that the ETEA protein, a member of the UBA-UBX family of proteins, targets and ubiquitinates neurofibromin. Furthermore, I found that the UBX domain of ETEA is critical for neurofibromin ubiquitination and degradation. Figure 7.1 summarizes the current working models that are presented in this dissertation.

We hypothesized that upregulation of neurofibromin is important in controlling heterozygous *NF1* stromal cells from enhancing NF1 development. Neurofibromin protein proteolysis has been demonstrated to contribute to Ras activation. This study provided evidence that proteins interacting with Ira2 in yeast both positively and negatively regulate its functions. Furthermore, this study also demonstrated that it is possible to positively regulate neurofibromin functions. By interfering with the proteins associated with the proteasome pathway, it is possible to prevent the RasGAP proteins Ira2/neurofibromin from protein degradation.

In addition, I also demonstrated that the protein kinase CK2 and deubiquitination enzyme Ubp6 can independently and positively regulate Ira2 activity. Whether these proteins identified in yeast cells have any functional role in regulating neurofibromin activity are clearly needed to be addressed. The fact that the UBA-UBX protein ETEA can negatively regulate neurofibromin and Gpb1 can negatively regulate Ira2 demonstrated that, at least in part, that the ubiquitin-associated protein pathway is conserved. Clearly, future studies will provide additional insights into functional regulation of ETEA and neurofibromin on human diseases.

Working Model
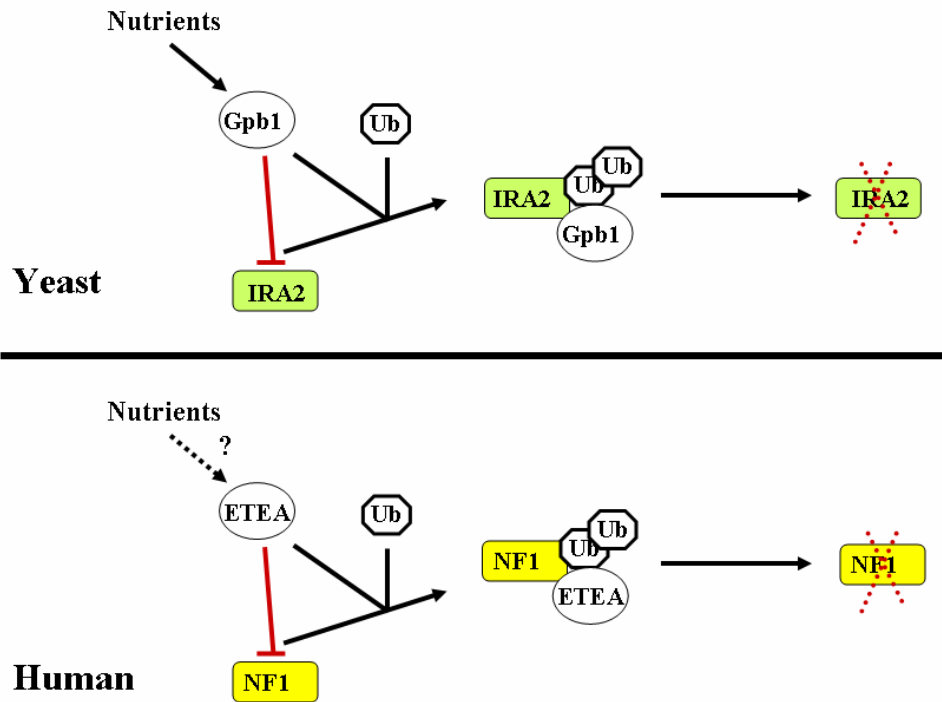

Figure 7.1: Working model for controlling Ira2 and neurofibromin proteins stabilization by Gpb1 in yeast and ETEA in human cells. (Yeast) Gpb1 negatively regulates Ira2 by inducing Ira2 ubiquitination. During glucose stimulation, Gpb1 down-regulates and ubiquitinates Ira2. (Humans) ETEA negatively regulates neurofibromin by directly binds and promotes ubiquitination of neurofibromin.

References

Ahmad, K.A., Wang, G., Slaton, J., Unger, G., and Ahmed, K. (2005). Targeting CK2 for cancer therapy. Anticancer Drugs *16*, 1037-1043.

Ahmed, K., Gerber, D.A., and Cochet, C. (2002). Joining the cell survival squad: an emerging role for protein kinase CK2. Trends Cell Biol *12*, 226-230.

Angers, S., Thorpe, C.J., Biechele, T.L., Goldenberg, S.J., Zheng, N., MacCoss, M.J., and Moon, R.T. (2006). The KLHL12-Cullin-3 ubiquitin ligase negatively regulates the Wnt-beta-catenin pathway by targeting Dishevelled for degradation. Nat Cell Biol *8*, 348-357.

Bader, J.L. (1986). Neurofibromatosis and cancer. Ann N Y Acad Sci *486*, 57-65.

Ballester, R., Marchuk, D., Boguski, M., Saulino, A., Letcher, R., Wigler, M., and Collins, F. (1990). The NF1 locus encodes a protein functionally related to mammalian GAP and yeast IRA proteins. Cell *63*, 851-859.

Bollag, G., and McCormick, F. (1991). Differential regulation of rasGAP and neurofibromatosis gene product activities. Nature *351*, 576-579.

Bourne, H.R. (1997). How receptors talk to trimeric G proteins. Curr Opin Cell Biol *9*, 134-142.

Bourne, H.R., Sanders, D.A., and McCormick, F. (1991). The GTPase superfamily: conserved structure and molecular mechanism. Nature *349*, 117-127.

Boyer, M.J., Gutmann, D.H., Collins, F.S., and Bar-Sagi, D. (1994). Crosslinking of the surface immunoglobulin receptor in B lymphocytes induces a redistribution of neurofibromin but not p120-GAP. Oncogene *9*, 349-357.

Cawthon, R.M., Weiss, R., Xu, G.F., Viskochil, D., Culver, M., Stevens, J., Robertson, M., Dunn, D., Gesteland, R., O'Connell, P*., et al.* (1990). A major segment of the neurofibromatosis type 1 gene: cDNA sequence, genomic structure, and point mutations. Cell *62*, 193-201.

Chu, S., DeRisi, J., Eisen, M., Mulholland, J., Botstein, D., Brown, P.O., and Herskowitz, I. (1998). The transcriptional program of sporulation in budding yeast. Science (New York, NY *282*, 699-705.

Cichowski, K., and Jacks, T. (2001). NF1 tumor suppressor gene function: narrowing the GAP. Cell *104*, 593-604.

Cichowski, K., Santiago, S., Jardim, M., Johnson, B.W., and Jacks, T. (2003). Dynamic regulation of the Ras pathway via proteolysis of the NF1 tumor suppressor. Genes Dev *17*, 449-454.

Colicelli, J. (2004). Human RAS superfamily proteins and related GTPases. Sci STKE *2004*, RE13.

Collins, S.R., Miller, K.M., Maas, N.L., Roguev, A., Fillingham, J., Chu, C.S., Schuldiner, M., Gebbia, M., Recht, J., Shales, M.*, et al.* (2007). Functional dissection of protein complexes involved in yeast chromosome biology using a genetic interaction map. Nature *446*, 806-810.

Colombo, S., Ma, P., Cauwenberg, L., Winderickx, J., Crauwels, M., Teunissen, A., Nauwelaers, D., de Winde, J.H., Gorwa, M.F., Colavizza, D.*, et al.* (1998). Involvement of distinct G-proteins, Gpa2 and Ras, in glucose- and intracellular acidification-induced cAMP signalling in the yeast Saccharomyces cerevisiae. Embo J *17*, 3326-3341.

Costa, R.M., Federov, N.B., Kogan, J.H., Murphy, G.G., Stern, J., Ohno, M., Kucherlapati, R., Jacks, T., and Silva, A.J. (2002). Mechanism for the learning deficits in a mouse model of neurofibromatosis type 1. Nature *415*, 526-530.

Dang, I., Nelson, J.K., and DeVries, G.H. (2005). c-Kit receptor expression in normal human Schwann cells and Schwann cell lines derived from neurofibromatosis type 1 tumors. Journal of neuroscience research *82*, 465-471.

Daston, M.M., and Ratner, N. (1992). Neurofibromin, a predominantly neuronal GTPase activating protein in the adult, is ubiquitously expressed during development. Dev Dyn *195*, 216-226.

Daston, M.M., Scrable, H., Nordlund, M., Sturbaum, A.K., Nissen, L.M., and Ratner, N. (1992). The protein product of the neurofibromatosis type 1 gene is expressed at highest abundance in neurons, Schwann cells, and oligodendrocytes. Neuron *8*, 415-428.

DeRisi, J.L., Iyer, V.R., and Brown, P.O. (1997). Exploring the metabolic and genetic control of gene expression on a genomic scale. Science (New York, NY *278*, 680-686.

Dohlman, H.G., and Thorner, J.W. (2001). Regulation of G protein-initiated signal transduction in yeast: paradigms and principles. Annu Rev Biochem *70*, 703-754.

Donovan, S., Shannon, K.M., and Bollag, G. (2002). GTPase activating proteins: critical regulators of intracellular signaling. Biochim Biophys Acta *1602*, 23-45.

Echard, A., Jollivet, F., Martinez, O., Lacapere, J.J., Rousselet, A., Janoueix-Lerosey, I., and Goud, B. (1998). Interaction of a Golgi-associated kinesin-like protein with Rab6. Science *279*, 580-585.

Edinger, A.L., Cinalli, R.M., and Thompson, C.B. (2003). Rab7 prevents growth factor-independent survival by inhibiting cell-autonomous nutrient transporter expression. Dev Cell *5*, 571-582.

Elsasser, S., Gali, R.R., Schwickart, M., Larsen, C.N., Leggett, D.S., Muller, B., Feng, M.T., Tubing, F., Dittmar, G.A., and Finley, D. (2002). Proteasome subunit Rpn1 binds ubiquitin-like protein domains. Nat Cell Biol *4*, 725-730.

Fabrizio, P., Gattazzo, C., Battistella, L., Wei, M., Cheng, C., McGrew, K., and Longo, V.D. (2005). Sir2 blocks extreme life-span extension. Cell *123*, 655-667.

Fabrizio, P., and Longo, V.D. (2003). The chronological life span of Saccharomyces cerevisiae. Aging cell *2*, 73-81.

Fabrizio, P., Pozza, F., Pletcher, S.D., Gendron, C.M., and Longo, V.D. (2001). Regulation of longevity and stress resistance by Sch9 in yeast. Science *292*, 288-290.

Gettemans, J., Meerschaert, K., Vandekerckhove, J., and De Corte, V. (2003). A kelch beta propeller featuring as a G beta structural mimic: reinventing the wheel? Sci STKE *2003*, PE27.

Ghaemmaghami, S., Huh, W.K., Bower, K., Howson, R.W., Belle, A., Dephoure, N., O'Shea, E.K., and Weissman, J.S. (2003). Global analysis of protein expression in yeast. Nature *425*, 737-741.

Guo, H.F., The, I., Hannan, F., Bernards, A., and Zhong, Y. (1997). Requirement of Drosophila NF1 for activation of adenylyl cyclase by PACAP38-like neuropeptides. Science *276*, 795-798.

Guterman, A., and Glickman, M.H. (2004). Complementary roles for Rpn11 and Ubp6 in deubiquitination and proteolysis by the proteasome. J Biol Chem *279*, 1729-1738.

Haas, A., Scheglmann, D., Lazar, T., Gallwitz, D., and Wickner, W. (1995). The GTPase Ypt7p of Saccharomyces cerevisiae is required on both partner vacuoles for the homotypic fusion step of vacuole inheritance. The EMBO journal *14*, 5258-5270.

Hanna, J., Hathaway, N.A., Tone, Y., Crosas, B., Elsasser, S., Kirkpatrick, D.S., Leggett, D.S., Gygi, S.P., King, R.W., and Finley, D. (2006). Deubiquitinating enzyme Ubp6 functions noncatalytically to delay proteasomal degradation. Cell *127*, 99-111.

Hanna, J., Meides, A., Zhang, D.P., and Finley, D. (2007). A ubiquitin stress response induces altered proteasome composition. Cell *129*, 747-759.

Harashima, T., Anderson, S., Yates, J.R., 3rd, and Heitman, J. (2006). The kelch proteins Gpb1 and Gpb2 inhibit Ras activity via association with the yeast RasGAP neurofibromin homologs Ira1 and Ira2. Mol Cell *22*, 819-830.

Harashima, T., and Heitman, J. (2002). The Galpha protein Gpa2 controls yeast differentiation by interacting with kelch repeat proteins that mimic Gbeta subunits. Mol Cell *10*, 163-173.

Harashima, T., and Heitman, J. (2005). Galpha subunit Gpa2 recruits kelch repeat subunits that inhibit receptor-G protein coupling during cAMP-induced dimorphic transitions in Saccharomyces cerevisiae. Mol Biol Cell *16*, 4557-4571.

He, Y.J., McCall, C.M., Hu, J., Zeng, Y., and Xiong, Y. (2006). DDB1 functions as a linker to recruit receptor WD40 proteins to CUL4-ROC1 ubiquitin ligases. Genes Dev *20*, 2949-2954.

Heriche, J.K., Lebrin, F., Rabilloud, T., Leroy, D., Chambaz, E.M., and Goldberg, Y. (1997). Regulation of protein phosphatase 2A by direct interaction with casein kinase 2alpha. Science *276*, 952-955.

Hirano, Y., and Ronai, Z. (2006). A new function for p53 ubiquitination. Cell *127*, 675-677.

Houlden, H., King, R.H., Muddle, J.R., Warner, T.T., Reilly, M.M., Orrell, R.W., and Ginsberg, L. (2004). A novel RAB7 mutation associated with ulcero-mutilating neuropathy. Annals of neurology *56*, 586-590.

Iacovides, D., O'Shea, C., Oses-Prieto, J., Burlingame, A., and McCormick, F. (2007). A critical role for arginine methylation in adenovirus-infected cells. J Virol.

Imai, Y., Nakada, A., Hashida, R., Sugita, Y., Tanaka, T., Tsujimoto, G., Matsumoto, K., Akasawa, A., Saito, H., and Oshida, T. (2002). Cloning and characterization of the highly expressed ETEA gene from blood cells of atopic dermatitis patients. Biochem Biophys Res Commun *297*, 1282-1290.

Ingram, D.A., Yang, F.C., Travers, J.B., Wenning, M.J., Hiatt, K., New, S., Hood, A., Shannon, K., Williams, D.A., and Clapp, D.W. (2000). Genetic and biochemical evidence that haploinsufficiency of the Nf1 tumor suppressor gene modulates melanocyte and mast cell fates in vivo. J Exp Med *191*, 181-188.

Issinger, O.G. (1993). Casein kinases: pleiotropic mediators of cellular regulation. Pharmacol Ther *59*, 1-30.

Izawa, I., Tamaki, N., and Saya, H. (1996). Phosphorylation of neurofibromatosis type 1 gene product (neurofibromin) by cAMP-dependent protein kinase. FEBS Lett *382*, 53-59.

Jacks, T., Shih, T.S., Schmitt, E.M., Bronson, R.T., Bernards, A., and Weinberg, R.A. (1994). Tumour predisposition in mice heterozygous for a targeted mutation in Nf1. Nat Genet *7*, 353-361.

Jin, J., Arias, E.E., Chen, J., Harper, J.W., and Walter, J.C. (2006). A family of diverse Cul4-Ddb1-interacting proteins includes Cdt2, which is required for S phase destruction of the replication factor Cdt1. Mol Cell *23*, 709-721.

Johannessen, C.M., Reczek, E.E., James, M.F., Brems, H., Legius, E., and Cichowski, K. (2005). The NF1 tumor suppressor critically regulates TSC2 and mTOR. Proc Natl Acad Sci U S A *102*, 8573-8578.

Kraakman, L., Lemaire, K., Ma, P., Teunissen, A.W., Donaton, M.C., Van Dijck, P., Winderickx, J., de Winde, J.H., and Thevelein, J.M. (1999). A Saccharomyces cerevisiae G-protein coupled receptor, Gpr1, is specifically required for glucose activation of the cAMP pathway during the transition to growth on glucose. Mol Microbiol *32*, 1002-1012.

Kulkarni, S.V., Gish, G., van der Geer, P., Henkemeyer, M., and Pawson, T. (2000). Role of p120 Ras-GAP in directed cell movement. The Journal of cell biology *149*, 457-470.

Lashkari, D.A., DeRisi, J.L., McCusker, J.H., Namath, A.F., Gentile, C., Hwang, S.Y., Brown, P.O., and Davis, R.W. (1997). Yeast microarrays for genome wide parallel genetic and gene expression analysis. Proceedings of the National Academy of Sciences of the United States of America *94*, 13057-13062.

Le, D.T., Kong, N., Zhu, Y., Lauchle, J.O., Aiyigari, A., Braun, B.S., Wang, E., Kogan, S.C., Le Beau, M.M., Parada, L.*, et al.* (2004). Somatic inactivation of Nf1 in hematopoietic cells results in a progressive myeloproliferative disorder. Blood *103*, 4243-4250.

Lebrin, F., Bianchini, L., Rabilloud, T., Chambaz, E.M., and Goldberg, Y. (1999). CK2alpha-protein phosphatase 2A molecular complex: possible interaction with the MAP kinase pathway. Mol Cell Biochem *191*, 207-212.

Leggett, D.S., Hanna, J., Borodovsky, A., Crosas, B., Schmidt, M., Baker, R.T., Walz, T., Ploegh, H., and Finley, D. (2002). Multiple associated proteins regulate proteasome structure and function. Mol Cell *10*, 495-507.

Legius, E., Marchuk, D.A., Collins, F.S., and Glover, T.W. (1993). Somatic deletion of the neurofibromatosis type 1 gene in a neurofibrosarcoma supports a tumour suppressor gene hypothesis. Nat Genet *3*, 122-126.

Lemaire, K., Van de Velde, S., Van Dijck, P., and Thevelein, J.M. (2004). Glucose and sucrose act as agonist and mannose as antagonist ligands of the G protein-coupled receptor Gpr1 in the yeast Saccharomyces cerevisiae. Mol Cell *16*, 293-299.

Li, Y., O'Connell, P., Breidenbach, H.H., Cawthon, R., Stevens, J., Xu, G., Neil, S., Robertson, M., White, R., and Viskochil, D. (1995). Genomic organization of the neurofibromatosis 1 gene (NF1). Genomics *25*, 9-18.

Longtine, M.S., McKenzie, A., 3rd, Demarini, D.J., Shah, N.G., Wach, A., Brachat, A., Philippsen, P., and Pringle, J.R. (1998). Additional modules for versatile and economical PCR-based gene deletion and modification in Saccharomyces cerevisiae. Yeast *14*, 953-961.

Lorenz, M.C., Pan, X., Harashima, T., Cardenas, M.E., Xue, Y., Hirsch, J.P., and Heitman, J. (2000). The G protein-coupled receptor gpr1 is a nutrient sensor that regulates pseudohyphal differentiation in Saccharomyces cerevisiae. Genetics *154*, 609-622.

Magherini, F., Busti, S., Gamberi, T., Sacco, E., Raugei, G., Manao, G., Ramponi, G., Modesti, A., and Vanoni, M. (2006). In Saccharomyces cerevisiae an unbalanced level of tyrosine phosphorylation down-regulates the Ras/PKA pathway. Int J Biochem Cell Biol *38*, 444-460.

Mangoura, D., Sun, Y., Li, C., Singh, D., Gutmann, D.H., Flores, A., Ahmed, M., and Vallianatos, G. (2006). Phosphorylation of neurofibromin by PKC is a possible molecular switch in EGF receptor signaling in neural cells. Oncogene *25*, 735-745.

Martin, G.A., Viskochil, D., Bollag, G., McCabe, P.C., Crosier, W.J., Haubruck, H., Conroy, L., Clark, R., O'Connell, P., Cawthon, R.M.*, et al.* (1990). The GAP-related domain of the neurofibromatosis type 1 gene product interacts with ras p21. Cell *63*, 843-849.

Meggio, F., and Pinna, L.A. (2003). One-thousand-and-one substrates of protein kinase CK2? Faseb J *17*, 349-368.

Minella, A.C., Welcker, M., and Clurman, B.E. (2005). Ras activity regulates cyclin E degradation by the Fbw7 pathway. Proc Natl Acad Sci U S A *102*, 9649-9654.

Narasimhan, M.L., Coca, M.A., Jin, J., Yamauchi, T., Ito, Y., Kadowaki, T., Kim, K.K., Pardo, J.M., Damsz, B., Hasegawa, P.M.*, et al.* (2005). Osmotin is a homolog of mammalian adiponectin and controls apoptosis in yeast through a homolog of mammalian adiponectin receptor. Molecular cell *17*, 171-180.

Nikawa, J., Cameron, S., Toda, T., Ferguson, K.M., and Wigler, M. (1987). Rigorous feedback control of cAMP levels in Saccharomyces cerevisiae. Genes Dev *1*, 931-937.

Niranjan, T., Guo, X., Victor, J., Lu, A., and Hirsch, J.P. (2007). Kelch repeat protein interacts with the yeast Galpha subunit Gpa2p at a site that couples receptor binding to guanine nucleotide exchange. J Biol Chem *282*, 24231-24238.

Park, J.I., Grant, C.M., and Dawes, I.W. (2005). The high-affinity cAMP phosphodiesterase of Saccharomyces cerevisiae is the major determinant of cAMP levels in stationary phase: involvement of different branches of the Ras-cyclic AMP pathway in stress responses. Biochem Biophys Res Commun *327*, 311-319.

Peeters, T., Louwet, W., Gelade, R., Nauwelaers, D., Thevelein, J.M., and Versele, M. (2006). Kelch-repeat proteins interacting with the Galpha protein Gpa2 bypass adenylate cyclase for direct regulation of protein kinase A in yeast. Proc Natl Acad Sci U S A *103*, 13034-13039.

Petroski, M.D., and Deshaies, R.J. (2005). Function and regulation of cullin-RING ubiquitin ligases. Nat Rev Mol Cell Biol *6*, 9-20.

Pinna, L.A. (1997). Protein kinase CK2. Int J Biochem Cell Biol *29*, 551-554.

Riccardi, V.M. (1992). Type 1 neurofibromatosis and the pediatric patient. Curr Probl Pediatr *22*, 66-106; discussion 107.

Rodriguez-Viciana, P., and McCormick, F. (2005a). Characterization of interactions between ras family GTPases and their effectors. Methods Enzymol *407*, 187-194.

Rodriguez-Viciana, P., and McCormick, F. (2005b). RalGDS comes of age. Cancer Cell *7*, 205-206.

Rodriguez-Viciana, P., Oses-Prieto, J., Burlingame, A., Fried, M., and McCormick, F. (2006). A phosphatase holoenzyme comprised of Shoc2/Sur8 and the catalytic subunit of PP1 functions as an M-Ras effector to modulate Raf activity. Mol Cell *22*, 217-230.

Salmena, L., and Pandolfi, P.P. (2007). Changing venues for tumour suppression: balancing destruction and localization by monoubiquitylation. Nat Rev Cancer *7*, 409-413.

Schubbert, S., Shannon, K., and Bollag, G. (2007). Hyperactive Ras in developmental disorders and cancer. Nat Rev Cancer *7*, 295-308.

Serra, E., Ars, E., Ravella, A., Sanchez, A., Puig, S., Rosenbaum, T., Estivill, X., and Lazaro, C. (2001). Somatic NF1 mutational spectrum in benign neurofibromas: mRNA splice defects are common among point mutations. Hum Genet *108*, 416-429.

Shannon, K.M., O'Connell, P., Martin, G.A., Paderanga, D., Olson, K., Dinndorf, P., and McCormick, F. (1994). Loss of the normal NF1 allele from the bone marrow of children with type 1 neurofibromatosis and malignant myeloid disorders. N Engl J Med *330*, 597-601.

Side, L., Taylor, B., Cayouette, M., Conner, E., Thompson, P., Luce, M., and Shannon, K. (1997). Homozygous inactivation of the NF1 gene in bone marrow cells from children with neurofibromatosis type 1 and malignant myeloid disorders. N Engl J Med *336*, 1713-1720.

Sprang, S.R. (1997). G protein mechanisms: insights from structural analysis. Annu Rev Biochem *66*, 639-678.

Tanaka, K., Nakafuku, M., Satoh, T., Marshall, M.S., Gibbs, J.B., Matsumoto, K., Kaziro, Y., and Toh-e, A. (1990a). S. cerevisiae genes IRA1 and IRA2 encode proteins that may be functionally equivalent to mammalian ras GTPase activating protein. Cell *60*, 803-807.

Tanaka, K., Nakafuku, M., Tamanoi, F., Kaziro, Y., Matsumoto, K., and Toh-e, A. (1990b). IRA2, a second gene of Saccharomyces cerevisiae that encodes a protein with a domain homologous to mammalian ras GTPase-activating protein. Mol Cell Biol *10*, 4303-4313.

The, I., Hannigan, G.E., Cowley, G.S., Reginald, S., Zhong, Y., Gusella, J.F., Hariharan, I.K., and Bernards, A. (1997). Rescue of a Drosophila NF1 mutant phenotype by protein kinase A. Science *276*, 791-794.

Thevelein, J.M., and de Winde, J.H. (1999). Novel sensing mechanisms and targets for the cAMP-protein kinase A pathway in the yeast Saccharomyces cerevisiae. Mol Microbiol *33*, 904-918.

Toda, T., Uno, I., Ishikawa, T., Powers, S., Kataoka, T., Broek, D., Cameron, S., Broach, J., Matsumoto, K., and Wigler, M. (1985). In yeast, RAS proteins are controlling elements of adenylate cyclase. Cell *40*, 27-36.

Tong, J.J., Schriner, S.E., McCleary, D., Day, B.J., and Wallace, D.C. (2007). Life extension through neurofibromin mitochondrial regulation and antioxidant therapy for neurofibromatosis-1 in Drosophila melanogaster. Nat Genet *39*, 476-485.

Upadhyaya, M., Ruggieri, M., Maynard, J., Osborn, M., Hartog, C., Mudd, S., Penttinen, M., Cordeiro, I., Ponder, M., Ponder, B.A.*, et al.* (1998). Gross deletions of the neurofibromatosis type 1 (NF1) gene are predominantly of maternal origin and commonly associated with a learning disability, dysmorphic features and developmental delay. Hum Genet *102*, 591-597.

van der Geer, P., Henkemeyer, M., Jacks, T., and Pawson, T. (1997). Aberrant Ras regulation and reduced p190 tyrosine phosphorylation in cells lacking p120-Gap. Mol Cell Biol *17*, 1840-1847.

Verhoeven, K., De Jonghe, P., Coen, K., Verpoorten, N., Auer-Grumbach, M., Kwon, J.M., FitzPatrick, D., Schmedding, E., De Vriendt, E., Jacobs, A*., et al.* (2003). Mutations in the small GTP-ase late endosomal protein RAB7 cause Charcot-Marie-Tooth type 2B neuropathy. American journal of human genetics *72*, 722-727.

Verma, R., Aravind, L., Oania, R., McDonald, W.H., Yates, J.R., 3rd, Koonin, E.V., and Deshaies, R.J. (2002). Role of Rpn11 metalloprotease in deubiquitination and degradation by the 26S proteasome. Science *298*, 611-615.

Viskochil, D., Buchberg, A.M., Xu, G., Cawthon, R.M., Stevens, J., Wolff, R.K., Culver, M., Carey, J.C., Copeland, N.G., Jenkins, N.A*., et al.* (1990). Deletions and a translocation interrupt a cloned gene at the neurofibromatosis type 1 locus. Cell *62*, 187-192.

Wallace, M.R., Marchuk, D.A., Andersen, L.B., Letcher, R., Odeh, H.M., Saulino, A.M., Fountain, J.W., Brereton, A., Nicholson, J., Mitchell, A.L*., et al.* (1990). Type 1 neurofibromatosis gene: identification of a large transcript disrupted in three NF1 patients. Science *249*, 181-186.

Wang, S., Zheng, H., Esaki, Y., Kelly, F., and Yan, W. (2006). Cullin3 is a KLHL10-interacting protein preferentially expressed during late spermiogenesis. Biol Reprod *74*, 102-108.

Welcker, M., and Clurman, B.E. (2008). FBW7 ubiquitin ligase: a tumour suppressor at the crossroads of cell division, growth and differentiation. Nat Rev Cancer *8*, 83-93.

Wichmann, H., Hengst, L., and Gallwitz, D. (1992). Endocytosis in yeast: evidence for the involvement of a small GTP-binding protein (Ypt7p). Cell *71*, 1131-1142.

Wyndham, A.M., Baker, R.T., and Chelvanayagam, G. (1999). The Ubp6 family of deubiquitinating enzymes contains a ubiquitin-like domain: SUb. Protein Sci *8*, 1268-1275.

Xu, G.F., Lin, B., Tanaka, K., Dunn, D., Wood, D., Gesteland, R., White, R., Weiss, R., and Tamanoi, F. (1990a). The catalytic domain of the neurofibromatosis type 1 gene product stimulates ras GTPase and complements ira mutants of S. cerevisiae. Cell *63*, 835-841.

Xu, G.F., O'Connell, P., Viskochil, D., Cawthon, R., Robertson, M., Culver, M., Dunn, D., Stevens, J., Gesteland, R., White, R.*, et al.* (1990b). The neurofibromatosis type 1 gene encodes a protein related to GAP. Cell *62*, 599-608.

Yang, F.C., Ingram, D.A., Chen, S., Hingtgen, C.M., Ratner, N., Monk, K.R., Clegg, T., White, H., Mead, L., Wenning, M.J.*, et al.* (2003). Neurofibromin-deficient Schwann cells secrete a potent migratory stimulus for Nf1+/- mast cells. J Clin Invest *112*, 1851-1861.

Yao, T., and Cohen, R.E. (2002). A cryptic protease couples deubiquitination and degradation by the proteasome. Nature *419*, 403-407.

Zhu, Y., Ghosh, P., Charnay, P., Burns, D.K., and Parada, L.F. (2002). Neurofibromas in NF1: Schwann cell origin and role of tumor environment. Science *296*, 920-922.

Zhu, Y., and Parada, L.F. (2001). Neurofibromin, a tumor suppressor in the nervous system. Exp Cell Res *264*, 19-28.
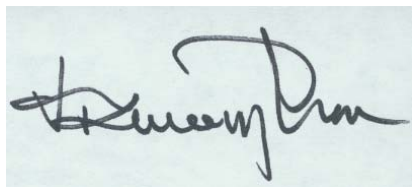
UCSF Library Release

The last page of your dissertation must have the following language:

Publishing Agreement

It is the policy of the University to encourage the distribution of all theses and dissertations. Copies of all UCSF theses and dissertations will be routed to the library via the Graduate Division. The library will make all theses and dissertations accessible to the public and will preserve these to the best of their abilities, in perpetuity.

Please sign the following statement:

I hereby grant permission to the Graduate Division of the University of California, San Francisco to release copies of my thesis or dissertation to the Campus Library to provide access and preservation, in whole or in part, in perpetuity.

3/31/08

_____   _____
Author Signature   Date

This page must be signed and dated by the author and include the correct pagination.